MODELING, FABRICATION AND CHARACTERIZATION OF COATED CALCIUM PHOSPHATE SCAFFOLDS PRODUCED BY 3D-PRINTING FOR TISSUE ENGINEERING APPLICATION

MARIA TOURI

FACULTY OF ENGINNERING
UNIVERSITY OF MALAYA
KUALA LUMPUR

2020

MODELING, FABRICATION AND CHARACTERIZATION OF COATED CALCIUM PHOSPHATE SCAFFOLDS PRODUCED BY 3D-PRINTING FOR TISSUE ENGINEERING APPLICATION

MARIA TOURI

THESIS SUBMITTED IN FULFILMENT OF THE REQUIREMENTS FOR THE DEGREE OF DOCTOR OF PHILOSOPHY

FACULTY OF ENGINNERING
UNIVERSITY OF MALAYA
KUALA LUMPUR

2020

UNIVERSITY OF MALAYA

ORIGINAL LITERARY WORK DECLARATION

Name of Candidate: MARIA TOURI

Matric No: HHS40001

Name of Degree: Doctor of Philosophy

Title of Thesis ("this Work"): **MODELING, FABRICATION AND CHARACTERIZATION OF COATED CALCIUM PHOSPHATE SCAFFOLDS PRODUCED BY 3D-PRINTING FOR TISSUE ENGINEERING APPLICATION**

Field of Study: Biomedical Engineering

I do solemnly and sincerely declare that:

(1) I am the sole author/writer of this Work;
(2) This Work is original;
(3) Any use of any work in which copyright exists was done by way of fair dealing and for permitted purposes and any excerpt or extract from, or reference to or reproduction of any copyright work has been disclosed expressly and sufficiently and the title of the Work and its authorship have been acknowledged in this Work;
(4) I do not have any actual knowledge nor do I ought reasonably to know that the making of this work constitutes an infringement of any copyright work;
(5) I hereby assign all and every rights in the copyright to this Work to the University of Malaya ("UM"), who henceforth shall be owner of the copyright in this Work and that any reproduction or use in any form or by any means whatsoever is prohibited without the written consent of UM having been first had and obtained;
(6) I am fully aware that if in the course of making this Work I have infringed any copyright whether intentionally or otherwise, I may be subject to legal action or any other action as may be determined by UM.

Candidate's Signature Date:

Subscribed and solemnly declared before,

Witness's Signature Date:

Name:

Designation:

MODELING, FABRICATION AND CHARACTERIZATION OF COATED CALCIUM PHOSPHATE SCAFFOLDS PRODUCED BY 3D-PRINTING FOR TISSUE ENGINEERING APPLICATION

ABSTRACT

A fully interconnected 3-dimensional scaffold with pre-determined dimensions and porosity can be attained by design-dependent rapid prototyping techniques which possess precise control over the internal and external architecture of the scaffolds thus they can overcome the problems associated with the process-dependent classical approaches. Interruption of vascular flow with fracture or surgical osteotomy results in a transient hypoxic gradient within the wound and subsequent tissue necrosis. Tissue engineering scaffolds with oxygen generating elements have shown to be able to increase the level of oxygen and cell survivability. In this study, biphasic calcium phosphate (BCP) scaffolds with the composition of 60% hydroxyapatite and 40% beta-tricalcium phosphate, which have shown a great potential for bone tissue engineering applications, were fabricated by robocasting technique. Then, the three-dimensional-printed scaffolds were coated with different ratios (1, 3 and 5 wt%) of an oxygen producing biomaterial, calcium peroxide (CPO), which encapsulated within a polycaprolactone (PCL) matrix through dip-coating, and used for in situ production of oxygen in the implanted sites. 3D-printed BCP scaffolds with 70% porosity and large pore size (500 μm) showed a compressive strength of ~21 MPa. The oxygen release behaviour was sustained and dependant on the concentration of CPO encapsulated in the PCL coating matrix. It was also demonstrated that the coated scaffolds, having 3% CPO in the coating system, could provide an increase of approximately 50% in the oxygen concentration and a great potential for promoting bone ingrowth with improving osteoblast cells viability, function and proliferation. The finite element modelling was used to calculate the stress fields in scaffolds and the predicted compressive strength of

the robocast scaffolds was ~24 MPa which is so close to the experimental result. Antimicrobial evaluations confirmed the inhibitory properties of the scaffolds on the growth of E. coli and S. aureus because of the release of calcium peroxide from the scaffolds. At in vivo part, a model of 15 mm segmental defect was made at the radius of rabbits. In the experimental group, defects were implanted using BCP scaffold coated with CPO. Control animals were implanted with uncoated BCP scaffolds. No implant was provided for the blank group. Bone repair was assessed by X-ray, biomechanical tests and histological observations at 3 and 6 months post-operation. The results showed that bone formation was increased at the interface and inside the inner pores of CPO coated scaffolds than those of uncoated scaffolds; biomechanical properties in the coated group were superior to those of the uncoated group. Our findings suggested CPO coated scaffolds had enhanced repairing ability in segmental bone defect in rabbit radius, and may serve as a potential material for repairing large bone defects.

Keywords: Oxygen-generating biomaterial; Scaffold; Additive manufacturing; Bone; Tissue engineering.

PEMODELAN, FABRIKASI DAN PENCIRIAN SKAFOLD KALSIUM FOSFAT BERSALUT YANG DIHASILKAN OLEH PERCETAKAN 3D UNTUK APLIKASI KEJURUTERAAN TISU

ABSTRAK

Skafold 3-dimensi penuh yang berkait dengan pre-dimensi ditetapkan terlebih dahulu dan porositi, dapat dicapai dengan teknik prototaip pantas yang bergantung pada rekabentuk kawalan tepat terhadap seni bina dalaman dan luaran skafold di mana ia dapat mengatasi masalah berkaitan dengan pendekatan klasik yang bergantung kepada kaedah pemprosesan sahaja. Gangguan aliran vaskular dengan fraktur atau pembedahan osteotomi mengakibatkan kecerunan hipoksik sementara di dalam luka dan tisu nekrosis. Skafold kejuruteraan tisu dengan unsur penjanaan oksigen telah menunjukkan peningkatan tahap oksigen dan kebolehan ketahanan sel. Dalam kajian ini, skafold kalsium fosfat bifasik (BCP) dengan komposisi 60% hydroxyapatite dan 40% beta-trikalsium fosfat, yang menunjukkan potensi besar untuk aplikasi kejuruteraan tisu tulang, telah direka dengan menggunakan teknik robocasting. Kemudian, cetakan skafold tiga dimensi disaluti dengan nisbah yang berlainan (1, 3 dan 5 wt%) daripada biobahan yang menghasilkan oksigen, kalsium peroksida (CPO), yang dikapsulkan ke dalam matriks polikaprolakton (PCL) melalui salutan dip, dan digunakan untuk penghasilan oksigen in-situ di bahagian implan. Cetakan skafold 3D BCP dengan kepekatan 70% dan saiz liang besar (500 μm) menunjukkan kekuatan mampatan ~ 21 MPa. Tingkah laku pelepasan oksigen dikekalkan dan bergantung kepada kepekatan CPO yang terkandung dalam matriks salutan PCL. Ia juga menunjukkan bahawa skafold bersalut, mempunyai CPO 3% dalam sistem salutan, berupaya memberikan peningkatan kira-kira 50% dalam kepekatan oksigen dan berpotensi besar untuk membantu penumbuhan semula tulang dengan meningkatkan daya, fungsi dan proliferasi sel osteoblast.

Model elemen finiti digunakan untuk mengira medan tegangan di skafold, dan kekuatan mampatan robocast skafold yang diramal adalah ~ 24 MPa iaitu menghampiri nilai hasil eksperimen. Evaluasi antimikrobia mengesahkan sifat-sifat penghalang skafold pada pertumbuhan E. coli dan S. aureus kerana pelepasan kalsium peroksida dari skafold. Untuk bahagian in vivo, model 15 mm defek-segmental dibuat di radius arnab. Dalam kumpulan eksperimen, defek telah diimplan menggunakan skafold BCP yang disalut dengan CPO. Kumpulan kawalan diimplan dengan skafold BCP yang tidak disalut. Tiada implan disediakan untuk kumpulan kosong. Pembaikan tulang dinilai oleh X-ray, ujian biomekanik dan pemerhatian histologi pada 3 dan 6 bulan selepas operasi. Hasilnya menunjukkan bahawa formasi tulang meningkat di pra-muka dan di dalam liang dalaman, bagi skafold yang bersalut CPO berbanding skafold yang tidak bersalut; sifat biomekanik dalam kumpulan bersalut lebih superior daripada kumpulan yang tidak bersalut. Penemuan kami mencadangkan skafold bersalut CPO telah meningkatkan keupayaan membaiki kecacatan tulang segment arnab, dan merupakan bahan yang berpotensi untuk membaiki defek tulang besar.

Kata Kunci: Biobahan penjanaan oksigen; Skafold; Pembuatan aditif; Tulang; Kejuruteraan tisu.

ACKNOWLEDGEMENTS

I cannot express enough thanks to my supervisor, Professor Dr. Ir. Noor Azuan Abu Osman for his continued support and encouragement.

My completion of this project could not have been accomplished without the support of Puan Hanie Nadia Shasmin.

TABLE OF CONTENTS

LIST OF FIGURES

LIST OF SYMBOLS AND ABBREVIATIONS

BCP	:	Biphasic calcium phosphate
HA	:	Hydroxyapatite
β-TCP	:	Beta-tricalcium phosphate
CPO	:	Calcium peroxide
MSC	:	Mesenchymal stem cell
PCL	:	Polycaprolactone
FEM	:	Finite element method
3D		3-Dimenthional

CHAPTER 1: INTRODUCTION

1.1 Background of study

Advancement of treatments for improving osteogenesis has been a great challenge in restoration of large and load bearing bone defects (Calori, Mazza, Colombo, & Ripamonti, 2011). The lesions of bone over a critical size will not be healed by the body and will form a nonunion (Petite et al., 2000), and in most cases external interference is required to restore normal processes (Bose, Vahabzadeh, & Bandyopadhyay, 2013). The use of bone grafts and tissue engineering are two of today treatments for bone reconstruction. Tissue engineering can be defined as using of scaffolds for repair or replacement of diseased or destroyed tissues. The scaffold supplies a beginning biomechanical profile for the replacement tissue until the cells create a sufficient extracellular matrix (Stock & Vacanti, 2001),(Ashman & Phillips, 2013). Bone tissue engineering is an outstanding method for bone reconstruction and it needs to design and process a 3D scaffold at first step (Johnson & Herschler, 2011),(Mouriño & Boccaccini, 2009).

The necessities for the material of the scaffold, beside the biocompatibility, also comprise the matching of its resorption kinetic with the formation kinetic of new bone tissue. The most encouraging materials for this application are calcium phosphates which have similarity to the chemical and phase composition of the bone mineral component. The solubility of tricalcium phosphate (TCP) is higher than hydroxyapatite (HA). Biphasic calcium phosphates (BCP, HA/TCP composites) have the capability of balancing resorption and biological behaviour depend on the HA/TCP ratio (Kubarev, Komlev, & Barinov, 2010).

BCP bioceramics consisting of HA ($Ca_{10}(PO_4)_6(OH)_2$) and β-TCP (beta-tricalcium phosphate, $Ca_3(PO_4)_2$), possess a broad application in tissue engineering because they can promote the ingrowth of bone in the implanted scaffolds. HA has the higher

mechanical strength and lower degradation rate compared to β-TCP, therefore the mechanical properties and degradation rate of the designed BCP scaffolds can be controlled by the HA/β-TCP ratio for various bone repair applications (LeGeros, Lin, Rohanizadeh, Mijares, & LeGeros, 2003),(Houmard, Fu, Genet, Saiz, & Tomsia, 2013). BCP in the composition of 60% HA and 40% β-TCP (in weight %), has been revealed a rapid new bone formation in both animals and humans and could persuade bone formation in large or long bone defects (Arinzeh, Tran, Mcalary, & Daculsi, 2005), (Broggini et al., 2015),(Bouwman, Bravenboer, Frenken, Ten Bruggenkate, & Schulten, 2017). Detsch et al. showed in their study that biphasic calcium phosphate ceramic with 60HA/40β-TCP presented outstanding osteoclastic proliferation, differentiation, and activation then it is the most promising surface to serve as 3D printed bone substitute scaffolds (Detsch et al., 2011).

Conventional scaffold fabrication techniques (particulate leaching, gas foaming, fibre networking, freeze casting, etc.) cannot control the size, geometry, interconnectivity, and the distribution of pores precisely. Other disadvantages include low and inhomogeneous mechanical strength, and limited control of external geometry which leads to problems in the fabrication of patient-specific implants. The classical approaches have remained process-dependent methods due to these limitations (Peltola, Melchels, Grijpma, & Kellomäki, 2008),(Billiet, Vandenhaute, Schelfhout, Van Vlierberghe, & Dubruel, 2012),(R. Touri et al., 2013). Rapid Prototyping (RP) techniques, design-dependent methods, can overcome these obstacles. RP techniques manufacture intricate 3D structures in a layer-by-layer way using a computer-aided design (CAD) model. Moreover, the ceramic scaffolds fabricated by RP techniques has improved mechanical properties compared to traditional fabrication methods (Sachlos & Czernuszka, 2003),(Hollister, 2005). Robocasting (direct write assembly or micro-robotic deposition) technique is outstanding for fabricating ceramic scaffolds in the

group of RP methods. It utilises water-based ink containing negligible organic content and doesn't require any sacrificial support material or mould. In this technique, a colloidal suspension (ink) is deposited through a cylindrical nozzle robotically. The ink has high viscosity and supports its weight throughout the assembling. Therefore, direct printing of a network of cylindrical ink rods will form a 3D structure (Smay, Cesarano, & Lewis, 2002),(Miranda, Pajares, & Guiberteau, 2008).

Tissue hypoxia frequently occurs after damages of tissues when the vascularization network is destroyed. Oxygen plays a critical role in multiple cellular functions during the healing process of bone fractures. Hypoxic wound and bacterial infection are some of the significant challenges after the scaffold implantation. Oxygen is essential for cell metabolism, preventing wounds from infection, collagen synthesis, extracellular matrix formation and almost all wound healing processes (Rodriguez, Felix, Woodley, & Shim, 2008),(Gordillo & Sen, 2003). Limited oxygen delivery can lead to cell apoptosis and subsequent chronic bacterial infection. Sufficient oxygen levels can increase cell proliferation, encourage cell differentiation, enhance extracellular matrix (ECM) synthesis and prevent infections (Guo & DiPietro, 2010),(Eisenbud, 2012).

Providing of supplemental oxygen to hypoxic bone remains a critical medical challenge with implications for tissue repair and regeneration as prolonged periods of ischemia can cause tissue necrosis. To prevent ischemia-related tissue death, several strategies like hyperbaric oxygen therapy, hemoglobin- and perfluorocarbon-based oxygen carriers, Lipid-based oxygen carriers, etc have been explored for provision of oxygen to various tissues but each of them has some problems with limited efficiency and slow development. A novel class of oxygen-generating biomaterials represents a viable solution for the direct provision of oxygen to hypoxic area (M. Touri, Moztarzadeh, Osman, Dehghan, & Mozafari, 2018b). Using of oxygen generating biomaterials is one of the recent developed strategies to increase the oxygen level to the

engineered tissues, especially at the early stages after implantation, while neovascularization is being formed. Tissue survival and decreasing of necrosis can be concluded from oxygen releasing biomaterials which provide a sustained release of oxygen to the cells (Pedraza, Coronel, Fraker, Ricordi, & Stabler, 2012a),(Oh, Ward, Atala, Yoo, & Harrison, 2009),(Harrison, Eberli, Lee, Atala, & Yoo, 2007).

1.2 Problem Statement

This study was decided to be done due to a combination of some problems and examine the recommended solution for eliminating these difficulties. The first problem is that the bone defects over a critical size will not be healed by the body and will form a non-union. This critical size according to the several studies is about 6 mm. It means that the bone defect larger than this length cannot be healed by the body and external intervention is required to restore the normal tissue. The length of the bone defect was considered 15 mm which is a proved by other studies that the body cannot heal this size of defect by own. There are some treatments for solving this problem which tissue engineering using a biodegradable scaffold is a way with lots of advantages that will be mentioned in the literature review.

Another problem is the fabrication method of the scaffold. The conventional methods are process-dependent and the desire design both internal and external which can meet our enquiries is so limited. Also, the ceramics scaffolds fabricated by traditional methods have weak mechanical strength and cannot be applied in load bearing locations. Therefore, we need a method for fabrication that be design-dependent to meet the required external geometry, internal structure such as pore shape and pore size, mechanical properties, etc. Additive manufacturing techniques can permit us to design the internal structure and subsequently control some properties like mechanical properties by varying the design.

The main problem and challenge in tissue engineering is the deficiency of oxygen in the wound area which leads to the cell death, bacterial infection, prolonged healing, etc. In bone tissue engineering, hypoxia in the bone defect can result in non-union. There are some procedures which can increase the level of oxygen in the defect area and avoid the tissue necrosis. In this study using of oxygen-generating biomaterials was chosen for in situ production of oxygen in the defect area for eliminating the hypoxia occurred due to the destroyed vascular. Some previous studies have used the oxygen-generating materials inside the scaffolds or any kind of implants but in this study theses biomaterials will be coated on the surface of scaffolds. The coating of oxygen-producing biomaterials for releasing oxygen has some merits compared to using in the bulk of implants. The coating can be applied on the implants which fabricated already by any technique but using of these materials in the bulk of implants is not possible for these implants. The hypoxia is severe in the first weeks after the defect created because the body can compensate the ischemia after a while then the coating can supply extra oxygen at the early stage of healing and inhibit the cell necrosis and subsequently the body can form the vascularization and provide sufficient oxygen for the wounded tissue.

1.3 Research Objectives

The main objective of this study is the treating of the 15-mm bone defect with an oxygen-generated scaffold and forming a union. It is expected that a coated scaffold with calcium peroxide (CPO, an oxygen-generating biomaterial) has an accelerated bone regeneration compared to a non-coated 3D-printed biphasic calcium phosphate scaffold. This study suggests several research objectives to be attained as follows:

1. Figuring out several in vitro tests to compare the capacity of two kinds of scaffolds (CPO coated vs non-coated) in numerous aspects such as SBF test, cell behaviour, antibacterial response, etc.

2. Investigating the effect of oxygen releasing scaffold on the proliferation, differentiation and expressing bone regeneration markers.
3. Figuring out in vivo test to compare the ability of coated and uncoated scaffolds in bone integration, scaffold degradation and bone filling in the defect.

CHAPTER 2: LITERATURE REVIEW

2.1 Bone biology

Bone is a mineralized connective tissue that displays four kinds of cells: osteoblasts, bone lining cells, osteocytes, and osteoclasts. Bone is comprised of cells and collagenous extracellular organic matrix, which is mainly type I collagen (85–95%) named osteoid that becomes mineralised by the deposition of calcium hydroxyapatite. Bone has significant functions in the body, like motion, support and protection of soft tissues, calcium and phosphate storage, and sheltering of bone marrow. Bone is extremely dynamic which is unceasingly resorbed by osteoclasts and neoformed by osteoblasts (Mohamed, 2008).

Osteoclasts are included in bone resorption that contributes to bone remodelling. When bone surfaces are neither in the formative nor resorptive phase, the bone surface is wholly lined by a layer of flattened and elongated cells called bone-lining cells. Via covering the bone surface, they defend it from any osteoclast resorptive activity. They may be reactivated to form osteoblasts. Osteocytes are entrapped osteoblasts. They are post-proliferative, expressing the most mature differentiation state of osteoblast lineage. The osteocytes inhabit lacunae, which are regularly dispersed, and numerous tiny canals named canaliculi emit from them in all directions. The canaliculi let the diffusion of materials within the bone. The cell-cell communication is also attained by interstitial fluid that currents among the osteocytes processes and canaliculi. Through the lacunocanalicular system, the osteocytes perform as mechanosensors as their interconnected network has the capability to sense mechanical pressures and loads, thus assisting the adaptation of bone to everyday mechanical forces. Via this approach, the osteocytes appear to perform as orchestrators of bone remodeling, throughout

adjustment of osteoblast and osteoclast actions (Florencio-Silva, Sasso, Sasso-Cerri, Simões, & Cerri, 2015),(Olszta et al., 2007).

Osteoblasts are cuboidal cells situated along the bone surface and are mostly recognised for their bone forming function. These cells demonstrate morphological characteristics of protein producing, comprising plentiful rough endoplasmic reticulum, noticeable Golgi apparatus, and numerous secretory vesicles. Osteoblasts secrete the osteoid for the bone matrix (Capulli, Paone, & Rucci, 2014). Osteoblasts are derivative of mesenchymal stem cells (MSC). For converting to osteoprogenitor lineage, MSC need the expression of particular genes comprising bone morphogenetic proteins (BMPs) and members of the Wingless (Wnt) pathways. The expressions of Runt related transcription factors 2 (Runx2) is critical for osteoblast differentiation and Runx2 upregulates the osteoblast-related genes like collagen type I, alkaline phosphatase (ALP), and osteocalcin (OCN) (Fakhry, Hamade, Badran, Buchet, & Magne, 2013). There is a proliferation phase when the osteoblast progenitors expressing Runx2 and collagen type I has been established during osteoblast differentiation. In the proliferation phase, osteoblast progenitors display alkaline phosphatase (ALP) activity, and are considered preosteoblasts. The transition of preosteoblasts to mature osteoblasts is characterized by an increase in the secretion of bone matrix proteins like OCN and collagen type I (Florencio-Silva et al., 2015).

2.2 Osteogenesis

Intramembranous and endochondral osteogenesis (ossification) are two types of bone formation which occurs in the flat and long bones, respectively. They commence through mesenchymal stem cells (MSCs) condensation. In intramembranous ossification, MSCs first differentiate into osteoprogenitors and subsequently develop mature osteoblasts which can experience apoptosis or convert to osteocytes. Cartilage

exists throughout the endochondral ossification dissimilar to the intramembranous ossification (Wu, Deng, Zhu, & Li, 2010).

Bone healing happens in three separate but overlapping stages: 1) the early inflammatory stage; 2) the repair stage; and 3) the late remodelling stage. In the inflammatory stage, a hematoma progresses in the fracture site throughout the initial few hours and days. Inflammatory cells and fibroblasts penetration results in the creation of granulation tissue, growth of vascular tissue, and migration of mesenchymal cells. During the repair stage, fibroblasts start to lay down a stroma which assists support vascular ingrowth. While vascular ingrowth develops, a collagen matrix is laid down as osteoid is secreted and successively mineralized, which results in the formation of a soft callus about the repair place. Lastly, the callus ossifies, creating a bridge of woven bone between the fracture fragments. Otherwise, if appropriate immobilization is not applied, ossification of the callus may not happen, and an unstable fibrous union may progress instead. Fracture healing is finalised throughout the remodelling stage in which the healing bone is reinstated to its original form, structure, and mechanical strength (Kalfas, 2001).

2.3 Bone reconstruction

Bone tissue possesses the exceptional inner repair capability to heal and remodel (Mouriño & Boccaccini, 2009) but critical-size bone defects cannot be repaired by the body and will form a nonunion (Petite et al., 2000), and in most cases external interference is required to restore normal processes (Bose et al., 2013). Significant bone loss can happen due to high-energy trauma, infection, tumour resection, developmental deformities, etc. The use of bone grafts and tissue engineering are two of today treatments for bone reconstruction (Ashman & Phillips, 2013). Autograft (a patient's own bone tissue) or allograft (bone tissue taken from another person), each process has

its own drawbacks including the requirement of secondary surgery, the limited amount of tissue that can be harvested, the possibility of graft rejection by the immune system, risk of infections and transmission of donor pathogens. Tissue engineering approaches are outstanding alternatives to overcome these problems and promote the regenerative ability of the host body. One of the main stages of bone tissue engineering is the design and processing of a porous 3D structure called a scaffold. Bone tissue engineering is an outstanding method for bone reconstruction and it needs to design and process a 3D scaffold at first step (Johnson & Herschler, 2011),(Mouriño & Boccaccini, 2009).

2.4 Tissue engineering and scaffold

The fundamental concept of tissue engineering comprises a scaffold that supplies an architecture or a preliminary biomechanical profile for the replacement tissue until the cells create an enough extracellular matrix. Throughout the formation, deposition, and organization of the newly generated matrix, the scaffold is degraded, finally leaving a vital tissue that restores, maintains, or improves tissue function (Stock & Vacanti, 2001).

In vivo, cells have the growth in three dimensions and complex cell-cell interactions then the absence of a 3D structure will cause cells to form a random 2D mono-layer (Billiet et al., 2012). An ideal scaffold must possess the following characteristics: (i) three-dimensional and highly porous with an interconnected pore network for cell growth and flow transport of nutrients and metabolic waste; (ii) biocompatible and bioresorbable with a controllable degradation and resorption rate to match cell/tissue growth in vitro and/or in vivo; (iii) appropriate surface chemistry for cell attachment, proliferation, and differentation and (iv) mechanical properties to match those of the tissues at the place of implantation (Hutmacher, 2000).

Bone regeneration embraces the series of biological events of bone induction and conduction, containing numerous cell types and intracellular and extracellular molecular-signalling pathways, with temporal and spatial order, to optimise skeletal repair and reinstate skeletal function. The most usual form of bone regeneration in the clinical setting is fracture healing in the clinical setting and the pathway comprises intramembranous and endochondral ossification. Bone scaffolds are made of synthetic or natural biomaterials that encourage the migration, proliferation and differentiation of bone cells for bone regeneration. An extensive variety of biomaterials and synthetic bone substitutes are presently used as scaffolds, including collagen, HA, β-TCP, calcium-phosphate cements, and glass ceramics (Dimitriou, Jones, McGonagle, & Giannoudis, 2011). The acceptance of these substitutes by host tissues is determined by two vital features: pore diameter and the porosity or interconnectivity. Minimum pore size of 100 μm is optimal for bone ingrowth whereas pore size more than 200 μm facilitates development of mature osteon (Bansal et al., 2009). The necessities that permit bone ingrowth are a porosity of 30–70 vol% and a pore diameter between 300 and 800 mm. Scaffolds for bone regeneration should also meet certain criteria regarding mechanical properties, which should be similar to those of the bone to be replaced (Detsch et al., 2011).

2.5 Scaffold's material and Calcium phosphates

There is an extensive diversity of biocompatible materials which comprises bioceramics, synthetic and natural biopolymers available for tissue engineering. Each material possesses its own characteristics, and within each family of materials there is a variety of properties and characteristics. The selection of materials consequently depends on the particular requirement dictated by the application and appropriate fabrication technique (Liu, Xia, & Czernuszka, 2007).

The necessities for the material of the scaffold, beside the biocompatibility, also comprise the matching of the kinetics of its resorption in time with the kinetics of the formation of new bone tissue. The most promising for these applications are materials on the basis of calcium phosphates, particularly HA, an equivalent of the mineral component of bone tissue by chemical and phase compositions. From the point of view of biocompatibility, hydroxyapatite appears to be the most appropriate ceramic material for hard tissue replacement implants. HA (chemical formula $Ca_{10}(PO_4)_6(OH)_2$) is the key mineral component of bones (Suchanek & Yoshimura, 1998).

Synthetic bioactive ceramics like some forms of calcium phosphates and combinations of them have been extensively studied as scaffold materials due to their structural and chemical similarity with the inorganic component of bone (Mouriño & Boccaccini, 2009). TCP and HA, and their combinations are the most frequently used bioceramics in scaffold fabrication. These two bioceramics have outstanding biocompatibility with hard tissues, and high osteoconductivity and bioactivity. They have neither antigenicity nor cytotoxicity and can be processed into porous form for use as bone substitutes or scaffolds (Liu et al., 2007). Though, HA is the least soluble calcium phosphate in physiological conditions. The kinetics of resorption can be administrated, adding a second more soluble phase to HA. The solubility of TCP is higher than HA. Biphase materials in the HA–TCP system were developed, the resorption ability and biological behaviour of which depend on the HA/TCP ratio (Kubarev et al., 2010). When used as a mixture, biodegradable HA/β-TCP have the ability to dissolve, break down, and allow new bone formation and remodelling required to reach optimal mechanical strength without interference. A completely nonresorbable graft material may hamper remodelling, cause strength lack of new bone and leave enduring stress risers in the fusion mass (Bansal et al., 2009).

For osteointegration, a bone tissue engineering scaffold should simulate the mechanical properties, morphology and composition of native bone tissues. Having an optimized degradation rate in balance with bone tissue regeneration rate is essential for the scaffolds applied in bone tissue engineering. Higher resorption rate of the scaffolds compared to new bone formation can decrease the bone healing or fusion (Karageorgiou & Kaplan, 2005). The ability of BCP (composite of HA and β-TCP) in increasing the vascularization, remodelling and ingrowth of bone and having higher bioactivity and osteoconductivity compared to phase-pure CPs have been proved in many in vivo studies (Arinzeh et al., 2005),(Detsch et al., 2011),(Tadic & Epple, 2004). Some recent studies have agreed on an optimized composition of 60HA/40β-TCP with the highest bone forming ability (Tadic & Epple, 2004),(Cho, Chung, & Rhee, 2011).

2.6 Scaffold Fabrication

Scaffolds have been manufactured in several ways, both by means of conventional scaffold fabrication techniques and more advanced methods. Traditional techniques for the fabrication of porous scaffolds like freeze drying, solvent casting, particulate leaching and gas foaming, etc. have shown some disadvantages such as the need for molds and special tools, poor control on the dimension, geometry, distribution and interconnectivity of pores, the use of organic solvents (leading to toxicity risks), lack of repeatability and weak mechanical properties. Furthermore, the scaffold design in classical approaches is basically dependent into the process. These problems can be solved by using a design-dependent method known as rapid prototyping which can be introduced as solid freeform fabrication (SFF) or additive manufacturing (AM) approaches.

Rapid prototyping (RP) is a layer by layer manufacturing process based on computer data such as CAD, CT, and MRI. Due to the ability of complex structures fabrication

with their intricate details, RP technologies is widely applicable in different fields such as engineering, manufacturing, aerospace, automotive, jewellery, coin, tableware, arts, and architecture. For example, in biomedical industry such as surgery planning, customized implants and prostheses, drug delivery devices, and tissue engineering, RP technologies play an increasingly important role. RP methods can apply either directly in which object is processed directly from a biomaterial or indirectly by using RP techniques to make a negative mould which is subsequently filled with castables such as ceramic slurry and then removed from the dried body. Schumacher *et al.* created porous HA, β-TCP, and BCP scaffolds by printing a negative mould with wax and infiltrating it with the ceramic slurry. There are more than 30 different RP technologies which are being applied in the different technologies and around 20 of them have biomedical applications (Popov et al., 2004),(Schumacher, Deisinger, Detsch, & Ziegler, 2010),(Billiet et al., 2012).

Despite some adaptations over the last few years, scaffold design techniques remained process-dependent by means of classical approaches. A more design-dependent method would be attractive, which can be attained by rapid prototyping techniques (Yeong, Chua, Leong, & Chandrasekaran, 2004),(Billiet et al., 2012),(J Russias et al., 2007). Complex three-dimensional (3D) objects can be manufactured by rapid prototyping processes in a layer-by-layer manner according to a model that can be designed by a computer-aided design (CAD) software or Computed Tomography (CT) and Magnetic Resonance Imaging (MRI) data (Bártolo, Almeida, Rezende, Laoui, & Bidanda, 2008). One of the critical applications of rapid prototyping is in biomedical industry such as tissue engineering, drug delivery, surgery devices, prostheses and implants. Using rapid prototyping techniques in tissue engineering can allow the fabrication of scaffolds with an accurate control over the external and internal complex

geometries, high mechanical strength and patient-specific structures (Peltola et al., 2008).

The working principle of some most famous techniques of rapid prototyping will be explained subsequently.

2.7 Stereolithography

SLA which developed by 3D systems in 1986, is considered to be the first commercially available SFF technique. An SLA apparatus consists of four main parts: 1) A liquid photo-curable resin reservoir, 2) A laser source (commonly UV light), 3) Controlling system for XY-movement of the light beam, 4) Vertical plane fabrication platform. 2D patterns of polymer produced by scanning the surface by single photon absorption. After finishing the 2D layer, to build-up a 3D construct, fabrication platform moves in Z-axis. To ensure good adherence of subsequent layers, typically step height of fabrication platform is smaller than curing depth. In most cases, washing-off excess resin and further UV curing are necessary as post-treatment steps (Melchels, Feijen, & Grijpma, 2010),(Arcaute, Mann, & Wicker, 2006).

2.7.1 Fused deposition modelling (FDM)

This technology was developed by Stratasys and is the second most widely used RP technology after stereolithography. In FDM a plastic filament is unwound from a coil, melt inside a heated liquefier, extrude through the nozzle, and finally solidify and adhere to the preceding layer. Extrusion nozzle moves over the table to form each layer of the required geometry. For each layer, the direction of material deposition (i.e., laydown pattern) can be changed to fabricate scaffolds with highly uniform internal honeycomb-like structures, controllable pore morphology, and complete pore interconnectivity (M. Touri, Kabirian, Saadati, Ramakrishna, & Mozafari, 2019).

2.7.2 Selective Laser Sintering (SLS)

SLS uses a CO2 laser to heat entire powder bed to just below the melting point of the material in order to minimize thermal distortion and facilitate fusion to the previous layer. A layer is drawn on the powder bed using the laser to sinter the material. The bed is then lowered and the powder-feed cartridge raised to spread a covering of powder by a counter-rotating roller. The sintered material forms the part and unsintered powder remains in place as a support material which removed once the part is complete (Pham, Dimov, & Lacan, 1999).

2.7.3 Three-Dimensional Printing (3DP)

This technique employs conventional inkjet technology and can be used to fabricate parts in a variety of materials including ceramics, metal, polymer, and metalceramic materials. The workflow can be described in three sequential steps: 1) The powder supply system platform is lifted and the fabrication platform is lowered on the layer; 2) The roller spreads the powder into a thin layer; 3) An inkjet head prints a liquid binder that bonds the adjacent powder particles together. As the complete construct is retrieved, any unbound powder is removed and a complex 3D part remains. While the surface finish is relatively poor and post-processing is required, 3DP can use a broad range of materials and the build time is shorter than other RP processes (Pfister et al., 2004).

2.7.4 Robocasting

Robocasting (direct-write assembly or micro-robotic deposition) deposits a colloidal suspension with high concentration through a nozzle to form rods of ink in a layered and controlled manner for building up a 3D–structure (Figure 2.1) (Miranda, Pajares, Saiz, Tomsia, & Guiberteau, 2008a),(Smay et al., 2002). It utilises water-based ink containing negligible organic content and doesn’t require any sacrificial support

material or mould. The ink has high viscosity and supports its weight throughout the assembling. This is an appropriate choice for the fabrication of tissue engineering scaffolds because of superior mechanical behaviour which enables them for load bearing applications (Hollister, 2005). Green parts have been formed by robocasting technique from structural ceramics like alumina and silicon carbide, bioactive glass and bioceramics like HA and β-TCP. The mechanical properties of this class of scaffolds can be similar to that of cancellous cortical bone by altering the sintering temperature and the size of the pores and rods (Dellinger, Cesarano, & Jamison, 2007).

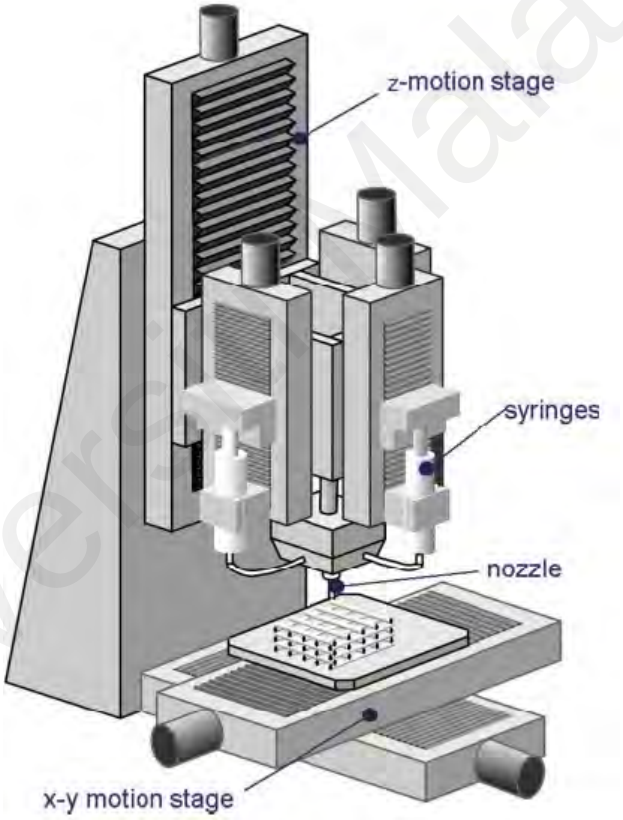

Figure 2.1: Schematic illustrations of robocasting technique (Lewis, Smay, Stuecker, & Cesarano, 2006)

2.8 Oxygen- generating biomaterials

Tissue hypoxia frequently occurs after damages of tissues when the vascularization network is destroyed. These hypoxic conditions could result in dying and necrosis of

leaving cells (Gholipourmalekabadi, Zhao, Harrison, Mozafari, & Seifalian, 2016). Oxygen plays a critical role in multiple cellular functions during the healing process of bone fractures. Oxygen concentration has important effects on some of the healing processes as follows: 1) aerobic metabolism of the cells, 2) activity of many enzymes such as cyclooxygenases involved in bone repair, 3) collagen synthesis, 4) expression of some angiogenic genes, and 5) proliferation and differentiation capacity of stem cells, chondrocytes and osteoblasts (Lu et al., 2013),(Carlier, Geris, van Gastel, Carmeliet, & Van Oosterwyck, 2015). Using of oxygen generating biomaterials is one of the recent developed strategies to increase the oxygen level to the engineered tissues, especially at the early stages after implantation, while neovascularization is being formed. Tissue survival and decreasing of necrosis can be concluded from oxygen releasing biomaterials which provide a sustained release of oxygen to the cells (Pedraza et al., 2012a),(Oh et al., 2009),(Harrison et al., 2007).

Solid inorganic peroxides, such as calcium peroxide, sodium percarbonate and magnesium peroxide are a group of oxygen-releasing biomaterials which can generate oxygen in aqueous liquids. It is known that solid peroxides can react with water and provide oxygen (Eq. 1). Hydrogen peroxide (H_2O_2), intermediate of this reaction, can be cytotoxic to the cells at high concentrations; although, mammalian cells can deal with low concentrations with their several defence mechanisms to convert it into oxygen and water. The rate of oxygen release has a critical importance in tissue formation, and can be controlled by incorporating the peroxide into hydrophilic or hydrophobic polymers for various tissue engineering applications. If solid peroxides are encapsulated in a hydrophobic material, the rate of oxygen release can be slowed down in a sustained manner because of the slow diffusion of water into the hydrophobic materials but in hydrophilic materials, quick water absorption leads faster decomposition and oxygen

generating. Thus, oxygen delivery and cytotoxicity must be in a thoughtful balance (Camci-Unal, Alemdar, Annabi, & Khademhosseini, 2013),(Steg et al., 2015).

$$2CaO_2 + 4H_2O \rightarrow 2Ca(OH)_2 + 2H_2O_2 \rightarrow 2Ca(OH)_2 + 2H_2O + O_2 \quad \text{(Eq. 1)}$$

Hypoxic wound (occurred due to the vascular disturbance) and bacterial infection are some of the significant challenges after the scaffold implantation. Oxygen is essential for cell metabolism, preventing wounds from infection, collagen synthesis, extracellular matrix formation and almost all wound healing processes (Rodriguez et al., 2008),(Gordillo & Sen, 2003). Limited oxygen delivery can lead to cell apoptosis and subsequent chronic bacterial infection. Sufficient oxygen levels can increase cell proliferation, encourage cell differentiation, enhance extracellular matrix (ECM) synthesis and prevent infections (Guo & DiPietro, 2010),(Eisenbud, 2012).

Providing of supplemental oxygen to hypoxic bone remains a critical medical challenge with implications for tissue repair and regeneration as prolonged periods of ischemia can cause tissue necrosis. To prevent ischemia-related tissue death, several strategies like hyperbaric oxygen therapy, hemoglobin- and perfluorocarbon-based oxygen carriers, Lipid-based oxygen carriers, etc have been explored for provision of oxygen to various tissues but each of them has some problems with limited efficiency and slow development. A novel class of oxygen-generating biomaterials represents a viable solution for the direct provision of oxygen to hypoxic area. CPO is a fast-releasing oxygen compound that appears promising for tissue viability applications which readily decomposes into oxygen and water, in the presence of water. Besides its stable oxygen releasing capability, CaO_2 also possesses antibacterial properties (M. Touri et al., 2018b).

Hypoxia at the bone fracture zone can cause cell death, belated chondrocyte and osteoblast differentiation and stalled healing (Lu et al., 2013). Low diffusion of oxygen throughout the scaffolds can hinder their applications. The diffusion of oxygen from capillaries is 100–200 μm in the tissues. To be specific, if the size of a scaffold is larger than 1 mm, simple diffusion of oxygen cannot be sufficient to hold on the viability of cells. Regarding tissue engineering of bone, the maximum penetration deepness of mineralized bone is 200 μm and only can be seen on the surface of the scaffolds (Farris, Rindone, & Grayson, 2016).

Oxygen plays a leading part in healing in addition to being a nutrient and antibiotic. The mechanism of how oxygen increases the bone healing is a novel paradigm which studying about that is still in progress. Hypoxia may influence the Wnt/β-catenin signalling route and can hinder Wnt processing and secretion, which turns β-catenin to unstabilized condition and reduces β-catenin level considerably (Verras, Papandreou, Lim, & Denko, 2008). Wnt signalling part is leading in the development and maintenance of several tissues such as bone. Whereas Wnt proteins can control cell growth, differentiation, function, and death by numerous routes, the Wnt/β-catenin or canonical pathway seems for impressing mainly the bone biology (Westendorf, Kahler, & Schroeder, 2004),(Rawadi & Roman-Roman, 2005). Wnt signalling augments bone formation by several mechanisms comprising regeneration of stem cells, trigger of preosteoblast division, activation of osteoblast production, and hindrance of osteoblast and osteocyte apoptosis (Krishnan, Bryant, & MacDougald, 2006). Lin et al theorised that increasing of oxygen concentration improves the bone formation through the osteogenic differentiation of bone marrow stromal cells (BMSCs), which is adjusted via Wnt3a/β-catenin signalling (Lin et al., 2014). Accruing evidence validates that Wnt/β-

catenin signalling pathway has a major part in bone repair and particularly it impresses the osteoblasts differentiation (Bao et al., 2017).

2.9 Case study

Sulaiman et al. in their study investigated the potential of HA or TCP/HA scaffold seeded with osteogenic induced sheep marrow cells (SMCs) for bone tissue engineering. HA-SMC and TCP/HA-SMC constructs were stimulated in the osteogenic medium for three weeks prior to implantation in nude mice. The HA-SMC and TCP/HA-SMC constructs were implanted subcutaneously on the dorsum of nude mice on each side of the midline. These constructs were harvested after 8 week of implantation. Constructs before and after implantation were examined through histological staining, scanning electron microscope (SEM) and gene expression analysis. The HA-SMC constructs revealed negligible bone formation. TCP/HA-SMC construct displayed bone formation eight weeks after implantation. The bone formation commenced on the surface of the ceramic and continued to the centre of the pores. H&E and Alizarin Red staining showed new bone tissue. Gene expression of collagen type 1 augmented meaningfully for both constructs, but higher for TCP/HA-SMC. SEM results indicated the formation of thick collagen fibers encapsulating TCP/HA-SMC more than HA-SMC. Cells attached to both constructs surface proliferated and secreted collagen fibers. Their findings propose that TCP/HA-SMC constructs with better osteogenic potential compared to HA-SMC constructs can be a potential candidate for the formation of tissue engineered bone (Sulaiman, Keong, Cheng, Saim, & Idrus, 2013).

Mayr et al. studied the degradation behaviour of pure HA, pure β-TCP and four BCP ceramics to investigate the effect of the phase composition to adapt for bone substitute materials. The chemical dissolution of each ceramic composition was examined by its release of calcium ions into a buffered solution. With lessening HA content in the

ceramics, the degradation rate augmented. Cell experiments were done with stimulated osteoclast-like cells. Using biochemical, genetic and microscopic analysis, the differentiation of the cells on the ceramic samples was carried out. The monocytic precursor cells differentiated into osteoclast-like cells on all ceramics. The strongest cell differentiation into osteoclast-like cells was discovered on ceramics with HA/β-TCP ratios of 80/20, 60/40 and 40/60. Cells on these ceramics possessed numerous nuclei and the largest cell size. As a outcome of resorption, lacunas were seen on all ceramics except β-TCP. All these experimental consequences verified the impact of the phase composition on degradation and resorption of calcium phosphate ceramics. Biphasic calcium phosphate ceramics with HA/β-TCP ratios of 80/20 and 60/40 showed the most capable properties to use as synthetic bone substitute materials since the implanted bone substitute materials should have optimized dissolution and resorption properties for integration in the physiological bone remodelling process (Mayr, Schlüfter, Detsch, & Ziegler, 2008).

Hwang et al. assessed the regeneration of three calcium phosphate synthetic block bone grafts in rabbit calvarial noncritical size defects. Four 8-mm-diameter defects were formed in each rabbit. Three defects, HA, β-TCP, and BCP, were implanted with one of three fabricated synthetic block bone graft materials. The fourth defect was occupied with blood clots. Samples were harvested at 4 and 8 weeks post operatively. Histological and histometrical findings showed that in the BCP group (60HA/40 β-TCP), the amount of newly formed bone was boosted more than for the other groups (Hwang et al., 2012).

Zou et al. stated in their research that calcium phosphate ceramics have been broadly used in clinics as bone grafts. Though, according to conventional techniques, it is problematic to produce calcium phosphate bone grafts with tailored internal porous

structures that may guarantee optimal biocompatibility and adequate mechanical properties. In this study, β-TCP bone scaffolds with well-defined inter-connective porous structures were produced by robocasting technique. The sintered β-TCP scaffolds supported the growth of mouse mesenchymal stromal cells (Zou et al., 2016).

Miranda et al. analysed the mechanical behaviour of β-TCP and HA scaffolds fabricated by robocasting technique under compressive stresses. Concentrated colloidal inks made with β-TCP and HA commercial powders were used to manufacture porous scaffolds comprising of a 3-D tetragonal mesh of interpenetrating ceramic rods. The compressive strength and elastic modulus of the scaffolds were measured by uniaxial testing to compare the relative performance of the selected materials. The consequences are compared with those stated in the literature for calcium phosphate scaffolds and human bone. The robocast calcium phosphate scaffolds were discovered to display outstanding mechanical performances in terms of strength, representing a promising potential of this kind of scaffolds for applying in load-bearing bone tissue engineering (Miranda, Pajares, et al., 2008a).

Abarrategi et al. in their study reported that porous ceramic scaffolds are extensively used in the tissue engineering field for their potential in medical applications as bone substitutes or as bone-filling materials. SFF fabrication methods permit production of ceramic scaffolds with fully controlled pore architecture, which opens new viewpoints in bone tissue regeneration materials. Though, slight experimentation has been done about biological properties and likely applications of SFF designed 3D ceramic scaffolds. Therefore, the biological properties of a specific SFF scaffold were assessed, both *in vitro* and *in vivo,* and the scaffolds were implanted in pig maxillary defect, which was a model for a probable application in maxillofacial operation. *In vitro* outcomes demonstrated excellent biocompatibility of the scaffolds, promoting cell

ingrowth. *In vivo* consequences showed that the material conducts adjacent tissue and permit cell ingrowth, as a result of the designed pore size. The data illustrated that SFF scaffolds have the application potentials for bone tissue engineering, with the chief benefit of being fully customizable 3D structures (Abarrategi et al., 2012).

Harrison et al. in this research stated that a restraining factor in regenerating large organs and healing large wounds entirely is the incapability to deliver oxygen to the affected areas for vascularization and healing to happen. An oxygen rich compound of sodium percarbonate was integrated into films of Poly(D,L-lactide–*co*–glycolide) (PLGA) and applied for in situ release of oxygen. Oxygen generation could be detected from the film over a period of 24 h. Once the oxygen-releasing biomaterials were located in contact with hypoxic tissue in a mouse model, reduced tissue necrosis and cellular apoptosis was noticed. This designates that promoted tissue viability could be preserved for numerous days by means of oxygen-producing biomaterials (Harrison et al., 2007).

Li et al. in their study mentioned that stem cell therapy possesses the potential to regenerate heart tissue injured by myocardial infarction (MI), but it experiences tremendously low efficiency. One of the main reasons is the poor cell survival under ischemic condition of the infarcted hearts. They assessed whether an oxygen-releasing system which sustainably provides oxygen to stem cells would enhance cell survival and cardiac differentiation in hypoxic condition imitating that of the infarcted hearts. The oxygen-releasing system comprised of hydrogen peroxide (H_2O_2)-releasing microspheres, catalase and an injectable, thermosensitive hydrogel. The microspheres were founded from PLGA and a complex of H_2O_2 and poly(2-vinlypyrridione) (PVP). The oxygen was produced after the released H_2O_2 was decomposed by catalase. The hydrogel was intended to progress the retaining of microspheres and stem cells in the

beating heart tissue throughout myocardial injection. The oxygen-releasing system was able to sustainably release oxygen for at least two weeks. The release kinetics was reliant on the ratio of H_2O_2/VP. The hydrogel possessed a stiffness similar to the heart tissue and could encourage the cardiosphere-derived cells (CDCs) to differentiate into cardiomyocytes. In hypoxic condition simulating the infarcted hearts (1% O_2), CDCs captured in the hydrogel experienced enormous cell death. Insertion of oxygen-releasing system in the hydrogel considerably increased cell survival; no cell death was detected after seven days of culture, and cells even grew after seven days. In hypoxic condition, cardiac differentiation of CDCs was totally supressed in the hydrogel, as verified at both mRNA and protein levels. Though, introduction of oxygen release reinstated the differentiation. The consequences proved that the developed oxygen-releasing system has promising potential to advance the efficiency of stem cell therapy (Li, Guo, & Guan, 2012).

Wang et al. in their study reported that many next-generation biomaterials will require the capability to not only encourage healthy tissue integration but to concurrently withstand bacterial colonization and subsequent biomaterials-associated infection. Antimicrobial nanofibers of polycaprolactone (PCL) were produced by incorporating calcium peroxide. PCL nanofibers comprising different ratios of calcium peroxide (1%, 5% and 10% (w/w)) were produced by means of an electrospinning technique. Antimicrobial assessments proved the repressive properties of the nanofibers on the growth of *E. coli* and *S. epidemidis* because of the release of calcium peroxide from the nanofibers. Examination of cell response presented that after 4 days of culture, osteoblast viability and morphology were both healthy. The consequences validated that oxygen-generating nanofibers could be designed and developed to afford a short-term peroxide-based antimicrobial answer as still preserving appealing tissue-integration properties (Wang et al., 2010).

Oh et al. mentioned in their research that one of the sustained challenges in engineering clinically applicable tissues is the formation of vascularization upon implantation *in vivo*. While the efficiency of an improved angiogenic answer by means of several growth factors has been revealed in numerous tissue systems, the rate of angiogenesis could not be expedited. They examined whether incorporating oxygen generating biomaterials into tissue engineered constructs would deliver a continued oxygen release over a prolonged period of time. They inspected whether oxygen generating biomaterials can preserve cell viability whilst likewise keeping structural integrity of a 3-D construct. Calcium peroxide-based oxygen generating powder was incorporated into the PLGA scaffolds. The scaffolds were considered to create oxygen over 10 days and concurrently uphold adequate mechanical integrity. Scaffolds comprising oxygen generating materials provided higher levels of oxygen when incubated in hypoxic conditions. Additional, these biomaterials could prolong cell viability growth in hypoxic conditions. The results designate that the usage of oxygen generating biomaterials may permit for augmented cell survivability whilst neovascularization is being formed after implantation. The scaffolds may play a vital role in tissue engineering where presently oxygen diffusion confines the engineering of large tissue implants (Oh et al., 2009).

Holzwart et al. in their study analysed the effect of low oxygen tensions on human multipotent mesenchymal stromal cells (MSC) and assessed proliferation, morphology, and differentiation. After transferring MSC from atmospheric oxygen levels of 21% to 1%, hypoxia-inducible factor (HIF-1α) expression was induced, representing effective oxygen decrease. Instantaneously, MSC showed a considerably different morphology with shorter extensions and broader cell bodies. MSC did not proliferate as fast as under 21% oxygen. Lessened oxygen tension strictly diminished osteogenic differentiation of human MSC. Raise of oxygen from 1% to 3% reinstated osteogenic differentiation.

Physiologic oxygen tension throughout *in vitro* culture of human MSC decelerates cell cycle progression and differentiation (Holzwarth et al., 2010).

Utting et al. investigated the effect of hypoxia on rat osteoblast function in long-term primary cultures. Decrease of pO2 from 20% to 5% and 2% diminished formation of mineralized bone nodules. Once pO2 was lessened more to 0.2%, bone nodule formation was nearly eliminated. The repressive effect of hypoxia on bone formation was partially because of reduced osteoblast proliferation. Hypoxia also abruptly decreased osteoblast alkaline phosphatase activity and expression of mRNAs for ALP and osteocalcin, signifying hindrance of differentiation to the osteogenic phenotype. Transmission electron microscopy demonstrated that collagen fibrils deposited by osteoblasts cultured in 2% O2 were less organized and much less rich than in 20% O2 cultures. The data proved the absolute oxygen necessity of osteoblasts for prosperous bone formation. They lately presented that hypoxia also performs in a mutual way as an influential stimulator of osteoclast formation. Their results could explain the bone loss which happens at the sites of fracture, tumors, inflammation and infection (Utting et al., 2006).

Forget et al. in their recent study stated that current organ transplantation protocols need the quick transference of freshly isolated donor tissue to the receiver patient at the place where the process is to be conducted. Throughout transport, the tissue graft can rapidly worsen due to oxygen deprivation. They reported the fabrication of oxygen-releasing coatings for upgraded tissue preservation. The coatings were organised by the encapsulation of calcium peroxide or urea peroxide microparticles between layers of octadiene plasma polymer films. Via altering the thickness of the plasma polymer coating and type of peroxide, formulations were gained that produce oxygen once exposure with aqueous solutions, as simultaneously restraining the quantity of toxic

reactive oxygen species created. The optimized coatings were examined in hypoxic conditions by means of the MIN6 β-cell line, which caused a sharply rise in the viability of cultured cells. The thin oxygen-releasing coatings can be deposited on an extensive variety of surfaces, generating a platform for oxygen supply with the potential to prolong the viability of transported tissues and elevate the time frame available for graft transportation (Forget et al., 2017).

2.10 Summary

Bone, is made of two different structures; cancellous and cortical bone. Cancellous, or the inner part of bone, is spongy in nature and cortical bone is the dense outer layer of bone. Both types of bone undergo dynamic remodeling, maturation, differentiation, and resorption that are controlled via interactions among osteocyte, osteoblast, and osteoclast cells. Osteoblasts are primarily responsible for new bone formation while osteoclasts are responsible for the resorption of old bone. Such a dynamic process involving osteoclasts and osteoblasts is known as bone remodeling, and is responsible for maintaining a healthy bone. Bone is well known for its self-healing abilities; While bone has limited regenerative capability, some injuries heal poorly due to anatomical location, patient age, or may be simply too large for the body to repair the defect by itself. Any space larger than ~6 mm will not heal naturally, and requires clinical intervention to ensure healing. Bone lesions above a critical size become scarred rather than regenerated, leading to non-union. Massive bone defects are a great challenge to reconstructive surgery. Significant bone loss is the sequela of high-energy trauma, infection, tumour resection, revision surgery and developmental deformities. Today treatment comprises: the use of bone grafts; bone substitutes; stem cells; growth factors; scaffolds and gene therapy.

Autografts (from the patient) is the therapeutically obvious gold standard in reconstructive surgery owing to high immunocompatibility. However, this concept is bound by several constraints (e.g. requirement of secondary surgery, limited amount of tissue that can be harvested, increased risk of infection or recurrent pain). Allograft (from a donor) or xenograft graftings are optional treatments, but each process has its own disadvantages including the possibility of graft rejection by the immune system, risk of infections and transmission of donor pathogens. To overcome these problems, tissue engineering approaches are emerging as convenient alternatives to promote the regenerative ability of the host body. One of the most important stages of bone tissue engineering is the design and processing of a porous, biodegradable three-dimensional structure called a 'scaffold', exhibiting high porosity, high pore interconnectivity and uniform pore distribution. These scaffolds should provide structural support for cells and the new tissue being formed, acting as a temporary extracellular matrix inducing the natural processes of tissue regeneration and development.

Without any three-dimensional supporting structures the cells will form a random two-dimensional mainly monolayer of cells. Thus, the primary function of a scaffold is to serve as an adhesion substrate for the cells. In addition, the scaffold provides temporary mechanical support and guidance to the growing tissue. Several requirements exist that a successful scaffold must meet: 1) the scaffold should have interconnecting pores that enable supply of nutrients and metabolites as well as cell ingrowth; 2) the pore size should be in the range of 5_10 times of the cell diameter; 3) the surface chemistry of the scaffold should favor cellular attachment, differentiation, and proliferation; 4) the scaffold should be made of a material with appropriate rate of degradation in order to allow the surrounding tissue eventually replace the scaffold; and 5) the scaffold should be easily fabricated into various shapes and sizes [8].

Scaffolds have been produced in various ways, both by using conventional scaffold fabrication techniques and more advanced methods. Conventional scaffold fabrication setups include techniques such as particulate leaching, gas foaming, fibre networking, phase separation, melt moulding, emulsion freeze drying, solution casting and combinations of those. There are several limitations involving these processing methods. Conventional methods are incapable of precisely controlling pore size, pore geometry, pore interconnectivity, spatial distribution of pore. Other reported disadvantages involve low and inhomogeneous mechanical strength, and difficulty in manufacturing patient specific implants (control over external geometry is limited). Despite some adaptations, over the years the scaffold design remains process-dependent by means of classical approaches. A more design-dependent method would be attractive, and this can be attained by Rapid Prototyping techniques.

By means of RP, an additive computer-controlled layer-by-layer process generates a scaffold. 3D computer models shape the external design, and such models can either be designed by CAD software or by modelling imaging data (CT, MRI). On the other hand, the internal architecture is determined by the processing of the CAD data into an STT file and subsequent slicing of the STT data (generation of the machine parameters). This directly indicates one of the greatest assets of RP: direct fabrication of scaffolds with a complex, patient specific external geometry in combination with a precise control over the internal architecture (limited by the resolution of the system).

Calcium phosphate ceramics, especially BCP composed of HA and β-TCP, are broadly used as bone-substitute material and in tissue-engineering applications because of being highly biocompatible, similarity to the mineral phase of bone and improving the formation of new bone inside the implanted scaffold.

The fracture of bone brings about the rupture of blood vessels which makes the fracture zone hypoxic. Oxygen lack may cause cell apoptosis, tissue necrosis, late tissue healing and bacterial infection. Adequate levels of oxygen augment extracellular matrix (ECM) synthesis, angiogenesis, cell differentiation, proliferation and migration. Hypoxia at the bone fracture zone can cause cell death, belated chondrocyte and osteoblast differentiation and stalled healing. Providing of supplemental oxygen to hypoxic bone remains a critical medical challenge with implications for tissue repair and regeneration as prolonged periods of ischemia can cause tissue necrosis. To prevent ischemia-related tissue death, several strategies like hyperbaric oxygen therapy, hemoglobin- and perfluorocarbon-based oxygen carriers, Lipid-based oxygen carriers, etc have been explored for provision of oxygen to various tissues but each of them has some problems with limited efficiency and slow development. A novel class of oxygen-generating biomaterials represents a viable solution for the direct provision of oxygen to hypoxic area.

CHAPTER 3: METHODOLOGY

This study was designed primarily to develop an oxygen delivery coating system was on the surface of 3D–printed bone scaffolds for supplying sustained oxygen release in order to tissue survival. It is expected that the oxygen releasing coating system could efficiently increase oxygen level which is essential mostly at the early stages of engraftment for preventing cell death due to hypoxia.

In the present study, an outstanding strategy has been considered regarding the oxygen-releasing scaffold. The BCP scaffolds were first fabricated using a 3D–printing method, robocasing, into desired structures suitable for bone tissue engineering. Then, different concentrations of CPO were employed as the oxygen generating agent encapsulated in a polycaprolactone (PCL) thin film coating on the scaffolds. The hydrophobic PCL was chosen to reduce the decomposition rate of CPO particles in the early stages of implantation. To understand the efficacy of the coated scaffold, the release kinetics of oxygen and biological investigation were studied in vitro. We intend to investigate how our oxygen-releasing scaffolds affect cell viability and proliferation, cell differentiation, apatite formation ability and antibacterial activity. These investigations were done to know whether our oxygen-releasing scaffolds can be an appropriate candidate for bone tissue engineering. We considered how an oxygen-generating coating of bone scaffolds can affect bone fracture healing in vivo. It is expected that this coating can enhance the oxygen level which is critical at the initial steps of implantation to prevent cell necrosis because of hypoxia.

The intention of the current study was to assess whether oxygen-generating coating enhances the osseointegration capability of BCP scaffold aimed for bone defect repair. For achieving this object, several experiments were done which they will be explained subsequently.

3.1 Fabrication of 3D–printed BCP scaffolds

The BCP scaffolds were fabricated using a 3D–printing method from two different starting materials, HA (Sigma-Aldrich, USA) and β-TCP (Sigma-Aldrich, USA). The lattice scaffolds with 15 mm length, 5 mm width and 3 mm thick were 3D–printed using a robocasting technique. The robocasting paste was an aqueous composition comprised of colloidal powders (60 vol% HA and 40 vol% β-TCP). The scaffolds were fabricated by sequentially printing cross-hatched layers of struts approximately 500 μm in width and gaps of approximately 500 μm between the struts. Subsequently, a sintering process was applied in air with the following schedule: 3 °C/min to 400 °C to allow organic decomposition, 5 °C/min to the target temperature (1190 °C), hold at that temperature for 2 h, and cooled down with the rate of 5 °C/min to room temperature.

3.2 PCL/CPO Coating on BCP scaffold

Polycaprolactone (PCL, Mw = 80,000, Sigma-Aldrich) pellets were dissolved in dichloromethane (DCM, Sigma-Aldrich) by stirring at room temperature (PCL/DCM 4% w/v). Various concentrations of CPO (CPO/PCL 1, 3 and 5 w/w) were added into the PCL solution and stirred. The sintered BCP scaffolds were coated by dipping into the coating solution, and the dipping-drying steps were repeated up to three times to get a thicker coating layer.

3.3 Scaffolds' Characterization

The density of the scaffolds ($\rho_{scaffold}$) was determined from the mass and dimensions of the sintered bodies. The theoretical densities of HA (3.16 g/cm^3) and β-TCP (3.14 g/cm^3) (Houmard et al., 2013) were used as references to calculate the total volume fraction of porosity according to Eq. 2 (R. Touri et al., 2013) where ρ_{solid} =3.152 g/cm^3 is the density of 60HA/40β-TCP composite calculated by the rule of mixtures.

$$P=1-(\rho_{scaffold}/\rho_{solid})=1-\rho_{relative} \quad \text{(Eq. 2)}$$

The microstructures of the scaffolds, before and after coatings, were observed using a scanning electron microscope (SEM, VEGA\\TESCAN, USA). In addition, the phase composition of the scaffolds was analyzed using XRD (PW 3710, Philips) and FTIR (Perkin Elmer, spectrum 400, USA) spectroscopy.

3.4 Mechanical Testing and Numerical Modelling

Compressive mechanical tests were performed on uncoated and coated BCP scaffolds of a dimension 15 × 5 × 3 mm (Omegadyne Inc., model LC203-1K) at a crosshead speed of 0.1 mm/min. Four samples were used to replicate this experiment. The stress-strain curve was obtained, and the compressive strength was determined from the maximum load recorded.

FEM can predict the mechanical behaviour of complex structures like multilayer systems (Zhao, Miranda, Lawn, & Hu, 2002) by providing the mechanical properties of included materials in the structure. Finite element simulation is able to compute the stress fields and evaluate the mechanical behaviour of the scaffolds under uniaxial compression. FEM was used to distinguish the fracture modes and estimate the strength of the robocast BCP scaffolds.

The most probable fracture was identified in the site of maximum stresses within the structure assuming a critical stress criterion (von Mises). This tactic has been used in the previous studies and outstanding outcomes have been shown for the compressive fracture modes of HA scaffolds (Miranda, Pajares, Saiz, Tomsia, & Guiberteau, 2007). Finally, the predictions of the modelled scaffold were compared to the experimental data from uniaxial compression tests.

FEM was done by ABAQUS/Standard/Simulia software in order to compare the stress fields in bare and coated scaffolds under compression. The model of scaffold possessed 7 orthogonal layers which were composed of parallel BCP rods. The diameter of the ceramic rods and their centre to centre distance in the printing plane were 500 and 1000 µm, respectively. The vertical space between the layers was around 300 µm because each layer had 100 µm overlapping with its neighbour.

FEM mesh of the scaffold consisted of more than 1,000,000 quadratic tetrahedral elements (C3D10). The sizes of the elements were different in the model. The element dimension was about 50 µm for a great part of the model. However, it decreased to around 4 µm at the overlapping site of the rods (Figure 3.1a). The stresses on the overlapping site of ceramic rods were the most applicable because the failure will initiate there throughout the testing. Mesh refinement can allow us to investigate the overlapping site stresses with more precision. Decreasing of the elements size were done in the high-stress locations according to sub-modelling technique and cannot be stretched to the entire model due to the limitations on the calculation time.

The compression was modelled by an algorithm in which a rectangular parallelepiped scaffold was set between two parallel rigid planes (Figure 3.1b). The rigid bottom plane was assumed to be fixed, although the top plane was allowed to move freely in the normal direction with an applied force (increased up to 1800 N). The contact between the rigid planes and the scaffold was supposed to be frictionless in the FEM. The material behaviour of the scaffold was presumed to be isotropic and elastic. The stress variation with the load was recorded during the simulation.

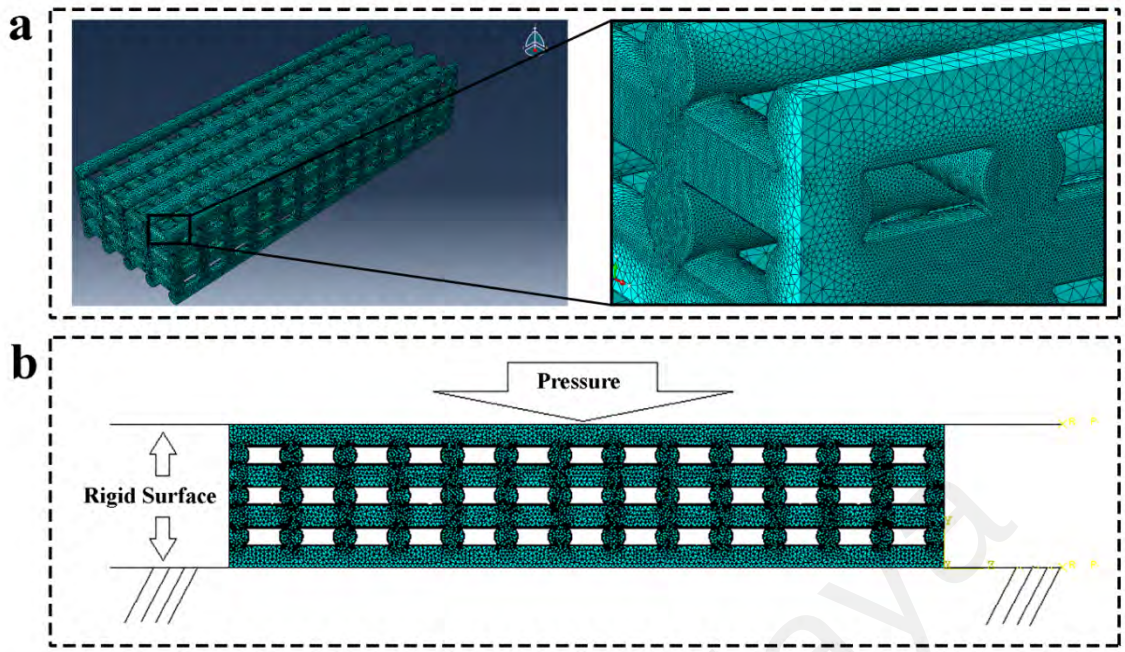

Figure 3.1: FEM mesh of the scaffold. Element C3D10 has been used for meshing the scaffolds. Most elements have the size of 50 µm in the model, excluding the overlapping site of the rods where the dimension is reduced to 4 µm. b) FEM was applied to model the scaffold located between two rigid and parallel planes in the mode of uniaxial compression.

3.5 Oxygen Release Behaviour

A blood gas analyser (OPTI CCA-TS, OPTI Medical, USA) was used to measure the oxygen concentration released from the coated scaffolds. The coated scaffolds with varied percentages of CPO (1, 3 and 5 wt%) were located individually in the 15 ml falcon tubes containing 6 ml serum-free media (Gibco) at the normoxic condition. The control tubes with only media were tested as well. The tubes remained closed to decrease the contamination. Once daily, a little amount of media from each tube was examined and this procedure continued for seven following days to quantify the dissolved oxygen concentration.

3.6 MTT Test

Cell proliferation was determined by 3-(4,5-dimethylthiazol-2-yl)2,5-diphenyltetrazolium bromide (MTT) assay at different time intervals to evaluate the effect of CPO content on supporting cell growth and viability. MG-63 cells were seeded into the uncoated and coated scaffolds with different ratios of CPO (1, 3 and 5 wt%) under a normoxic condition (21% O_2, 5%CO_2) with an initial inoculum of 10,000 cells per sample. MG-63 is a commonly used osteoblastic model to study bone cell viability, adhesion, and proliferation on the surfaces of biomaterials (Wandiyanto et al., 2019). After 1, 3, 7 and 14 days of cell culture, 10 mL MTT solution (5 mg/mL; Sigma Aldrich, USA) was prepared and 100 μL of it (0.5 mg/mL in PBS) was added into each well containing scaffolds and incubated for 4 h at 37 °C. Next, the medium was decanted and 100 mL dimethyl sulfoxide (DMSO, Sigma Aldrich, no. D8418, US) was added and the optical density (OD) values were read on a spectrophotometer at 570 nm wavelength. The yellow tetrazolium salt is metabolized by viable cells to purple crystals of formazan which are solubilized in DMSO (Kargozar et al., 2016). The cultures without the scaffolds or tissue culture plate (TCP) were considered as negative controls.

3.7 Confocal Microscopy

The influence of different concentrations of CPO on cellular responses of the scaffolds was examined using a confocal laser scanning microscope (Eclipse E800; Nikon, Tokyo, Japan). Dialkylcarbocyanine also called “DiI” [1,1′-dioctadecyl-3,3,3′,3′-tetramethyl-indocarbocyanine perchlorate; $DiIC_{18}(3)$] was used to stain the MG-63 cells (with an initial inoculum of 10,000 cells per sample) on the coated and uncoated scaffolds (after 3 days). DiI is a lipophilic and orange-red fluorescent dye which consists of a hydrophilic head and two lipophilic hydrocarbon side chains. DiI can insert into the plasma cell membrane through its hydrophobic chains (C. Cheng, Trzcinski, & Doering, 2014). The scaffolds were stained in 1–2 mg/mL DiI solution. After labeling, the

scaffolds were rinsed with phosphate buffered saline solution (PBS) and then examined by confocal microscope at an excitation wavelength of 549 nm with a 20× lens to investigate the cell proliferation.

3.8 ALP Activity

Cell differentiation was investigated by ALP activity. ALP is an early marker of osteoblasts differentiation and mineralisation (Lee, You, & Kim, 2015). The osteogenic potential of the uncoated and PCL/CPO (1, 3 and 5 wt%) coated BCP scaffolds were assessed by ALP activity assay. In this respect, Saos-2 (Sarcoma osteogenic) cells were incubated on the scaffolds with a culture medium (Gibco, USA) for three different times (1, 7 and 14 days). After each time point, the cell/scaffold constructs were washed with PBS for removing the medium and the cells were lysed by Tris-Triton buffer (20 mM Tris, 1% Triton X100). The cell lysates were incubated with ALP solution (para-Nitrophenylphosphate (pNPP) liquid substrate system, Sigma, USA) at 37 °C for 30 min. ALP activity was determined by measuring the formation of p–nitrophenol (pNP) from pNPP. Then, 1 M NaOH was added to terminate the enzymatic reaction. The supernatant was transferred to the microtiter plate after centrifugation at 16,000g for 10 min and the absorbance was measured at 405 nm (SpectraFluor plus, Tecan). Finally, a standard curve was plotted using pNP amount to determine the ALP activity. The tissue culture plate (TCP), a culture sample exclusive of scaffolds, was studied as the negative control.

3.9 Simulated Body Fluid (SBF) Test

SBF was prepared according to Kokubo technique in which the concentration of the ions was similar to those in human blood plasma (Kokubo & Takadama, 2006). Uncoated and coated scaffolds with various percentages of CPO were soaked in 40 ml of SBF and located in an incubator shaker to mimic the dynamic condition of the body

at 37 °C for 21 days. Three replicates were utilised for each sample and apatite mineralisation on the surface of the scaffolds was analysed by SEM.

3.10 Antibacterial activity

3.10.1 Determination of the minimum inhibitory concentration (MIC) and minimum bactericidal concentration (MBC)

MIC and MBC are significant parameters for quantifying the activity of an antibacterial material against the infecting pathogens. MIC and MBC tests were done to evaluate the antibacterial behaviour of CPO. Staphylococcus aureus (S. aureus, gram-positive) and Pseudomonas aeruginosa (P. aeruginosa, gram-negative) were chosen in this study because they seem to have a significant role in the bacterial infection of wounds (Bjarnsholt et al., 2008). The coated scaffolds had three amounts of CPO (1%, 3%, and 5%, polymer base). The amount of CPO which was added to PCL for coating on 3% CPO-coated scaffold was 0.012 gr. This value was measured by a digital scale to perform the MIC test.

MIC is the minimum concentration of an agent which inhibits the observable growth of an organism (Qi, Xu, Jiang, Hu, & Zou, 2004). The MIC of CPO particles was determined by using the serial dilution method. 13 tubes with 1 ml of liquid Muller Hinton Broth (MHB) medium were required for each bacterium. Test tubes with the numbers 1 and 2 received 1 ml suspension with 12,000 μg ml^{-1} CPO sonicated for 10 min at the frequency of 28 kHz. The CPO concentration in tube 1 and 2 reached 6000 μg ml^{-1} after mixing with the culture media. Subsequently, 1 ml from tube 2 was transferred to tube 3 and blended thoroughly. This process was continued successively up to tube 12. Lastly, 1 ml of tube 12 and 0.9 ml of tube 1 were disposed for achieving the same quantity of the tubes. Tubes 2–13 received 0.1 ml of standard microbial suspension (S. aureus and P. aeruginosa) comprising 1.5 $\times 10^8$ CFU/ml microorganism

and then were placed in an incubator at 35 °C for 24 h. Afterwards, the microbial growth was investigated through a visual check. There were two control samples in this experiment: positive (tube 1 holding CPO and MHB medium, lacking inoculum) and negative (tube 13 having inoculum and MHB medium, lacking CPO). The negative control presented the microbial growth without CPO. The test tubes numbered 2–13 for each bacterium located in a 24-well plate. All the trials were performed three times.

MBC is the minimum concentration of an antibacterial agent which kills 99.9% of bacteria (Qi et al., 2004). For measuring the MBC, a loopful of the MIC samples without apparent growth were taken, sub-cultured on Muller Hinton Agar (MHA) plates and incubated at 35 °C for 24 h. The sample without colonies on the MHA was determined as the CPO concentration with the bactericidal result.

3.10.2 Disk diffusion test

Escherichia coli (E. coli, gram-negative) organism can cause numerous infections related to devices (Wang et al., 2010). S. aureus is the main origin of major bone and joint infections in all ages except neonates (Mal, Berendt, & Peacock, 2002). In this study, E. coli and S. aureus bacterial strains were chosen for investigation of the antimicrobial behaviour of CPO-coated scaffolds because the fabricated scaffold has a bone tissue engineering application. The Kirby-Bauer technique is a useful test which can investigate the prior antimicrobial activity of certain agents. The antibacterial agent spread around the experimental sample towards the agar. The concentration of the antibacterial agent will be superior besides the test specimen, but it will be decreased gradually by the increase of distance from the specimen. “Inhibition zone” is a region in which the concentration of antibacterial material is larger than the effective one and in this area, no bacteria can grow. Hence, a stronger antibacterial property will make a

bigger clear area around the test sample (Ghafari-Nazari et al., 2012),(Rajendran, Barik, Natarajan, Kiran, & Pattanayak, 2014),(Zhou et al., 2015).

The antibacterial activity of CPO-coated BCP scaffolds against E.coli and S. aureus were assessed by the Kirby-Bauer process, while the uncoated BCP scaffold was represented as a control specimen. E. coli and S. aureus suspension covered the agar plates. Afterwards, uncoated and coated scaffolds (with three distinctive percentages of CPO) were located on the plates and incubated at 37 °C for 24 h. Lastly, the inhibition zone of the samples was investigated.

3.11 In Vivo Test

3.11.1 Surgical Procedure

This animal study was conducted in accordance with the guidelines of national institute of health for the care and use of laboratory animals (Council, 2010). Local ethics committee for animal experiments at faculty of veterinary medicine, University of Tehran approved the design of the experiments. A segmental radial bone defect model was implemented in rabbits adapted from Kasten et al. as described previously (Kasten et al., 2008). The local ethics committee for animal experiments approved the design of the experiment. Two types of scaffolds were tested, including bare and uncoated BCP scaffold (BCPS) and CPO coated BCP scaffold (CPO/BCPS). Thirty-six adult male New Zealand white rabbits (3–3.5 kg) rabbits were randomly divided into three groups in two time points (3 and 6 months): (1) BCPS (n = 12); (2) CPO/BCPS (n = 12); (3) empty defect (control, n = 12). Three samples for histology and three samples for biomechanical tests were harvested and analyzed per time point in each group. The surgical instruments were sterilized via autoclave before the surgery. Anesthesia was induced by an intramuscular injection of ketamine (35 mg/kg) and xylazine (5 mg/kg) and maintained through endotracheal intubation using isoflurane 2-2.5%. The surgical

procedures were performed using aseptic technique. Briefly, after clipping of forearm and disinfection, the animal was positioned in the dorsal recumbency, and a craniomedial incision of 3 cm was performed in the midsection of left radial diaphysis. For exposing the bone, soft tissues were dissected and retracted. A 15-mm long segmental defect was made by an orthopedic saw in midshaft radius (Figure 3.2a) and the defect was irrigated with 0.9% sterile saline solution. Figure 3.2b illustrates the removed segment of radius besides the scaffold. The ulna was left intact. BCPS and CPO/BCPS were press fitted in the bone defects of rabbits (Figure 3.2c) and nothing were inserted in the empty control group. The muscles and skin were sutured in layers. The rabbits were caged and water and food were supplied ad libitum. To manage the pain and avoid infection, animals were injected tramadol (5mg/Kg), Ketoprofen (3mg/kg) and enrofluxacin (15mg/Kg) perioperatively and also for 3 days' post-operatively. At 3 and 6 months after operation, the rabbits were euthanized as follows. Initially, anaesthesia was induced with intramuscular injection of ketamine and xylazine. Then, venous access was obtained via the ear and Thiopental Sodium (100 mg/kg) was injected intravenously.

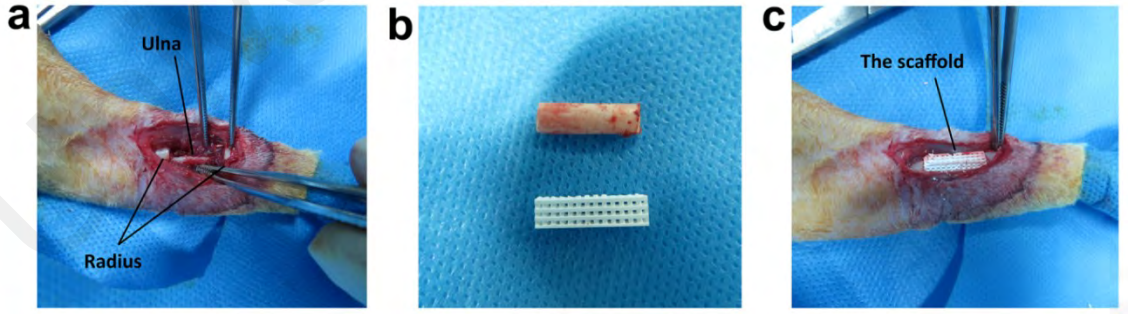

Figure 3.2: Rabbit radial segmental bone defect and 3D-printed scaffold implantation. (a) A 15-mm radial segmental defect was created in the midshaft of rabbit radius, (b) 15-mm removed segment of radius besides the robocast scaffold, (c) The scaffold was implanted into the defect.

3.11.2 Radiological Assessment

To evaluate the repair process, the rabbits were examined by X-ray machine (Toshiba, Tokyo, Japan) at 3 and 6 months' post-surgery or post-operatively.

3.11.3 Histological Evaluation of New Bone

The specimens experienced the following procedures respectively: fixing in 10% buffered formaldehyde, decalcifying in 10% EDTA, dehydrating by an ethanol series, clearing with xylene, and embedding into paraffin. Samples' sections were made via a microtome. Serial sections were stained through some approaches for microscopic evaluations, as follows.

3.11.3.1 Hematoxylin and Eosin and Masson's Trichrome Staining

Sections were stained by hematoxylin and eosin (H&E) and Masson's trichrome and inspected via a light microscope for the new bone histology. The area fraction of new bone in the bone defects were calculated by means of Image J software. Three serial sections were used for each sample to take the average for statistical analysis.

3.11.3.2 Immunohistochemistry

For supplying a comprehensive investigation of bone regeneration process, expression of two protein markers comprising osteonectin and osteocalcin were identified by means of immunohistochemistry staining. Accordingly, decalcified sections with paraffin were mounted on silane coated slides, dewaxed by downward concentrations of alcohol and rehydrated. The slides were dipped into 3% hydrogen peroxide for blocking endogenous peroxidases and rinsed in running tap water for 10 minutes. Then, they were dipped in Tris solution. For antigen retrieval, they were placed in 10 mM citrate buffer, incubated at 120°C for 10 min and cooled. Blocking buffer (10% fetal bovine serum) was added onto the sections of the slides. 100 µl primary antibody was added to the slides and they were incubated for a day at 4 °C followed by

washing with citrate buffer. 100 µl secondary antibody was poured on the slides and they were incubated at room temperature for 1 h after washing with citrate buffer and running tap water, dehydration the tissue slides through alcohol, clearing in xylene and mounting. The slides were then examined microscopically.

3.11.4 Biomechanical Evaluation

Immediately following sacrifice in two time points (3 and 6 months), three removed radius and ulna per group were enclosed in hydrated gauze and conserved frozen for mechanical testing. As mentioned, there were three groups: (1) BCPS; (2) CPO/BCPS; (3) blank. Meantime, three normal samples were harvested arbitrarily from the right forearms of experimental rabbits in order to compare the biomechanical properties of the groups with an intact normal bone. Before testing, the soft tissues surrounding the samples were removed, and then each sample was fixed on the mechanical testing device (Universal Testing Machine, SANTAM Company, Tehran, Iran) with a span of 30 mm. A three-point bending test was carried out with 1 mm/min displacement rate till the fracture of radius. Maximum force (F_{max}) was set down at the fracture point of the sample and mean magnitudes of F_{max} were likened amongst the groups.

3.11.5 Statistical analysis

The numerical data are represented as average ± standard deviations. Significant variances were analyzed by Graph-Pad Prism version 8. Statistical significance was considered at $P < 0.01$.

CHAPTER 4: RESULTS

4.1 Scaffolds' Characterization

4.1.1 Morphological Observations

The 3D–printed scaffolds exhibited porosity of ~70%, as determined by measurement of their mass and dimensions, after applying Eq. (2). The optical micrograph (b) and SEM-taken macrostructures of the sintered and uncoated scaffolds (a,c) are demonstrated in Figure 4.1. The robocast scaffold was porous with high interconnectivity. The size of the open macropores was 500 μm in the printing plane and 300 μm in the vertical direction. The dimension and volume fraction of the scaffold's pores have a significant effect on the bone formation both in vitro and in vivo. The size of the pores has a critical range in any scaffold and can fluctuate with the type of cell or engineered tissue. The pore sizes larger than 300 μm are capable of promoting new bone and capillary generation in bone tissue engineering (O'brien, 2011),(Murphy, Haugh, & O'brien, 2010). These micrographs demonstrated the excellent capability of the robocasting technique in the production of periodical scaffolds with an accurate controlled and interconnected macro-porosity. This macro-porosity should also provide transport pathways for nutrients, oxygen, and wastes necessary to maintain living cells within the scaffolds. It is known that there are some important requirements for the scaffolds in tissue conduction processes, including the scaffolds' geometry and pore dimensions that promote cell seeding, proliferation, vascularization and bone formation inside the scaffolds (Karageorgiou & Kaplan, 2005).

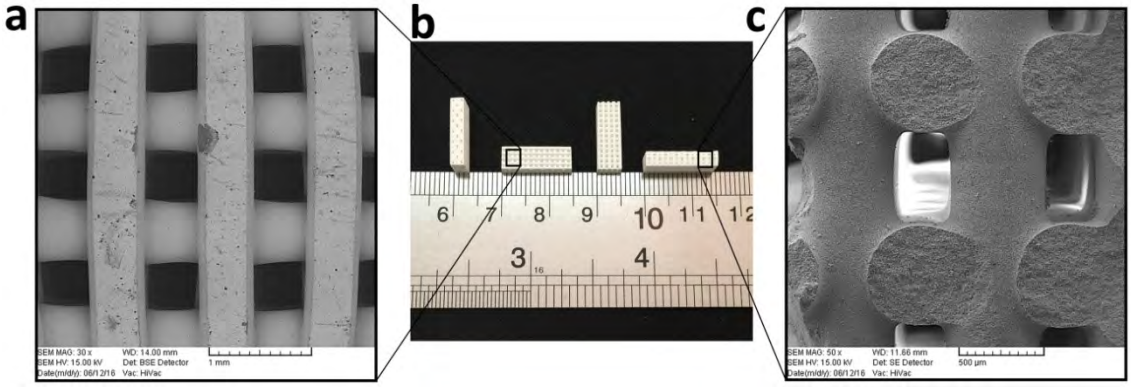

Figure 4.1: Visualisation of the sintered robocast BCP scaffolds. Optical (b) and SEM view from the top (a) and cross-section (c) of the ceramic scaffold.

The typical morphologies of the surface of the rods in the 3D–printed scaffolds before and after applying the PCL-CPO hybrid coatings are shown in Figure 4.2. The 60HA/40β-TCP composite surfaces exhibited separated particles among micro-pores (Figure 4.2a) that the presence of micro-porosity in BCP rods, could be a key factor to explain enhanced bone ingrowth performance of such materials. After coating (Figure 4.2b), the scaffolds were covered partially with PCL-CPO thin layers. At a higher magnification (Figure 4.2c), the coating layer was observed to cover the surfaces and some CPO powders were finely dispersed in the form of particles (indicated by arrows).

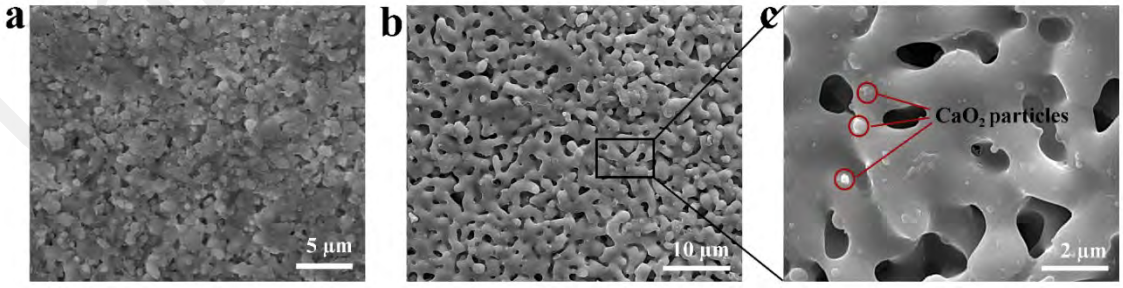

Figure 4.2: SEM micrographs showing the morphology of the rod surface of BCP scaffolds. (a) without and (b-c) with PCL-CPO hybrid coating. Arrows (c) indicate CPO powders were finely dispersed in the form of particles.

4.1.2 Phase Composition and Chemical Structure

The crystalline phases in the uncoated and coated scaffolds were detected by XRD (see Fig. 4). By using X'Pert HighScore software, XRD analysis of the samples revealed crystalline HA, β-TCP and CPO phases with main sharp peaks identified by PDF reference patterns 00-0090432, 01-070-2065 and 01-085-0514, respectively. The sharp characteristic peaks of BCP have been in accordance with the peaks of the standard spectrum of reference patterns of HA and β-TCP. The prominent peaks in PCL-CPO coated BCP scaffolds apart from the CPO and BCP peaks at around 2Θ of 21° and 23° could be attributed to PCL (Gautam, Chou, Dinda, Potdar, & Mishra, 2014). Also, it can be noted that the peak at around 2Θ of 25° was attributed to calcium peroxide. The BCP spectrum not only showed the presence of HA and β-TCP phases, but the presence of a-TCP phase was also detectable (L. Xie et al., 2016). This example indicated that α-TCP crystals could be generated in 60HA/40β-TCP scaffolds during the sintering treatment at 1190 °C.

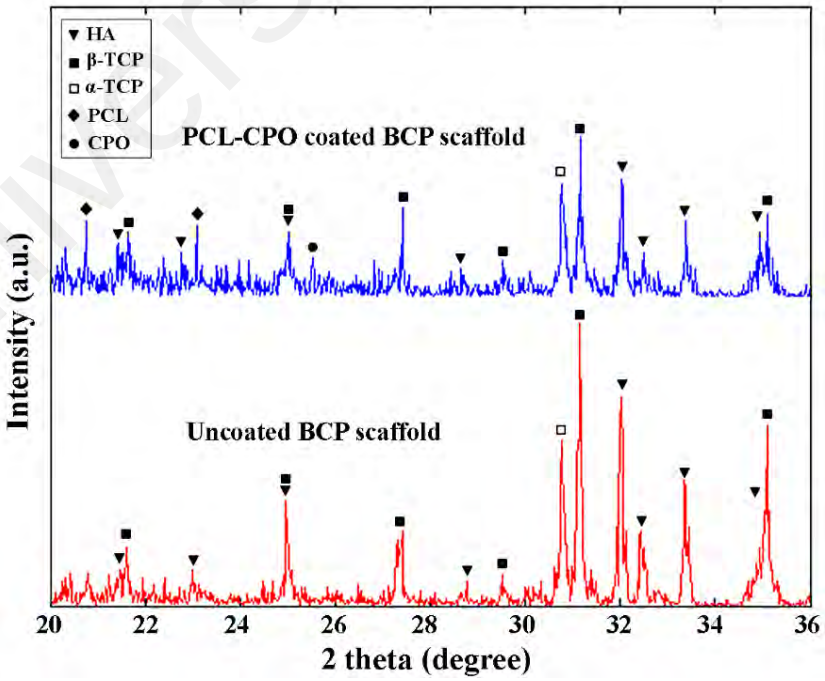

Figure 4.3: XRD patterns of the uncoated BCP and PCL-CPO coated BCP scaffolds.

Figure 5.3 shows the FTIR spectra of the uncoated and coated (with different concentration of CPO in the PCL coating layer) BCP scaffolds. For the BCP powder, resonances associated with the stretching mode of PO_4 group, were observed at 570, 603 and 1041 cm^{-1}. Also the absorption at 3570 cm^{-1} was assigned to OH group. The spectrum of PCL/CPO coated BCP scaffold was characterized by absorption bands arising from BCP, PCL and CPO. The PCL/CPO coated BCP scaffold represented typical structural bands of pure PCL (C=O, C-O, and C-H), HA (P-O and O-H), β-TCP (P-O) and CPO (O-O). As the results showed, PO_4 groups in PCL/CPO coated scaffolds were more intense than BCP powder. Absorption bands at 561–609 cm^{-1} groups of BCP. Bands at 1240, 1727, 2865 and 2949 cm^{-1} associated with the PO_4 in PCL/CPO coated BCP scaffolds spectra associated with the formation of C-O-C asymmetric stretching, carbonyl stretching, symmetric CH_2 stretching and asymmetric CH_2 stretching due to the presence of PCL ligands. The peak positions centered at 1334 and 1420 cm^{-1} may arise from the O-O bands corresponding to the peroxide (O_2^{2-}) ions of CaO_2 particles (Baghbani et al., 2012),(Elzein, Nasser-Eddine, Delaite, Bistac, & Dumas, 2004),(T.-W. Kim et al., 2012),(S. Cheng et al., 2009).

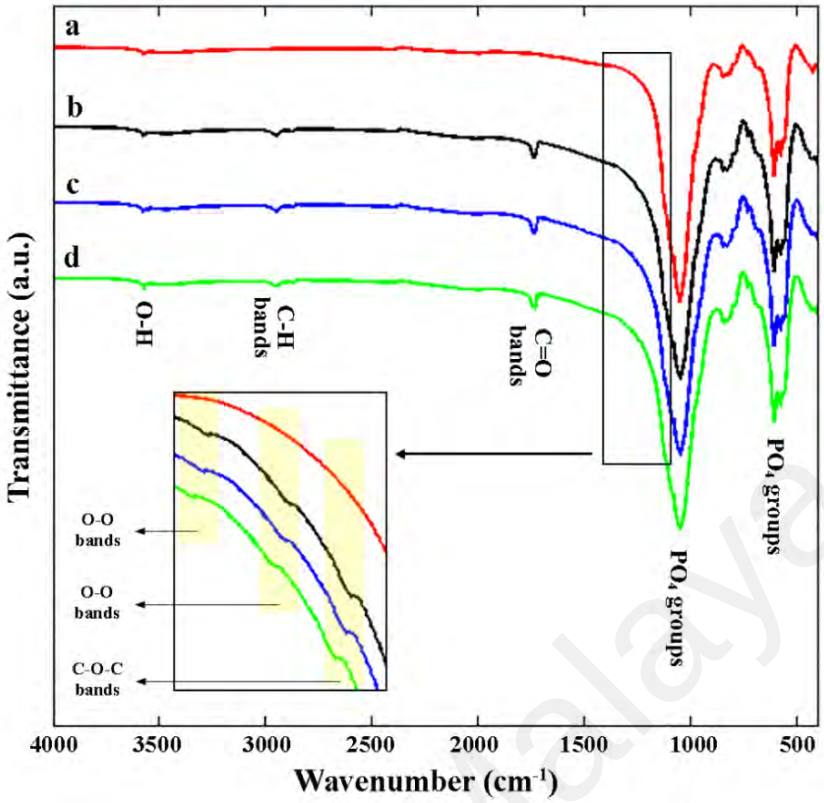

Figure 4.4: FTIR spectra of the uncoated BCP and PCL-CPO coated BCP scaffolds containing 1, 3 and 5% CPO in the PCL coating layer (a-d), respectively.

4.2 Mechanical testing and numerical modelling analysis (FEM analysis of scaffolds)

The results of compressive strength test proved that the scaffolds were well designed for the purpose of implanting in the radius of rabbit. Appropriate bone repair needs load bearing throughout the healing time and the scaffold must behave like the healthy bone under the load. In other words, the elastic modulus of scaffold must be alike to that of bone and If the difference be high, the repairing process will be lengthened (Dellinger, Wojtowicz, & Jamison, 2006). The compressive mechanical properties of the robocast scaffold (E=8.4 MPa, σ=21 MPa (M. Touri et al., 2018b)) were so similar to the radius of rabbit (E=11 MPa (Franklyn & Field, 2013), σ=20.5 MPa (Sharifi, Khoushkerdar, Abedi, Asghari, & Hesaraki, 2012),(Özkadif, Eken, Beşoluk, & Dayan, 2015)).

Figure 4.9 shows the stress–strain behaviour of the uncoated and coated scaffolds, responding to an applied load. A compressive load was applied to each sample at a constant speed until a failure occurred. The scaffolds exhibited a typical brittle stress–strain curve, an initial elastic linear region, a maximum stress, and a stress drop followed by an ultimate failure. This stress–strain behaviour is also observed in ceramic foams (H. W. Kim, Knowles, & Kim, 2004). As compared to the uncoated scaffolds, the maximum stress of the coated scaffolds was slightly higher and the stress region dropped, while the elastic modulus was roughly same.

The ABAQUS FEM software has been used for stress analysing and estimating the maximum compressive strength of the scaffolds. The loads will be mainly compressive in a wide range of the bone implants applications (Miranda, Pajares, & Guiberteau, 2008). Thus, the computations were accomplished in the compression mode. The stress and displacement fields are denoted by σ and u, respectively.

The mechanical properties of the BCP rods (Elastic modulus (E) = 64.4 GPa, Fracture strength (σ_F) = 51.6 MPa, Poisson's ratio (ν) = 0.28) were used as input parameters for the simulation and they were determined from the rule of mixture equation using the inherent mechanical properties of HA rods (E = 82 GPa, σ_F = 68 MPa, ν = 0.28) and β-TCP rods (E = 38 GPa, σ_F = 27 MPa, ν = 0.28) (Martínez-Vázquez, Perera, Miranda, Pajares, & Guiberteau, 2010),(Miranda, Pajares, Saiz, Tomsia, & Guiberteau, 2008b). The radius of fillets between the rods plays a major role in stress concentration and it is around 100 µm.

Figure 4.5 represents the displacement contour for the scaffold which was compressed between two parallel rigid planes. The displacement contour shows that the scaffold movement is proportional to the distance from the fixed bottom. The part close to the top plane is displaced by 0.008 mm from its first location.

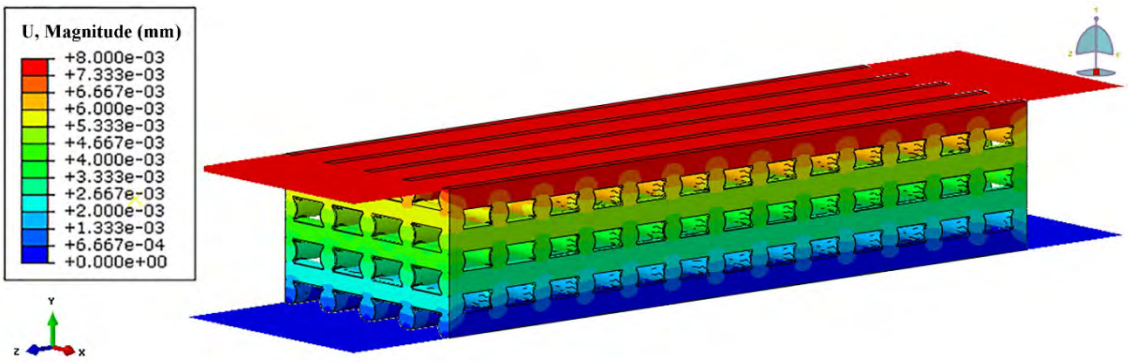

Figure 4.5: Displacement distribution for the modelled scaffold.

Figure 4.6 demonstrates the contour of von Mises stresses at the critical load of 1800 N which causes a fracture in the uniaxial compression experiment. During the normal compression to the top plane, σ reached its highest level in where the rods of neighbouring layers have been joined together.

The result of the simulation also shows that the maximum stresses are located at the edges of the scaffold. This happens because of two reasons: 1. Bending of the top layer makes a sag in the middle of the scaffold and reduces the pressure on the middle section; 2. Lateral rods carry the load in only one side, and therefore an extra bending stress is added to this section. It is expected that the location of maximum stresses shall be on the interface zone of the rods because this zone is subjected to stress concentration and the radius of the fillet between the rods controls the stress.

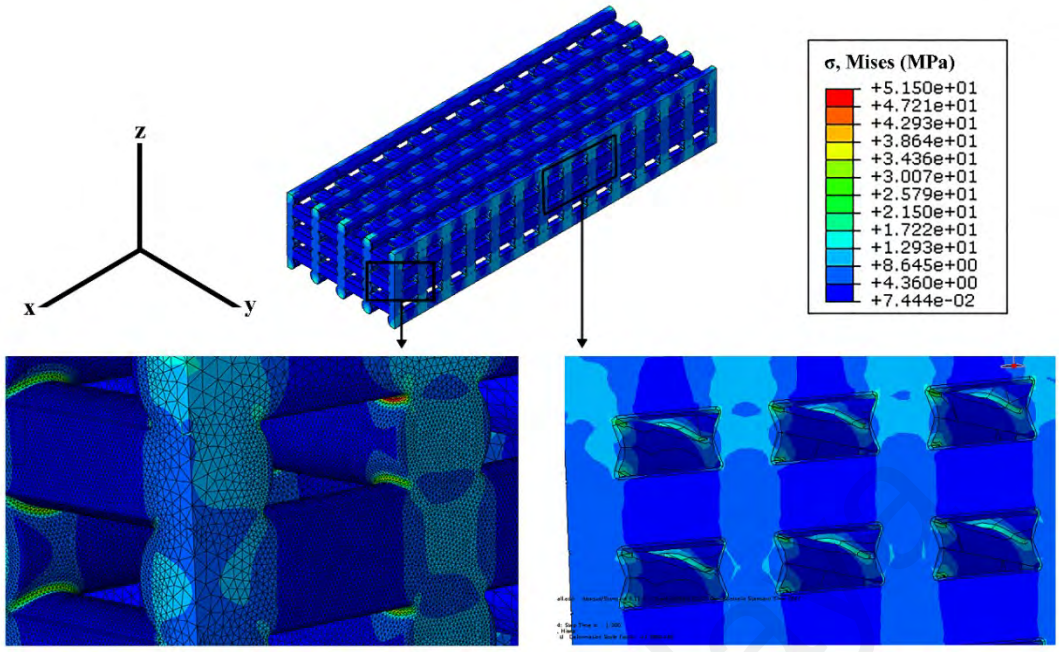

Figure 4.6: The contour of stress shows the stresses established in the scaffold after applying a compression load of 1800 N. Maximum stresses are located in the sides of the scaffolds and stress concentration is in the interface of the rods.

If the corner fillet radius would be zero, then the stress would be infinite theoretically and the result would be changed by mesh size, but if a fillet is considered between the rods, then the stress will be converged by decreasing the mesh size (Figure 4.7). The graph shows a falling trend with the decrease of mesh size and it reaches a plateau mode after 50 µm of mesh size. The amount of maximum stress/applied pressure ratio is equal to 2.1 in the mesh size of 50 µm which is the size of most meshes in the stimulated scaffold.

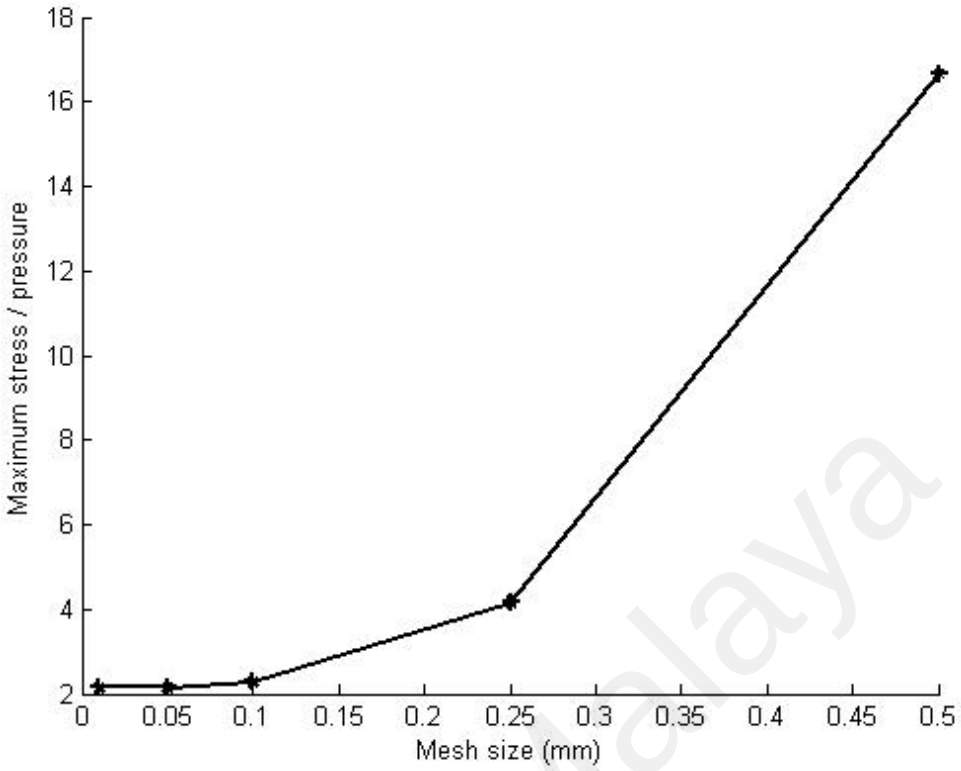

Figure 4.7: Maximum stress/applied pressure per mesh size for the simulated robocast scaffold.

The reduction of mesh size increases the number of elements and the duration of the simulation. Sub-modelling FEM technique is used to increase the accuracy and decrease the simulation time. In this technique, the elements around the stress concentration point are selected and exported in a separate file. The displacement boundary conditions of the submodel elements are applied from the whole model displacement. Figure 4.8 demonstrates the result of submodel stress concentration. It was concluded that the stress was changed gradually from the maximum location, so the stress change per element remained a low value which indicates the high quality of the results. In addition, the simulation time was lowered to 1/100 of the whole model simulation.

Figure 4.8 also shows the contour of stress computed by FEM (at 1800 N load) which presents the maximum stress in every point of the BCP rods. The region near the joints (demonstrated with dot) will be responsible for the crack initiation. The cracks

will be commenced adjacent to the joints and spread in the perpendicular orientation of the rods. The stresses on the centre of the rod (specified via x) will cause no noticeable fracture because they have smaller magnitude and the compressive stresses located in layer-to-layer contact regions would hamper the propagation of such cracks.

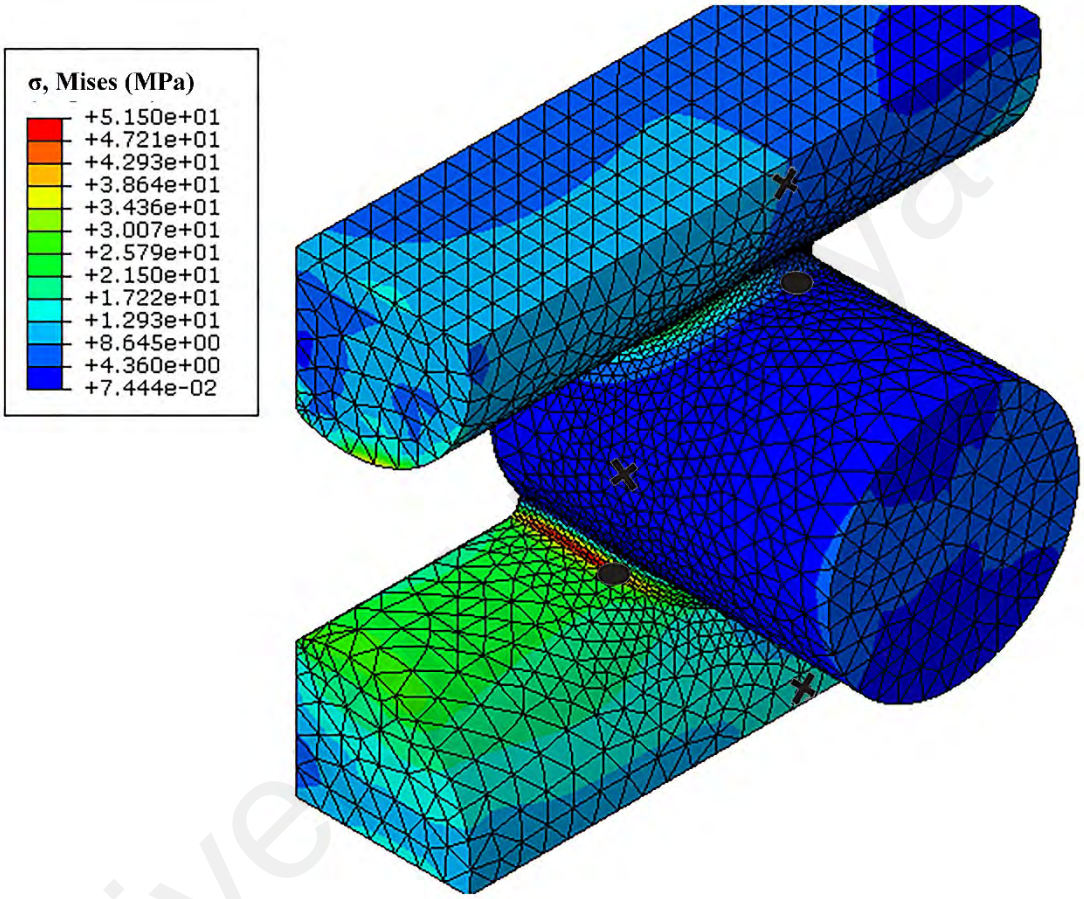

Figure 4.8: Submodel stress concentration. The contour of stress demonstrates the maximum stresses formed during uniaxial compression (1800 N) of the robocast BCP scaffold. The region demonstrated with dot represents the highest stresses responsible for the crack initiation and the region specified by x causes no noticeable fracture.

Figure 4.9 compares the compressive strengths of the scaffold obtained from FEM and the experimental test. The compressive strengths predicted by FEM seem to agree with the experimental one and the difference is less than 10%. The maximum compressive strength of the scaffold obtained from FEM and the experiment was around

24.5 and 21 MPa, respectively. This slight difference proves the capability of FEM to predict the fracture behaviour of robocast scaffolds. Figure 4.9 also demonstrates stress-displacement plots created by FEM and the experimental compression tests of the uncoated and coated scaffolds. It can be concluded from the experimental test results that the compressive strength of the BCP scaffolds was increased from around 21 to 23 MPa after PCL coating. The finite element analysis (FEA) data was approximately matching for bare BCP and PCL-coated scaffolds with just 2% difference because the thickness of the coating is negligible compared to the diameter of the rod.

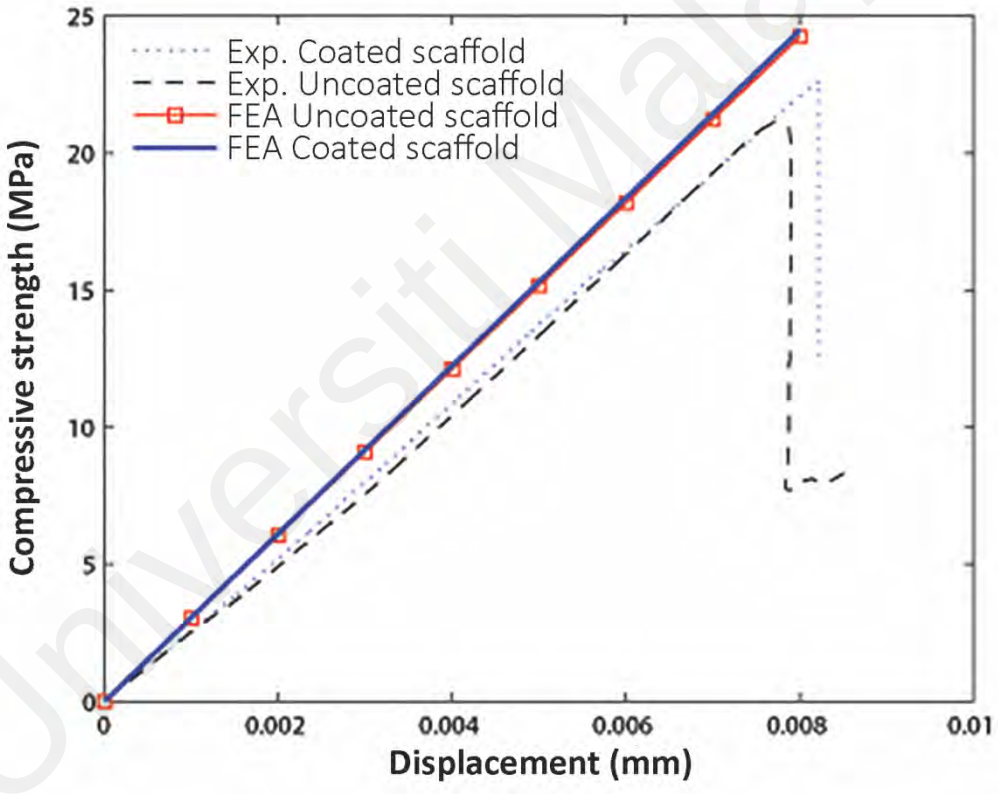

Figure 4.9: The comparison of compressive strength generated by FEM and actual experiment for the bare and PCL-coated BCP scaffolds.

Several researchers have used FEM to calculate the stress fields and predict the mechanical behaviour of robocast HA or β-TCP scaffolds. They have reported that the

compressive strengths predicted by FEM simulation were positively proved by comparing with experimental data obtained from the uniaxial compression test. This can justify that the selected methodology is potent for the optimisation. Among several fabricating systems, the robocasting has the capacity to produce porous calcium phosphate scaffolds with controlled architecture and the mechanical response of the scaffolds fabricated by this technique can be simulated via FEM. The results of these analysis supply valuable insight into the mechanical behaviour of robocast scaffolds for bone tissue engineering applications (Martínez-Vázquez et al., 2010),(Miranda, Pajares, & Guiberteau, 2008),(Miranda et al., 2007),(Martínez-Vázquez, Miranda, Guiberteau, & Pajares, 2013),(Entezari, Zhang, Chen, & Li, 2014).

Computer-aided manufacturing techniques (like robocasting) are perfect for designing and producing porous scaffolds and can optimise the biological and mechanical properties of the scaffolds to an unachievable extent with other methods. Improving the mechanical responses of the scaffolds has a high priority because the weak mechanical properties can hinder their widespread application for repairing the defects in the load-bearing bones. To carry out this optimisation, a predictive tool will be needed as a design aid for the ideal scaffold architecture. FEM Predictions can determine how the mechanical behaviour of the structure will be changed by varying geometrical parameters (rod width, distance, interpenetration, relative angles, etc.). FEM is a potent tool to predict the mechanical response of the scaffolds created with robocasting or other solid freeform fabrication procedures. Improving the scaffolds' mechanical behaviour via a smart design is essential for their application in load-bearing bone tissue engineering.

4.3 Oxygen Release Performance

CPO releases oxygen upon exposure to water. Forming of hydrogen peroxide and its decomposing into oxygen happen in the first and second step, respectively. The CPO powders with three doses were captured in the PCL coating on the BCP scaffolds, and their oxygen releasing performance were evaluated. Figure 4.10 demonstrates the daily oxygen concentration in the control sample (just media) and solutions having PCL/CPO coated BCP scaffolds at normoxia. The oxygen concentration was declined slowly in the control sample and confirmed that the control was not able to generate oxygen. A significant increase in the oxygen concentration with slight fluctuation could be observed in the solutions with the CPO-coated scaffolds.

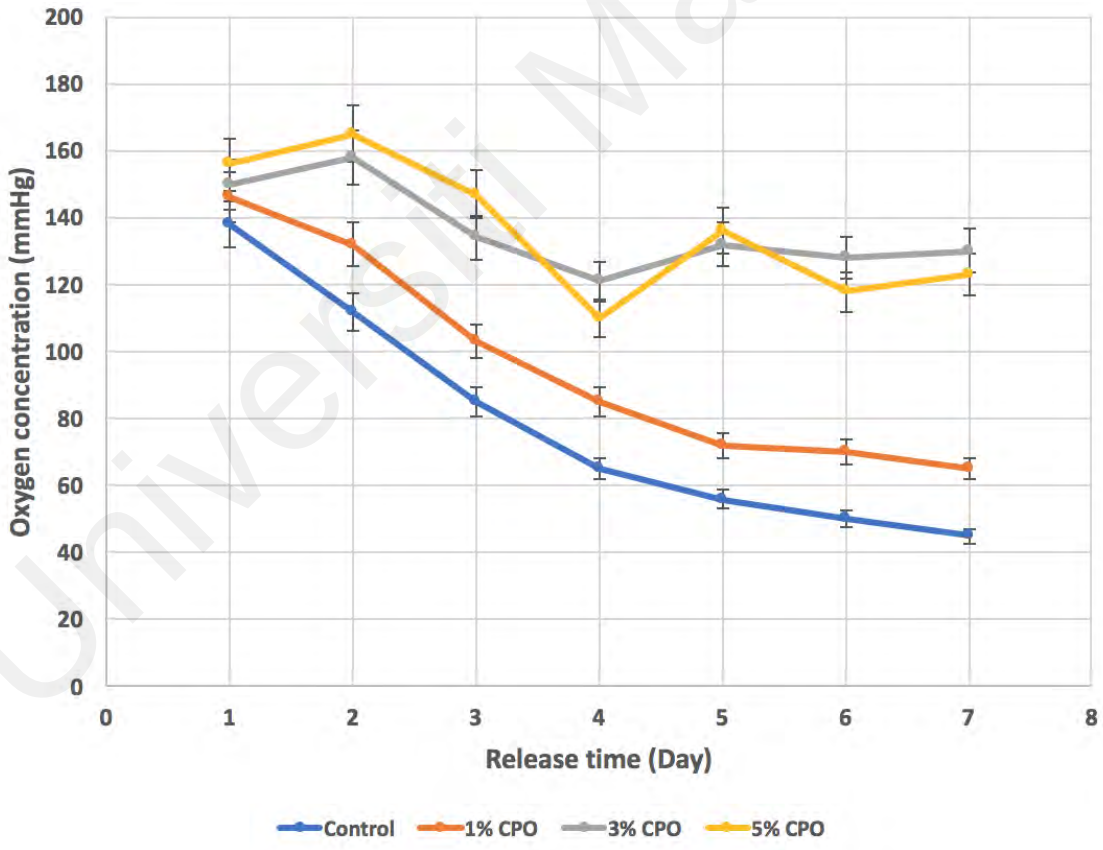

Figure 4.10: The oxygen-releasing behaviour of CPO coated scaffolds under the normoxic condition.

Small bubbles of oxygen formed on the scaffolds after a while when the CPO-coated scaffolds were located in the media. The results presented a noticeable increase in oxygen level during seven days. Throughout the experiment, the pH of the solutions was in the range of 7.1–7.6.

The release profile varied according to the CPO amount and none of the CPO-coated scaffolds showed any burst release. 5% CPO-coated scaffolds demonstrated the highest release within days 1 to 3. However, the scaffolds coated with 3% CPO possessed a supreme level of oxygen in the final days. Scaffolds having 1% CPO in their coating showed the lowest profile for producing oxygen through the whole release days.

In this study, we encapsulated CPO (as an oxygen-releasing biomaterial) within the PCL coating layer on the BCP scaffolds for function in hypoxic conditions. Without encapsulation, peroxide-based compounds release oxygen rapidly as soon as exposure to water. This leads to a burst release of oxygen which is acute and temporary for using (Northup & Cassidy, 2008).A diffusional barrier is created by encapsulating the solid peroxide within a hydrophobic biomaterial. This will decrease the reactivity of the solid peroxide, and therefore will regulate the oxygen release for several days. The reactivity of the encapsulated CPO is significantly modulated by its loading and the rate of water diffusion into the PCL layer. In situ oxygen generation is moreover reliant on the surrounding oxygen conditions. Several studies confirmed that using of CPO in tissue engineered constructs would supply a sustained oxygen release over an extended period (Oh et al., 2009),(Pedraza, Coronel, Fraker, Ricordi, & Stabler, 2012b).

4.4 MTT Test

The results of cell-viability study are presented in Fig. 7. The cell number on the scaffolds was evaluated over time. MTT assay results revealed that the scaffolds had no cytotoxic effect on the osteoblasts after 3, 5 and 7 days of incubation. The cell proliferation rate improved along with increasing the incubation time, which demonstrates the inducting effect of the scaffolds on the metabolic activity of the osteoblasts (Kargozar et al., 2017). The oxygen generating scaffolds with 1% CPO showed approximately equivalent activity compared to BCP only scaffolds. The best result was related to 3% CPO-coated scaffolds, which promoted osteoblast proliferation and along with increasing the incubation time, better cell proliferation rate was also visible compared with the other groups. The cell viability as well as the cell proliferation of 3% CPO-coated BCP scaffolds was significantly higher than the uncoated BCP and also other coated scaffolds at each time point which proved that 3% CPO as an oxygen producing element could be an optimal amount for using in the coating systems for tissue engineering applications. The cell viability of the coated scaffolds with 5% CPO were lower than 3% CPOcoated scaffolds. Many studies have demonstrated the cytotoxity of H_2O_2 to the cells in high doses where the killing of cells is mediated by the generation of reactive oxygen species (ROS) (Wang et al., 2011).

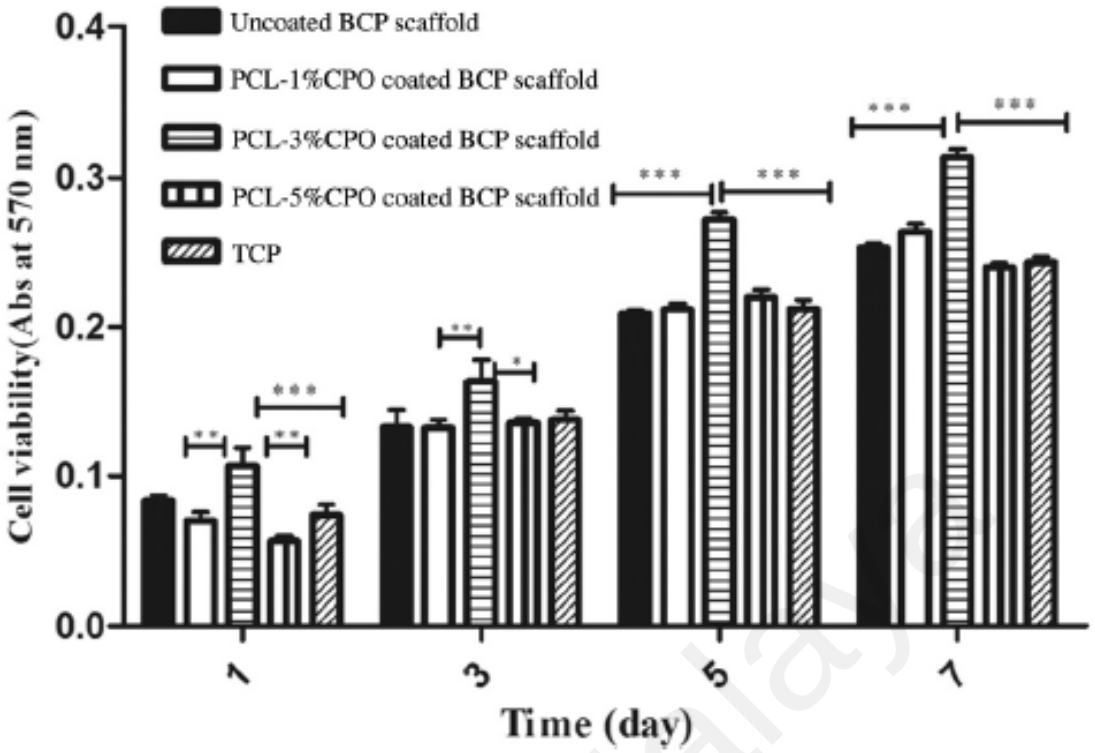

Figure 4.11: Cell viability on the scaffolds as a function of CPO (wt%).

4.5 Confocal Microscopy

Confocal images were studied to observe the cellular responses of the scaffolds. Figure 4.12 shows live osteoblasts in the scaffolds with and without oxygen release behaviour. At 7 days after cell seeding, the images showed cell attachment and proliferation on the strand surfaces of the scaffolds. When the cells are seeded onto the scaffolds, the production of oxygen from the scaffolds appears to improve cell viability. Confocal images also showed that the osteoblasts could attach and grow on the CPO-coated or uncoated BCP scaffolds, but the cells could spread better on the CPO-coated scaffold. Coupled with the data of MTT test, the scaffolds containing CPO at the concentrations of 1 and 3 percentages, could maintain a better cell viability over time. The coated scaffold containing 3% CPO had a significant increase in cell proliferation. Compared with the uncoated scaffolds, 1 and 3% CPO-coated scaffolds with oxygen

release ability exhibited higher cell density, enhanced viability and proliferation of cells than those without oxygen release ability. However, it has been shown in Figure 4.12d that the cell numbers were reduced by high amount of H_2O_2 which might be cytotoxic to the osteoblasts in the coated scaffolds with 5% CPO. After the cells had spread over the entire scaffolds' surfaces, they began to fill the interconnected pore network over time. In addition, cells incubated with CPO-coated scaffolds tended to form larger cellular spheroids, because of either growth of the cells into clusters or aggregation. These results indicated that the proposed oxygen generating scaffolds could be useful for extending cell viability of engineered tissues in vivo until host vascularization is formed. With vascularization of tissue scaffolds estimated at 0.5–1 mm per day in tissue, maintaining cell viability for 10 days could possibly allow for centimeter sized tissue scaffolds to be used. In addition, they can be effective for adjusting the ischemia condition which is common in engineered tissue after implantation (Cao et al., 2006),(Giuliani et al., 2005).

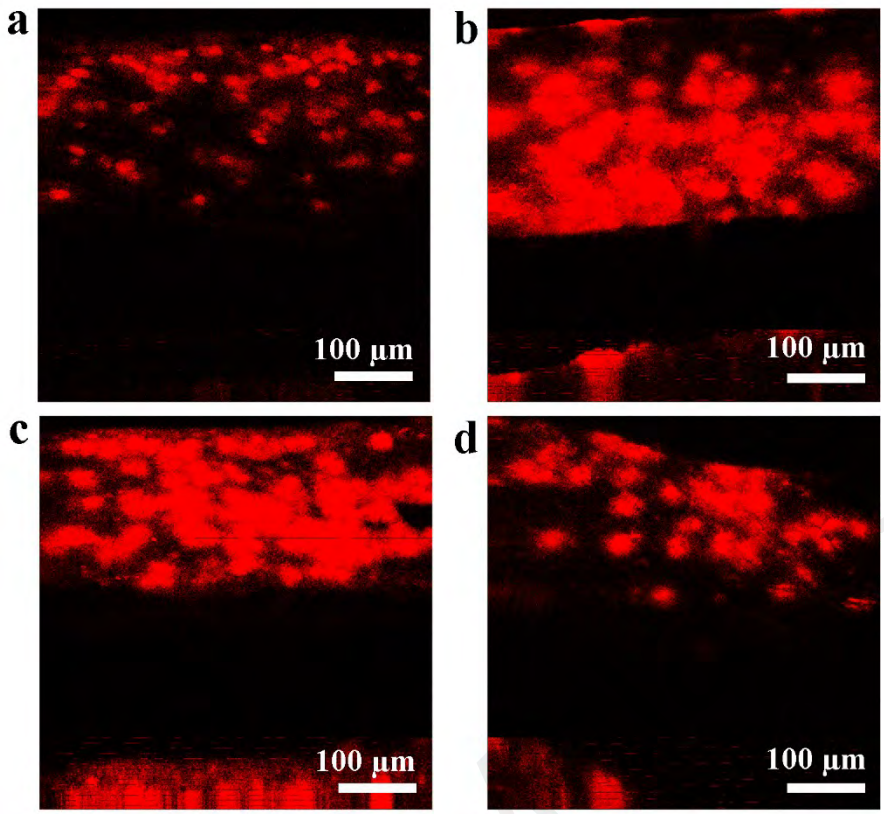

Figure 4.12: Laser confocal microscope photographs of osteoblast cells on (a) uncoated BCP scaffold, and (b-d) CPO-PCL coated BCP scaffolds with 1, 3 and 5% CPO, respectively.

4.6 ALP Activity

ALP is a phenotypic marker expressed throughout the proliferation and differentiation of osteoblasts. In vitro ALP activity can be a predictor for the in vivo bone formation capability (Prins et al., 2014). Hence, the ALP assay was done by Saos-2 (human osteosarcoma) cells to investigate the biocompatibility and bone generation capacity of the scaffolds because these scaffolds were designed for applying in bone tissue engineering. Figure 4.13 presents the results. ALP activity of the coated and uncoated scaffolds was increased during the 14-day culture period. The coated scaffolds presented higher levels of ALP activity in comparison with the uncoated one and this result can predict that the coated scaffolds will have a higher capacity for bone

formation. The ALP production at the 1st day was approximately at the same level for all samples. The cell activity on the 7th day was higher for the coated scaffolds with 3% and 5% CPO compared to the other samples and roughly the ALP level of the uncoated and coated scaffolds with 1% CPO were similar. The ALP formation level of the cells on the 14th day was higher again for the coated scaffolds with 3% and 5% CPO compared to the other specimens. The coated scaffold with 5% CPO showed the maximum ALP activity during all days.

The results show that the CPO coating encouraged the osteogenic differentiation of Saos-2 cells and the ALP activity was elevated with the increase of CPO percentage in the scaffolds' coating layer. This can be related to the oxygen released from the coated scaffolds. Several studies have proved that the elevated ALP activity occurs with the increase of oxygen level (He, Genetos, Yellowley, & Leach, 2010),(Tuncay, Ho, & Barker, 1994). Hypoxia can significantly decline the osteoblast's ALP activity and the expression of mRNAs for ALP (Utting et al., 2006). It can be concluded that the ALP production or activity, as an indicator of early osteoblastic differentiation, is changed as a function of oxygen level. According to Figure 4.10, the coated scaffolds with 3% and 5% CPO possessed the higher level of released oxygen then they presented the elevated ALP activity compared to the other scaffolds. The findings of this in vitro study propose that the oxygen-releasing coating on the BCP scaffolds creates a prominent advanced biomaterial for bone tissue engineering applications.

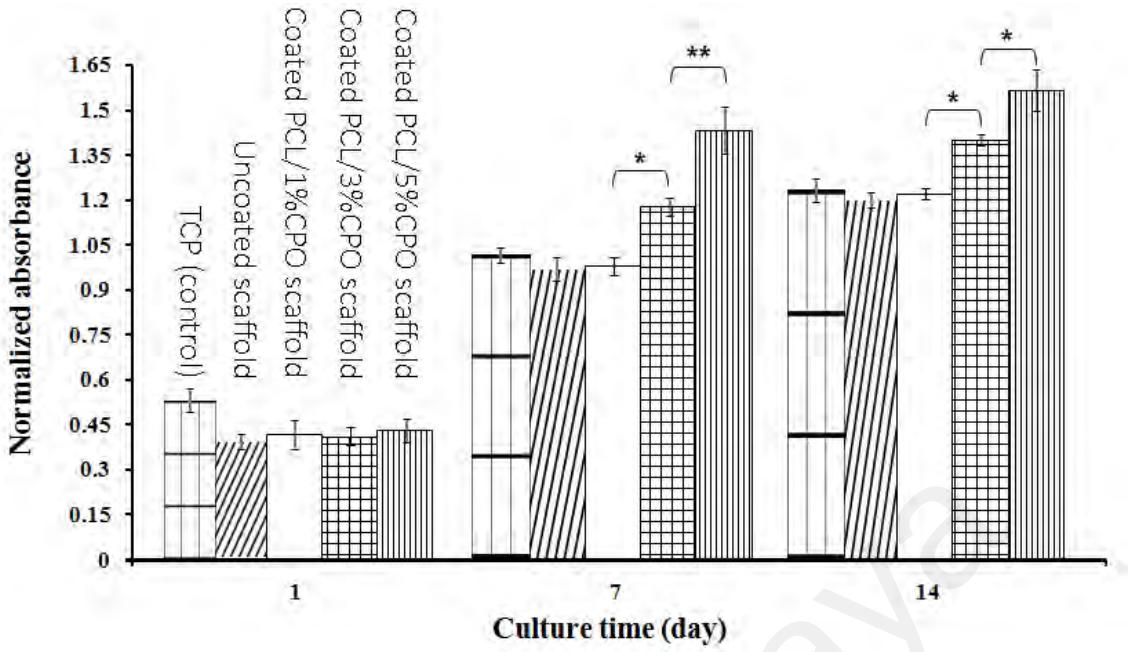

Figure 4.13: ALP activity of Saos-2 cells on the uncoated and PCL/CPO (1, 3 and 5 wt%) coated BCP scaffolds after culturing for 1, 7 and 14 days. The ALP formation level of the cells was higher for the coated scaffolds with 3% and 5% CPO compared to the other specimens.

4.7 In Vitro Behaviour in SBF

Apatite formation ability on the biomaterial's surface in SBF is mostly utilised for predicting the in vivo bone-bonding capability of bioceramics and bioceramic/polymer composites (Julie Russias et al., 2007),(Roohani-Esfahani, Nouri-Khorasani, Lu, Appleyard, & Zreiqat, 2010). Figure 4.14 shows some micrographs related to the surface of uncoated and coated scaffolds after a 21-day immersion in SBF. Precipitation of calcium phosphate happened over the entire samples after the SBF immersion. Higher magnification images show the calcium phosphate aggregates on the scaffolds' surface. The coated scaffolds revealed a superior capability of the precipitation compared to the uncoated one. Thus, it seems that the CPO particles played the role of a driving force for apatite formation. The micrographs also show that the apatite precipitation on the coated scaffolds was increased and aggregated with the increase of

CPO percentage. It may relate to the releasing of calcium hydroxide and hydrogen peroxide, the product and intermediate of CPO reaction with water. Calcium hydroxide can take part in the hard tissue bridge formation. It is done by the activating of some tissue enzymes such as alkaline phosphatase which helps HA sedimentation (Estrela & Holland, 2003). Furthermore, several publications have been reported that the release of hydrogen peroxide accelerates the formation of HA in SBF solution which leads to promoting osseointegration (Baker, Assis, Higa, & Costa, 2009),(Randorn, Kanta, Yaemsunthorn, & Rujijanakul, 2015),(Karthega, Nagarajan, & Rajendran, 2010).

The results indicated that the BCP scaffolds coated with 3% and 5% CPO had high apatite formation ability. It can be said that these scaffolds can bond to the living bone in a short time after the implantation because a high degree of apatite formation on the surface of a material in SBF can lead to a high degree of its in vivo bone bioactivity (Kokubo & Takadama, 2006).

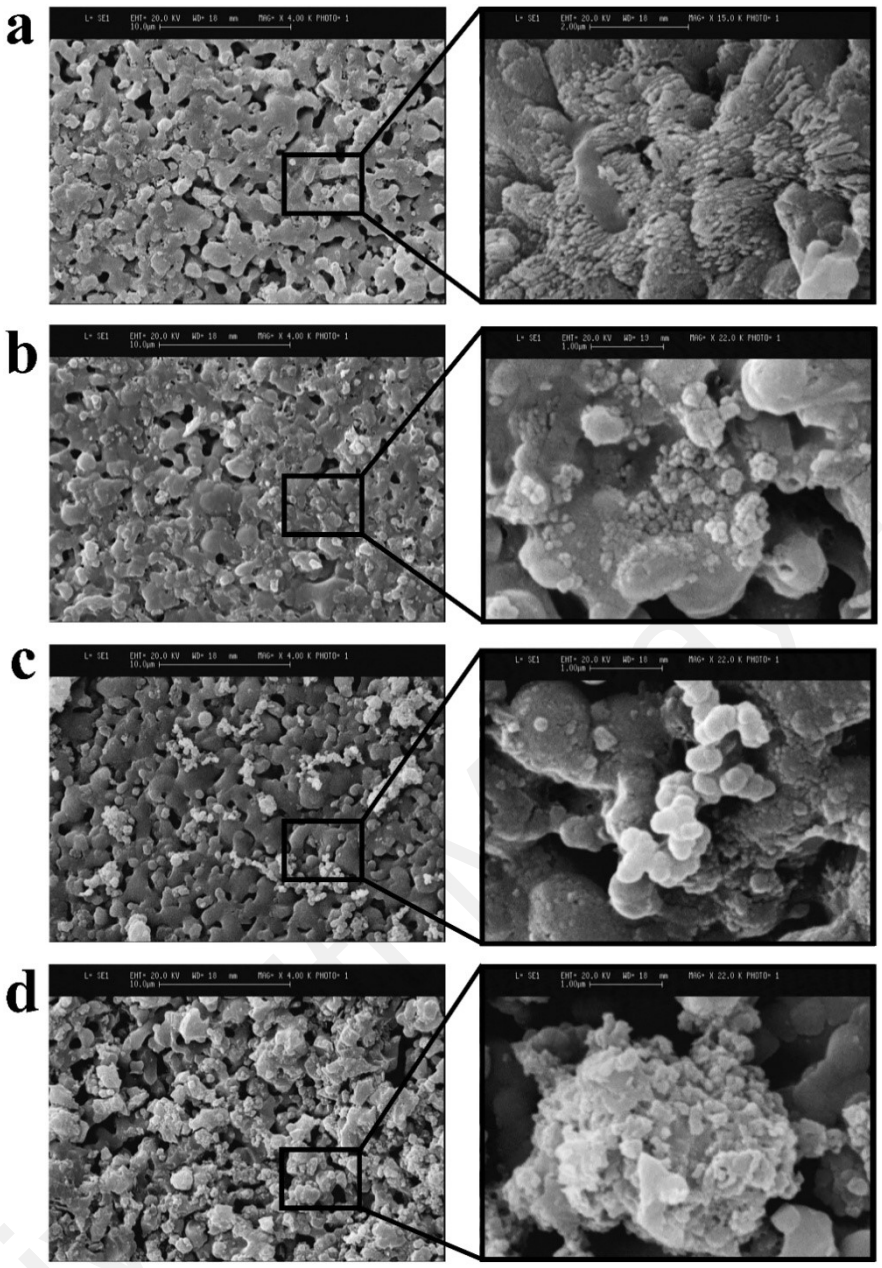

Figure 4.14: SEM micrographs were taken from the surface of the uncoated (a) and coated BCP scaffolds with 1%, 3% and 5% CPO (b-d, respectively) after 21-day soaking in the SBF solution.

4.8 Antibacterial Activity Assessment

Bacterial infection is one of the main problems associated with the implanted biomedical devices. Several strategies have been established to avoid the bacterial colonisation and following biofilm formation on the surface of the implants. Modifying

the surfaces to be anti-adhesive and applying the antimicrobial agents in the bulk or coating of the implants are some of these strategies. Innovative approaches are still required not just for inhibiting the bacterial infection but also for instantaneously developing healthy tissue integration (Wang et al., 2010),(Khoo et al., 2009).

4.8.1 MIC and MBC

CPO (CaO_2) is a solid peroxide with the colour of white or yellow. When CPO is exposed to hydrous media, it is decomposed and releases oxygen. In addition to its ability of oxygen releasing, it is also capable of disinfection. Thus, it has been broadly utilised in medicine. CPO forms hydrogen peroxide and calcium hydroxide ($Ca(OH)_2$) after dissolving in water. The sterilisation properties of calcium hydroxide stem from its ability to increase the pH of a solution by dissociation of hydroxyl ions. The high pH may affect the bacteria through destroying their membranes, denaturation of the structural proteins and enzymes, and damaging the DNA. However, the antibacterial mechanism of CPO may arise from the releasing of reactive oxygen species (ROS). Hydrogen peroxide may generate oxygen free radicals and react with macromolecules (such as membrane lipids and DNA) which leads to the bacterial death. Thus, high pH and ROS may be the sterilisation mechanism of CPO (Ma, Zhang, Zhao, Guo, & Lin, 2007),(Mura et al., 2005),(Yong Liang & Wang, 2016).

The bacteria were cultured in MHB liquid media containing CPO for 24 h, and Figure 4.15 presents the results. The bacteria suspensions without CPO became turbid, signifying the fast proliferation of bacteria within the MHB medium (sample B6 for S. aureus and D6 for P. aeruginosa in Figure 4.15). Corresponding to the reduction of CPO concentration within the MHB medium, bacteria suspensions were still clear up to the CPO concentration achieved 0.094 mg/ml for S. aureus (sample D1 in Figure 4.15) and 0.375 mg/ml for P. aeruginosa (sample A5 in Figure 4.15). Since MIC is the minimum

concentration of an antibacterial agent which is able to hinder the growth of bacteria, the MIC of CPO is 0.094 mg/ml and 0.375 mg/ml for S. aureus and P. aeruginosa, respectively. Subsequently, the samples with higher CPO concentration than the MIC were cultured on the MHA plates. It was concluded once the CPO concentration reached 0.187 mg/ml for S. aureus (sample C6 in Figure 4.15) and 0.75 mg/ml for P. aeruginosa (sample A4 in Figure 4.15), the bacteria suspension did not become turbid. Therefore, the MBC of CPO was identified as 0.187 mg/ml and 0.75 mg/ml for S. aureus and P. aeruginosa, respectively.

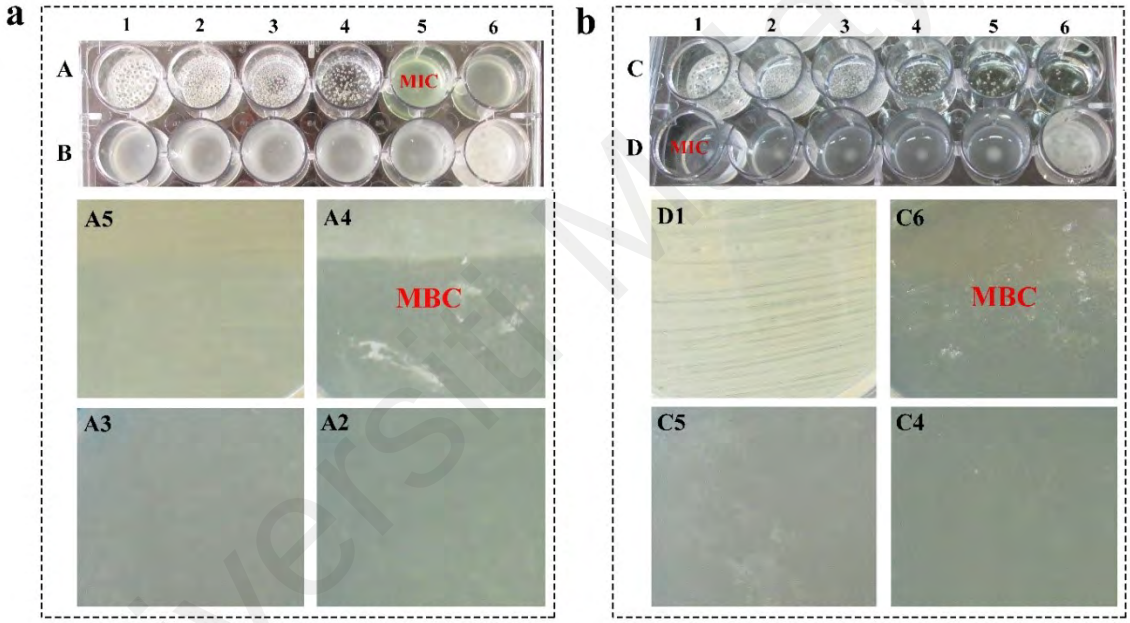

Figure 4.15: First part from the top presents the MIC test in which the turbidity of bacteria suspensions with different concentrations of CPO can be observed. The bottom part is related to the MBC test which demonstrates the cultured bacteria suspensions (obtained from the samples of the MIC test) on agar plates and the colonies of bacteria can be observed in the sample with a concentration less than the MBC. Section (a) was done for S. aureus and (b) for P. aeruginosa.

Some small bubbles can be observed in the samples with higher CPO concentration than the MIC in Figure 4.15. These bubbles are related to the oxygen produced during

the reaction of CPO and water. The oxygen bubbles can be a visual reason for inhibiting bacteria in the samples.

According to the MIC and MBC results, CPO possessed superior antibacterial activity against S. aureus than P. aeruginosa. This happened probably because of the capability of P. aeruginosa for generating biofilm (Chiang & Burrows, 2003) which can confuse the straight act of CPO against the bacterial cell.

4.8.2 Disk Diffusion

Figure 4.16 shows the inhibition zone of the CPO coated scaffolds after 24-h incubation. An inhibition zone around the CPO coated scaffolds proves the bacteriostatic effect of CPO. The inhibition zone was increased from 1 to 5 wt% CPO in the coated scaffolds. Hydrophobic PCL was used for the scaffolds' coating to reduce the rate of CPO release and avoid the cytotoxicity of a burst release. Although, the diameter of the inhibition zone will be increased by the higher amount of CPO and using a hydrophilic polymer for coating. CPO can hinder the growth of bacteria efficiently with its reaction products (calcium hydroxide, hydrogen peroxide and oxygen) acting as the biocides.

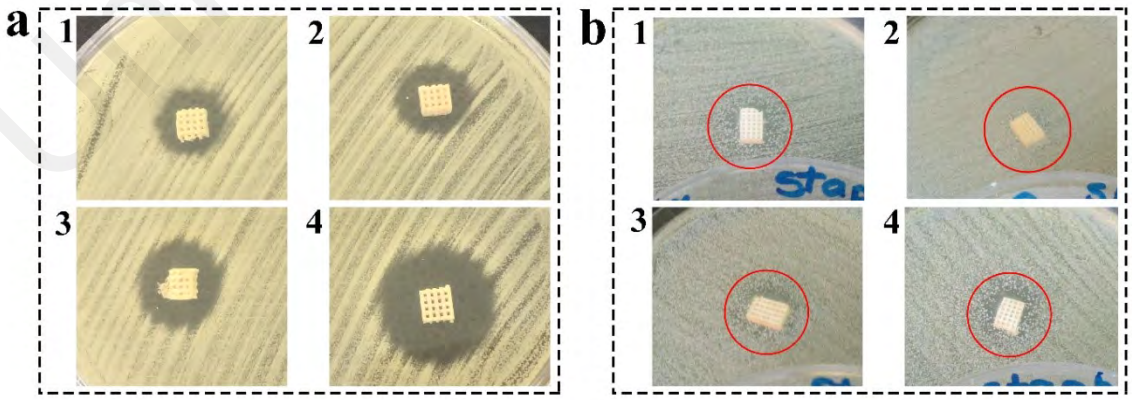

Figure 4.16: Inhibition zone of uncoated (1) and coated BCP scaffolds with 1%, 3% and 5% CPO (2–4, respectively) against E. coli (a) and Staphylococcus aureus (b) after 24-h incubation on the agar.

Calcium hydroxide is converted to calcium and hydroxyl ions when it is exposed to the aqueous environments. It possesses some properties affecting vital tissues like encouraging the deposition of hard tissue and inhibiting bacteria. The fatal effects of calcium hydroxide on the bacterial cells are mainly due to the production of hydroxyl ions. These free radicals are severe oxidizers with intense reactivity and can affect the bacteria through the subsequent mechanisms: 1) Harming the cytoplasmic membrane of the bacteria due to lipid peroxidation and destruction of phospholipids, 2) Protein denaturation due to alkalinisation, and 3) Damage to the DNA (Mohammadi, Shalavi, & Yazdizadeh, 2012),(Sladdin & Lynch, 1983),(Siqueira Jr & Lopes, 1999).

Hydrogen peroxide is well-known for being an effective biocide. It eliminates the bacteria and stops biofilm creation by protein oxidising and generating oxygen radicals (Wang et al., 2011). It is able to limit the biofilm growth even at the low concentrations. This is done by hindrance of glycolysis and suppressing the regulatory gene of biofilm besides the minimum hurt to the adjacent host tissue (Siqueira Jr & Lopes, 1999),(Baldeck & Marquis, 2008).

Oxygen has an outstanding role in preventing the surgical wound infections. Decreasing of infection by supplementary oxygen is mediated by ROS (including H_2O_2, superoxide (O_2^-) and free radicals). Almost all the wound-related cells own particular enzymes which can produce ROS from oxygen. The extent of superoxide generation (a major element to kill the pathogens by oxidising) via leukocytes is dependent on the level of oxygen. ROS play a critical role as the cellular messengers in stimulating the main routes related to lesion repairing and infection prevention (Rodriguez et al., 2008),(Guo & DiPietro, 2010),(Sen, 2003).

The results of the agar diffusion test depend on the solubility of the specimen in the agar rather than just its effectiveness against the organism (Basrani et al., 2003),(de

Almeida Gomes et al., 2006). In this study, CPO was incorporated in the PCL coating and CPO releasing was dependent on the degradation of PCL. The CPO-coated scaffolds were in contact with the bacteria just for 24 h in the disk diffusion test. Then, the CPO powders would not have enough time to be released and kill the bacteria due to the low degradation rate of PCL. It can be said that the antibacterial activity of the CPO-coated scaffolds is time-dependent.

CPO inhibited E. coli more strongly than S. aureus. The membrane structure of gram-positive and gram-negative bacteria are different and the major dissimilarity is related to their peptidoglycan layer thickness. The gram-positive bacteria have a thicker wall compared to the gramnegative bacteria (J. S. Kim et al., 2007). The inferior efficiency of CPO against S. aureus can be affected by the thicker wall.

An inhibition zone around the uncoated BCP scaffolds (Figure 4.16 a1 and b1) proves their bacteriostatic effect which may arise from the production of ROS on their surface with fatal damage to the bacteria (Ragab et al., 2014). However, the bactericidal effect of coated BCP scaffolds is related to just CPO because PCL covers all the surface of the BCP scaffolds. All the CPO-coated scaffolds with 1%, 3% and 5% could inhibit the E. coli growth remarkably (Figure 4.16 a2–4). The CPO-coated scaffolds with 3% and 5% presented an inhibition zone against S. aureus (Figure 4.16 b3–4), but the 1% CPO-coated scaffold did not have a clear inhibition zone (Figure 4.16 b2). It can be concluded that the amount of 1% CPO is too low to have an inhibitory effect against S. aureus.

The decreasing of bacterial growth can decline the opportunity of biofilm progress. A steady release profile can eliminate pre-operative organisms and subsequently, the possibility of bacteria colonising over the implants will be decreased. The in vitro antimicrobial experiments present the antibacterial activity of CPO-coated BCP

scaffolds. Thus, they look potent for being an antibacterial scaffold applied in bone tissue engineering.

These results reveal that the oxygen-generating scaffolds can be designed to provide a short-term peroxide-based antibacterial activity. CPO, a cost-effective biomaterial, has been used as an oxygen generating and biocidal agent. Wang et al. also used CPO in nanofibers to act as an antibacterial agent (Wang et al., 2011). Using these antibacterial scaffolds can kill the bacteria in the early stage of implantation and prevent the biofilm formation.

4.9 In Vivo Test

All of the rabbits survived and didn't have any fractures or infections post-surgery.

4.9.1 Radiological Assessment

Imaging is one of the key investigations in bone tissue engineering research. X-ray examination is chiefly applied for evaluating the osseointegration between the scaffold and host bone.

The scaffolds were implanted skilfully in the absence of any displacement or fracture on the surgery day. The empty group had a 15-mm defect precisely in the radius midsection (Figure 4.17a). Scaffold and host bone merging increased in implanted groups gradually and new callus in CPO/BCPS group was more than BCPS group (Figure 4.17b,c). There was a major improvement of bone regeneration in group CPO/BCPS compared to the group BCP alone at 6 months post-surgery (Figure 4.18b,c). CPO/BCPS group presented the best result and whole bridging was apparent between the bony ends lengthways the radius boundary. The empty group had clear radius defects all the time and the segmental defect was non-healed, so non-union was revealed at 3 and 6 months after surgery (Figure 4.17a and Figure 4.18a).

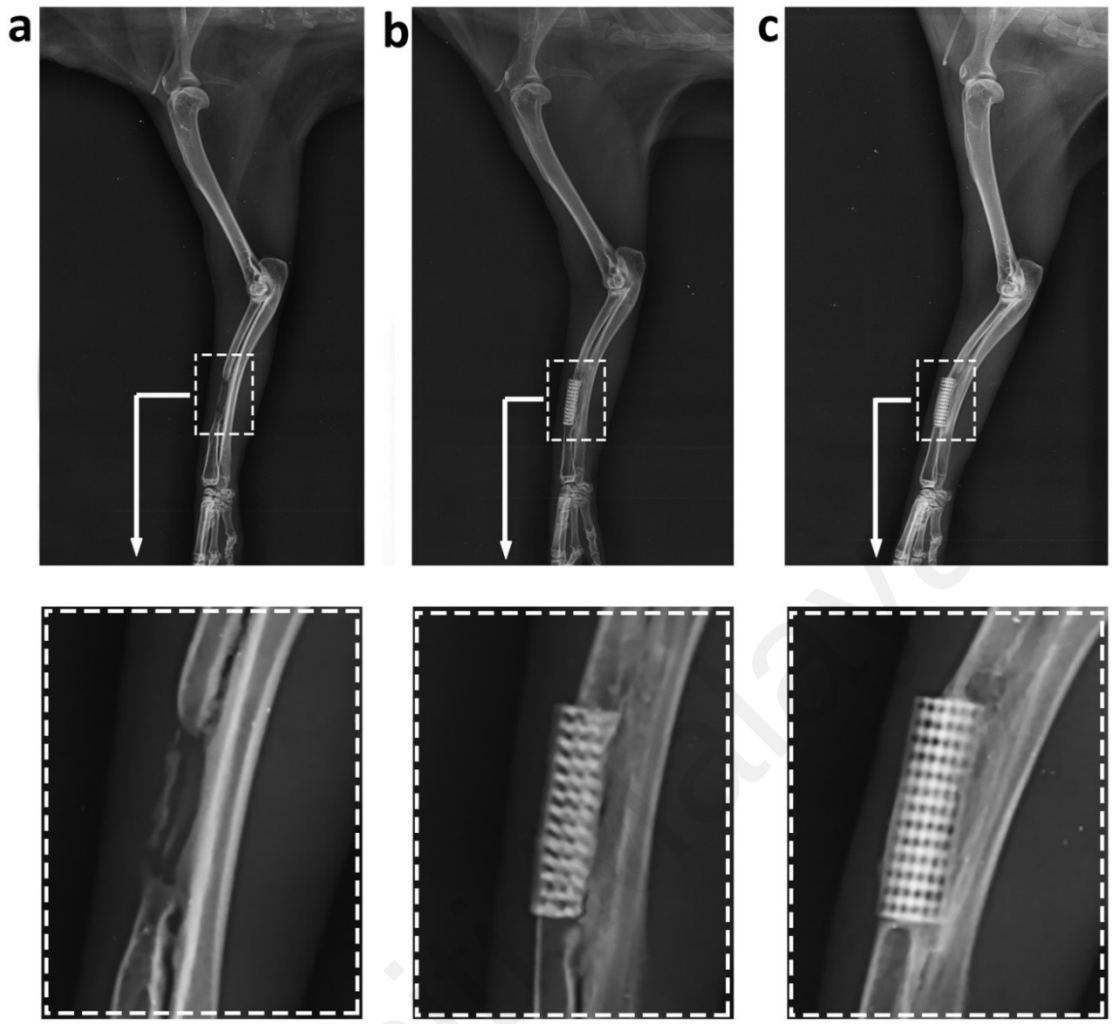

Figure 4.17: Illustrative radiographs of radial segmental defects without (a) and with scaffold implantation (b: BCPS, c: CPO/BCPS) taken 3 months post-operatively. The CPO/BCPS group showed more bone filling in the defect compared to BCPS group. The segmental defect was not healed after 3 months in the empty group.

Radiographs exhibited that segmental defects implanted with BCP scaffolds having oxygen generating coating amalgamated at the proximal and distal host bone–scaffold interfaces at 6 months postoperatively (Figure 4.19). The porous look of the scaffolds at a few days after operation (Figure 4.19b), slowly converted to more radiopaque appearance at 6 months after operation, representing that mineralization occurred in the pores of the CPO/BCPS (Figure 4.19a). New bone was shaped around the periphery of the scaffolds as well as along the host bone and completely filled the segmental defect.

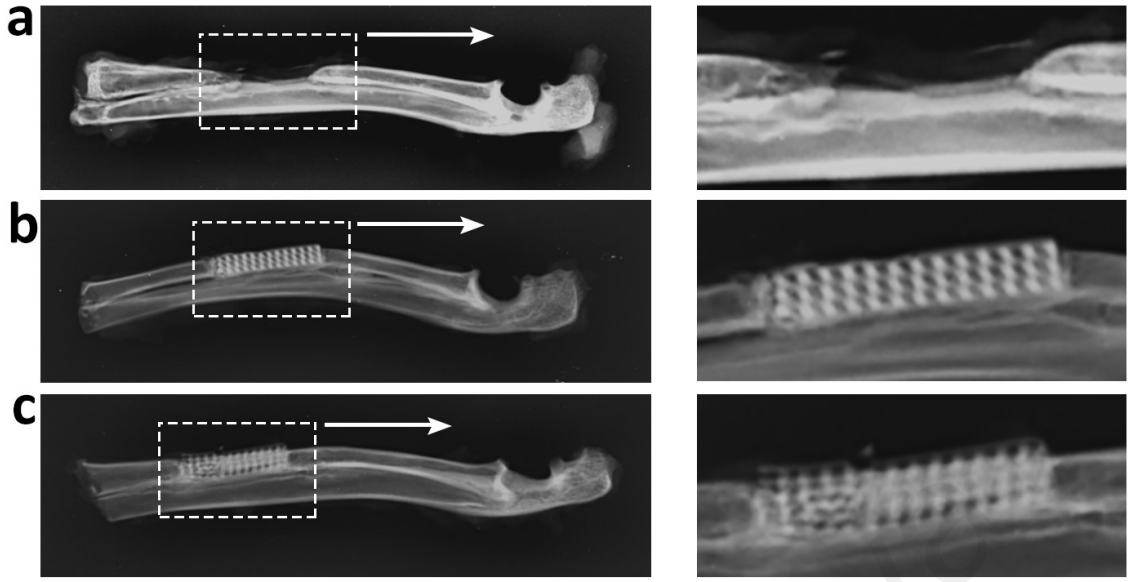

Figure 4.18: Illustrative radiographs of radial segmental defects without (a) and with implantation of scaffolds (b: BCPS, c: CPO/BCPS) taken at month 6 post-operatively. There was a major improvement of bone regeneration in CPO/BCPS group compared to BCPS group. The segmental defect was not healed after 6 months in the blank group.

At 3 and 6 months after operation, new bone progressively augmented at the interface between the implant and host bone and internal pores of BCPS and CPO/BCPS groups (Figure 4.17b,c and 4.18b, c). The results of empty group revealed that no rabbit attained repair by themselves, additional demonstrating that the segmental defect length was appropriate as experimental model of bone defect in rabbits. In the CPO/BSPS group, the presence of more mineralized bone tissue interrupted between the fracture area in radius and more osseointegration between the host bone and the implant was detected compared to the non-coated scaffold group.

Figure 4.19: Radiographs of CPO/BCPS group at 6 months (a) and day 0 (b) postoperatively. The scaffold pores became radiopaque at 6 months, representing mineralization happening in the pores.

4.9.2 Histological Findings

4.9.2.1 New Bone Area Percentage

In this study, the scaffolds without and with CPO coating at a macropore dimension of 500 μm and porosity of 70% were inserted to 15-mm bone defects. The effect of scaffolds was explored for bone regeneration after 3 and 6 months' post-implantation in the radius of rabbit. There were no sign of inflammation and infection at defect site in all treated and control animals. Histological outcomes revealed that new bone could develop or migrate into the central of scaffolds throughout the macropores, where CPO/BCPS groups presented improved osteogenic effects as against both blank group and BCPS. Macroscopically, a connective tissue formed in blank group after 3 months'

post-surgery. In addition, a well-defined continuous layer of new bone was formed in the defect site in groups grafted with scaffolds (Figure 4.20).

As represented in Figure 4.21, the blank group was poorly healed through new bone even after 6 months. Histological examination confirmed that new bone slowly amplified at the interface between the implant and host bone and within the interior pores in the course of time in the implanted groups, and protracted to the centre of scaffold. The new bone mass and maturity in CPO/BCPS group were significantly enhanced in contrast to BCPS group at the two time points evaluated, which presented that the coating of CPO could efficiently encourage new bone formation (Figure 4.20,21). The scaffold fragments were detected in the scaffold groups which according to radiological and histological data, the degradation of scaffolds in CPO/BCPS group was more than the BCPS group and after 6 months they could completely match themselves with the host bone and newly formed bone.

Masson's trichrome staining revealed that collagen fibers were more formed in the defects treated with scaffolds in comparison with blank group over all the time periods. Moreover, the results of Goldner's trichrome staining showed considerably more new bone formation with collagen alignment in the defects treated with CPO coated scaffolds, compared with uncoated scaffolds (Figure 4.20,21). According to several literatures, trichrome staining specifies woven and mineralized bone tissue with blue and red colour, respectively (Song et al., 2014),(S. A. Park et al., 2018),(Chen et al., 2013). As seen in Figure 4.20 and 4.21, the new bone formed in the defect after 3 months, turned from woven to mineralized bone in 6 months. The attendance of vessels can be surely distinguished once erythrocytes seem in the pink colour. It shows that neovascularization was happened in the new bone formed inside the coated scaffolds.

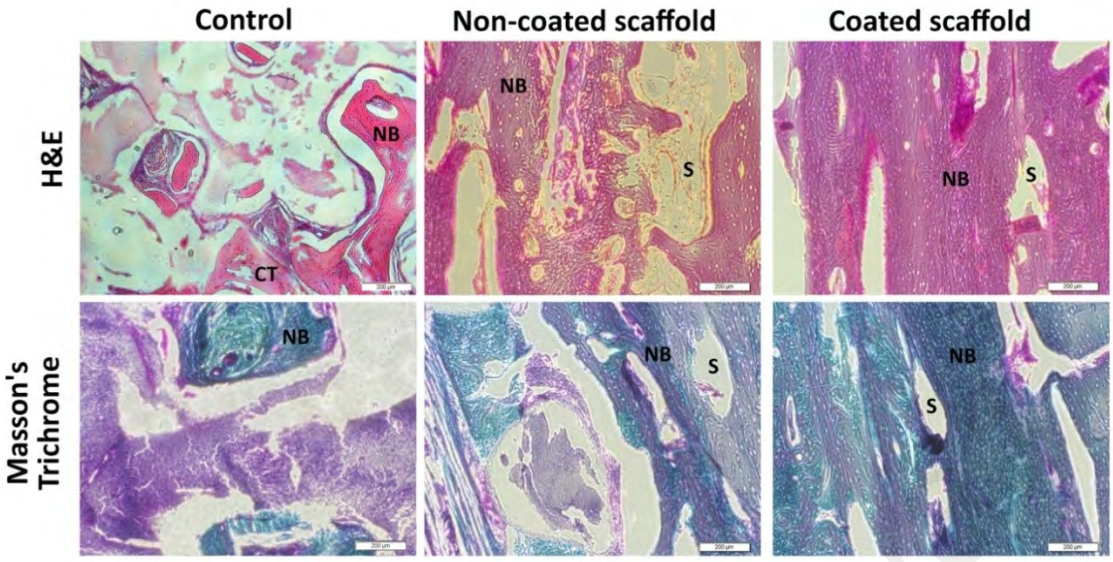

Figure 4.20: Representative sections of decalcified histology of radial segmental bone defects at 3 months of post-surgery. H&E stained sections at month 3 showed formation of connective tissue in control group and more newly formed bone in coated scaffolds group than that in non-coated one. Masson's trichrome staining confirmed more new woven bone (blue colour) formation in CPO coated scaffold, compared with uncoated one (NB, New Bone; S, Scaffold; CN, Connective Tissue; white bar = 200 μm).

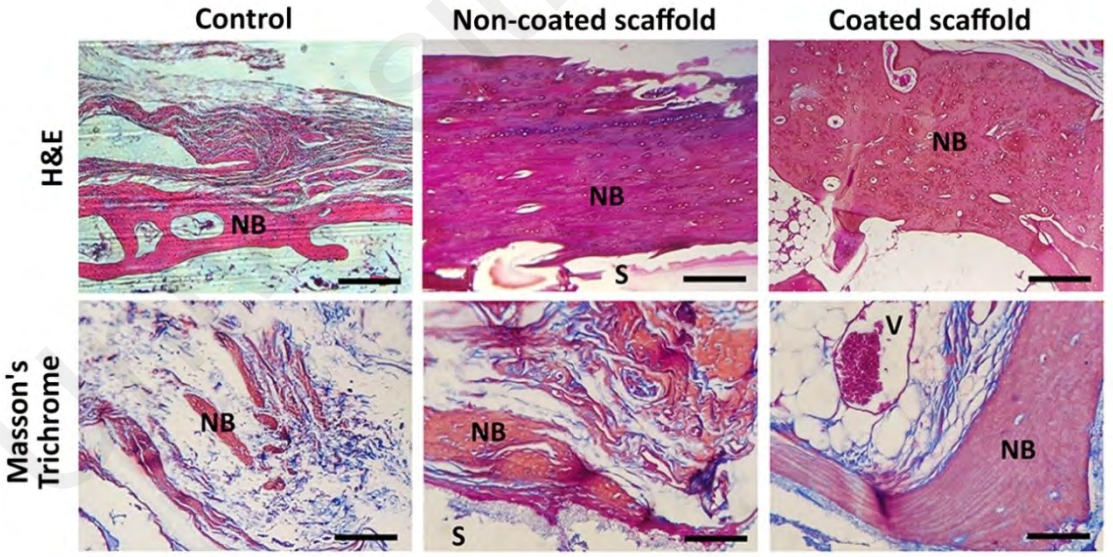

Figure 4.21: Representative sections of decalcified histology of radial segmental bone defects at 6 months of post-surgery. H&E stained sections at month 6 showed poorly healing of control group and more newly formed bone in coated scaffolds group compared to non-coated one. Masson's trichrome staining confirmed more new mineralized bone (red colour) formation in CPO coated scaffold, compared with uncoated one (NB, New Bone; S, Scaffold; BV, Blood Vessel; black bar = 200 μm).

The quantitative results of histomorphometry analysis represented considerably more new bone formation in the coated scaffolds within 6 months' post-surgery compared to uncoated scaffolds and control groups, as exhibited in Fig. 8a. New bone volume fractions in the control, BCPS and CPO/BCPS groups were about 5, 45 and 85%, respectively. The amount of newly formed bone in the CPO/BCPS group was nearly 2 times higher than the BCPS. H&E staining could distinguish the mineralized bone tissue and mature osteocytes existed in that (Fig. 8B). According to H&E staining of the coated scaffolds in Fig. 7 and Fig. 8b (larger magnification), the newly formed lamellar bone within the coated scaffolds demonstrated osteons comprising Haversian canals. The detection of Haversian canals, lamellae, lacuna and osteocytes in the newly formed bone inside the scaffold specifies a regular mineralized bone formation.

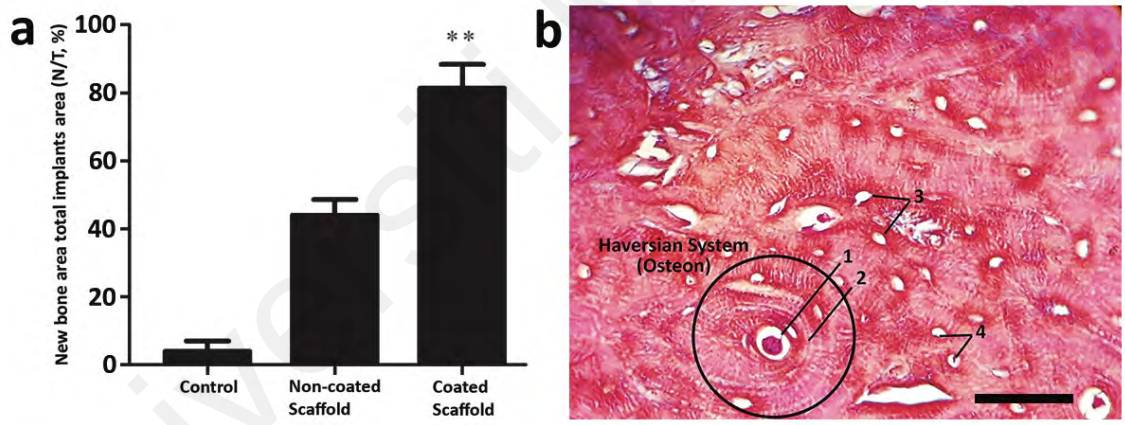

Figure 4.22: a) Bone volume inside the segmental bone defects in the groups of control, non-coated and coated scaffolds following 6 months of post-surgery. The coated scaffold group displayed nearly 2 times more new bone formation in the defect compared to non-coated scaffold (p < 0.01). b) H&E staining – detailed investigation of new lamellar bone within the coated scaffold presenting osteons. (1, Haversian canal; 2, lamellae; 3, lacuna; 4, osteocyte; black bar = 100 μm).**

4.9.2.2 Osteogenic Markers Expression In Situ

Osteonectin (ON) and osteocalcin (OC), noncollagenous extracellular matrix proteins, are early and late markers for osteoblast differentiation respectively (Kato et al., 2013). ON and OC are mainly made by osteoblasts and secreted throughout the differentiation and mineralization procedure of osteoblasts. ON, the most plentiful non-collagenous protein in the mineralized bone matrix, sticks selectively to both hydroxyapatite and collagen and connects the bone mineral and collagen phases, possibly commencing active mineralization in skeletal tissue. OC designates the mineralization process in bone formation done through the calcification of the osteocytes in the collagen layer. Indeed, OC influences the hydroxyapatite nucleation because of its high affinity for calcium ions, a property gained by the γ-Carboxyglutamic acid residues (Ozdemir, Kurtis, Tuter, Senguven, & Yildirim, 2016),(Tsao et al., 2017).

For proving osteogenic differentiation and mineralization in the scaffolds inside bone defect locations, ON and OC were distinguished via immunofluorescence staining in decalcified paraffin sections. After 6 months as shown in Figure 4.23 and 4.24, the stained specimens revealed a significant upsurge expression of osteogenic markers ON and OC in the defects treated with the scaffolds in comparison with the empty control. Both proteins ON and OC were over-expressed in the defects treated with coated scaffolds at 6 months of post-surgery demonstrating higher osteogenic differentiation and bone mineralization compared to uncoated scaffolds group.

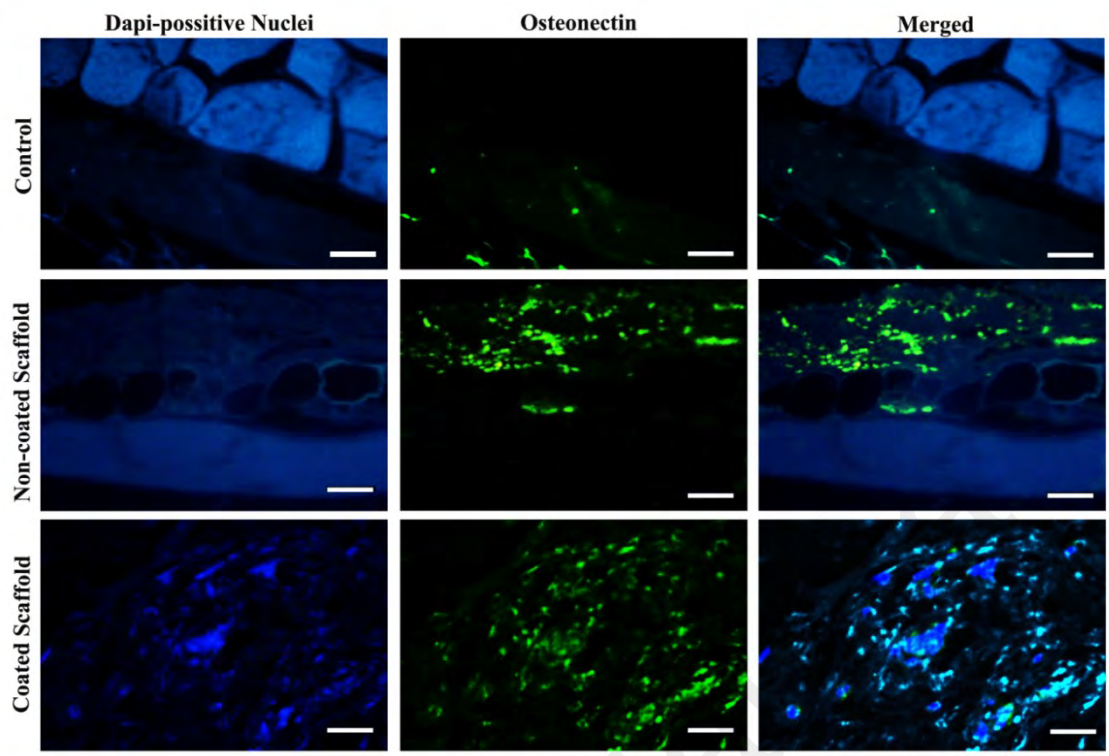

Figure 4.23: Representative immunohistochemistry of osteonectin expression in the rabbit radial defects after 6 month's post-implantation. Immunohistochemistry staining verified osteocalcin expression on the new bone with more and stronger fluorescence signals in the scaffolds, particularly coated scaffolds, compared to control group in the segmental defects, indicating higher osteogenic differentiation and bone mineralization (white bar = 200 μm).

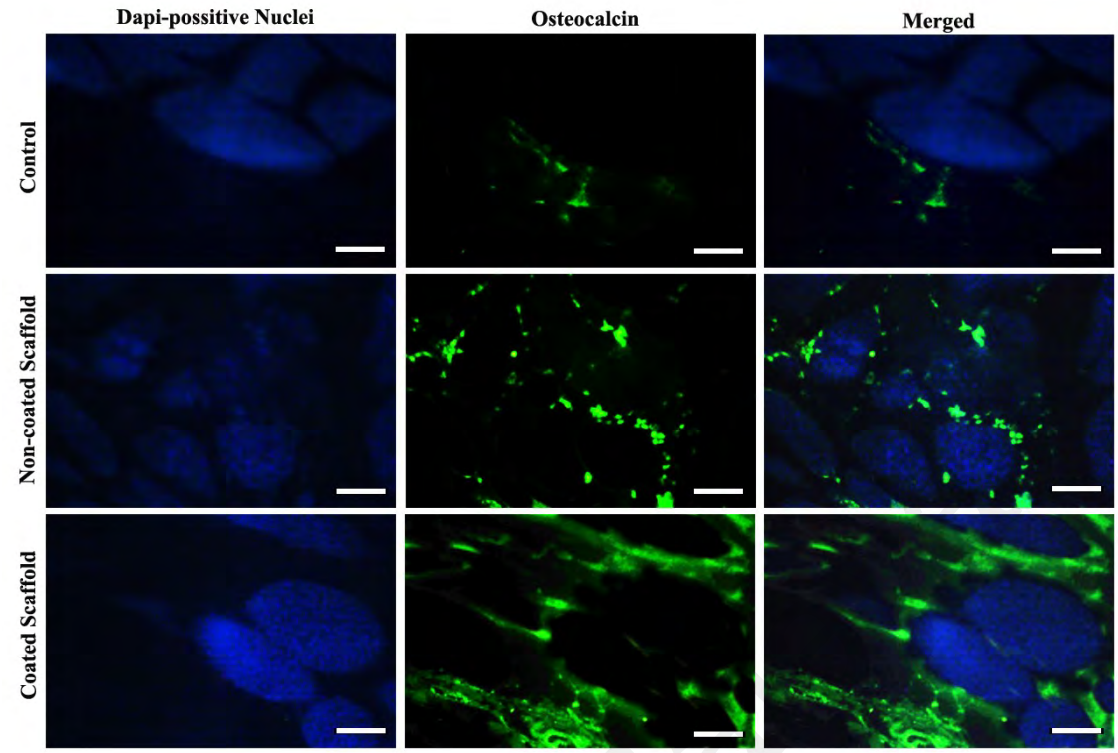

Figure 4.24: Representative immunohistochemistry of osteocalcin expression in the rabbit radial defects after 6 month's post-implantation. Immunohistochemistry staining proved osteocalcin expression on the new bone with more and stronger fluorescence signals in the scaffolds, specifically coated scaffolds, compared to control group in the segmental defects, indicating higher osteogenic differentiation and bone mineralization (white bar = 200 μm).

4.9.3 Biomechanical Findings

One of the major indexes for investing the quality of bone healing, is biomechanical testing (D. Xie et al., 2015) which was determined by three-point bending test. The maximal forces of radial bone in CPO/BCPS group after 3 and 6 months were 134 and 150 N, respectively, which were considerably higher than the F_{max} of BCPS group with 92 and 127 N at every time interval (Figure 4.25). Amid the groups, the highest and lowest mechanical properties are dedicated to CPO/BCPS and blank groups, respectively. F_{max} of the intact normal bone was 170 N which is higher than that in CPO/BCPS, BCPS and control groups, and the differences were statistically significant ($P < 0.01$). Compared to the normal bone, F_{max} value in CPO/BCPS group (6 months post-operation) reached to 88.2%, indicating the remarkable repairing effect of CPO

coated scaffolds on segmental defects. Higher in vivo biomechanical stability is an evidence for the speedier bone regeneration in CPO/BCPS group. These results showed that porous BCP scaffolds modified with CPO possessed outstanding biomechanical properties and the potential for reconstruction of radial bone defect in rabbits.

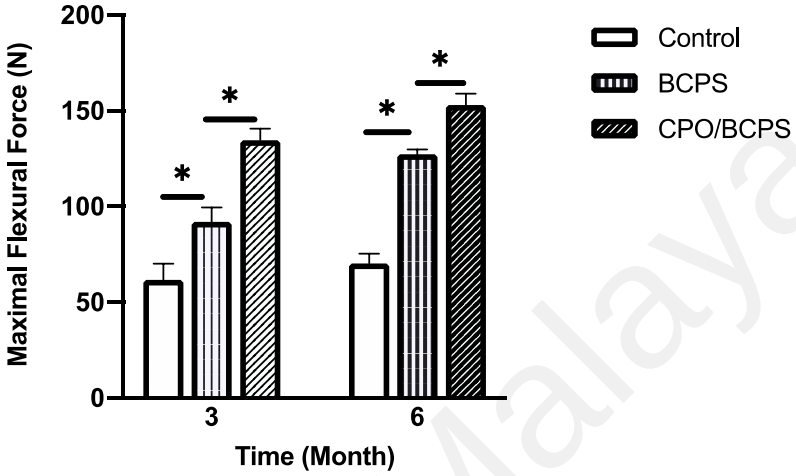

Figure 4.25: Maximal flexural force in the groups of control, BCPS and CPO/BCPS at 3 and 6 months after surgery.

CHAPTER 5: DISCUSSION

Wound healing signifies an arranged compensation which happens after each surgery and traumatic injury. Discovering the hindrances of wound healing and evolving a proper treatment strategy to control the obstructions is the first step for accomplishing a healed wound. Hypoxia occurs due to disrupting of vasculature and is one of the main limitations for wound healing. Rectifying of wound-hypoxia is essential to supply sufficient O_2 which supports the growth of regenerating tissues (Mouriño & Boccaccini, 2009).

Reduced oxygen tension strictly decreases the osteogenic differentiation of MSC. Raising of oxygen from 1% to 3% reinstates the osteogenic differentiation (Holzwarth et al., 2010). Interference of vascular flow with fracture or surgical osteotomy causes a temporary hypoxic slope in the wound, with oxygen tension dropping to 0–2% in the central wound area (Salim, Nacamuli, Morgan, Giaccia, & Longaker, 2004). Hypoxia weakens the osteogenic differentiation through the reduction of alkaline phosphatase activity and expression of osteogenic markers (Hsu, Chen, & Wei, 2013). Elevation of alkaline phosphatase activity with increasing of oxygen concentration was presented in our previous publication (M. Touri, Moztarzadeh, Osman, Dehghan, & Mozafari, 2019) and since alkaline phosphatase (ALP) is a helpful marker of bone formation and osteoblasts differentiation (Bao et al., 2017) then, the increasing of its activity due to increased oxygen pressure will affect the bone regenerating.

The oxygen concentration may impact on the osteogenic markers like ON and OC and subsequently on the bone formation. Lin et al. showed that increasing of oxygen pressure with HBO increased the expression of osteogenic markers of BMSCs like alkaline phosphatase activity, type I collagen and osteocalcin (Lin et al., 2014). Park et al. in their research showed that a human osteosarcoma cell line unceasingly exposed to

2% O_2 for up to 96 h would express reduced levels of the late bone marker osteocalcin (J. Park, Park, Kim, Park, & Baek, 2002). Utting *et al.* investigated that reduction of pO_2 to 2% declined the formation of mineralized bone. The repressive impact of hypoxia on bone formation is somewhat because of reduced osteoblast proliferation. Hypoxia moreover severely lowers osteoblast alkaline phosphatase (ALP) activity and expression of mRNAs for ALP and osteocalcin, signifying hindrance of differentiation to the osteogenic phenotype. They moreover revealed that hypoxia affected the collagen fibrils deposited by osteoblasts which were less organized and less abundant (Utting et al., 2006).

In rabbits, measuring of pO_2 in hematoma 4 days after the fracture showed average values of 0.8% O_2 (Brighton & Krebs, 1972). It is demonstrated in our previous publications that the 3%CPO-coated scaffolds could save the pO_2 from hypoxic zone (M. Touri, Moztarzadeh, Osman, Dehghan, & Mozafari, 2018a),(M. Touri, Moztarzadeh, et al., 2019) and this increase of oxygen concentration may save the fracture healing from the demerits of hypoxia. Considered together, these results can confirm the higher collagen fibre extent and osteocalcin expression by oxygen generating scaffolds and assist to clarify the bone loss which happens at the site of fracture with uncoated scaffold which doesn't have any oxygen supplier for compensating the hypoxia.

Examination of undecalcified sections for new bone percentage showed earlier and more bone formation in CPO/BCPS compared to BCPS group at each assessed post-operation time point, suggesting an encouraging bioengineering approach for bone repair applications, ascribed to their supreme treatment efficiency, where CPO had a leading part in bone healing improvement by its straight oxygen release into healing area and the indirectly encouraged cell behavior in development of osteogenesis.

According to the Figure 4.17 and 4.18, it seems that the CPO-coated scaffolds had more osseointegration and biodegradation compared to uncoated scaffolds. As osteoinduction (Okubo et al., 2000),(Yoshida et al., 1998) and osseointegration (Danesh-Sani, Shariati-Sarabi, & Feiz, 2012),(Granström, 2003) may rise with the increasing of the partial pressure of oxygen then CPO-coated scaffolds due to generating oxygen, may have more osteoinduction and osseointegration. Osteoinduction indicates the employment of immature cells and the inspiration of these cells to develop into preosteoblasts in a bone healing condition like a fracture (Albrektsson & Johansson, 2001). Numerous factors impress the biodegradation and resorption of calcium phosphate materials after implantation and cell mediated resorption has a leading part in the degradation of CPs. Several cell types are included in the degradation process by phagocytic mechanisms and osteoblasts can be categorized in this group (Heymann, Pradal, & Benahmed, 1999),(Sheikh et al., 2015). According to the results of MTT assay, alkaline phosphatase activity and histological investigations, it can be concluded that the activity of osteoblasts is higher in the CPO-coated scaffolds due to having more oxygen concentration. More degradation of new mineralized bone formation in the coated scaffolds may relate to the having more osteoinduction and osteoblasts activity in oxygen generating scaffolds.

In this study, a porous BCP scaffold with oxygen releasing ability was developed to rescue osteoblasts, restore normal function and improve bone repair after acute trauma. The scaffold was capable to deliver oxygen to osteoblast cells and increase their function and their survival. It demonstrated that oxygen generating materials have a positive impact on osteogenesis in which the mechanism is activation of osteoblasts. Oxygen can apparently increase the proliferation and differentiation of BMSCs. It is supposed that an oxygen enriched microenvironment is capable to improve *in situ* bone formation. Definitely, hypoxia has been indicated to limit osteogenesis through

reduction pre-existing osteoblast functions including alkaline phosphatase activity, calcium deposition and collagen synthesis. Furthermore, oxygen tension in normal range favors the osteogenic differentiation of MSCs.

With respect to animal study, it seems that the designed coated-scaffolds are able to effectively induce new bony tissue formation due to the release of oxygen *in situ* and the lesion site was significantly healed. The results indicate that supplemental oxygen in the defect site is able to accelerate healing time. The existence of oxygen in high level enhances bone regeneration through promoting alkaline phosphatase activity, angiogenesis and osteoblast differentiation (Al Hadi, Smerdon, & Fox, 2015). The mechanism of accelerated vessel growth by supplemental oxygen is through vascular endothelial growth factor (VEGF). VEGF is vital for stimulating angiogenesis in the wound area. Supplemental oxygen encourages the level of VEGF mRNA in endothelial cells and macrophages and elevates the expression of VEGF protein at wounds in vivo (Gordillo & Sen, 2003).

CHAPTER 6: CONCLUSION

6.1 Conclusion

Hypoxia, the result of disrupted vasculature, is one of the major challenges after scaffold implantation which can lead to tissue necrosis and can be categorized in the main limiting factors for fracture healing. Remedying hypoxia by supplying additional oxygen, can increase the cell proliferation, encourage the cell differentiation and prevent the infections and will majorly affect bone healing. Repairing the large defects of bone has still remained a challenge in clinical orthopedic surgery. Developing an engineered scaffold with a sustained oxygen release is an outstanding way for addressing the challenges of oxygen deficiency.

In this study, the bioceramic scaffolds were fabricated from biphasic calcium phosphate (BCP) powder with the composition of 60% hydroxyapatite (HA) and 40% betatricalcium phosphate (β-TCP). BCP ceramics are able to be tremendous scaffolds in bone tissue engineering for having bioactivity, osteointegrativity and osteoconductivity. The Robocasting technique was utilised for producing a porous structure comprising interpenetrated ceramic rods in a 3-dimensional tetragonal mesh. The scaffold was modelled by the finite element method (FEM) for computing the stress fields and predicting their mechanical performance. Calcium peroxide (CPO), as an oxygen-producing and antimicrobial biomaterial, was mixed with a polycaprolactone (PCL) solution and was coated on the scaffolds by the dip-coating method. The coating layer possessed three different percentages of CPO (1, 3 and 5 wt%). The oxygen-releasing profile proved that this design of coating-scaffold could be effective as a system of oxygen delivery. Qxygen release behaviour was sustained and dependant on the concentration of CPO encapsulated in the PCL coating matrix. It was also demonstrated that the coated scaffolds, having 3% CPO in the coating system, could provide a great potential for promoting bone ingrowth with improving osteoblast cells viability and

proliferation. According to the antibacterial investigations, releasing of CPO from the scaffolds could inhibit the growth of E. coli and S. aureus. Simulated body fluid (SBF) tests confirmed that the coated scaffolds because of CPO particles on their surface presented superior apatite precipitation in comparison with the uncoated one. The differentiated osteoblastic function was monitored by measuring the alkaline phosphatase (ALP) activity. The coated BCP scaffolds with 3% and 5% CPO exhibited higher ALP activity compared to the other samples. The results demonstrated that the proposed bioceramic-based scaffolds containing oxygen-generating coating could be optimised to supply an antibacterial performance, ideal mechanical properties, increased cell proliferation, improved ALP activity and higher apatite formation ability.

The present study investigated that how an oxygen-generating coating on the scaffold affects the bone regeneration. For this purpose, uncoated and 3%CPO coated BCP scaffolds fabricated by robocasting were implanted in the segmental bone defect of rabbit's radius and their capability of new bone formation were compared. For in vivo test, a 15-mm segment of bone was removed from the mid-shaft of radius thus; radial critical-sized defects were created in New Zealand White rabbits. CPO-coated and uncoated BCP scaffolds were implanted in the defects of experimental and control group, respectively. The empty group received no implantation. Repairing of Bone was investigated via X-ray, histological analysis and biomechanical tests at 3 and 6 months post-operatively, with immunohistochemical examinations at 6 months after operation. The CPO-coated scaffold compared to uncoated one presented augmented ability of osteogenesis because of having more osseointegration according to radiological observations, about 2 times higher newly formed bone based on histomorphometry analysis, over-expression of osteogenic markers including osteocalcin and superior biomechanical properties.

This study demonstrated that the applied oxygen generating coating could extend cell viability under hypoxic conditions. CPO was used as an oxygen generating element capable of sustained and localized oxygen release when encapsulated within the PCL matrix as a coating on the 3D–printed BCP scaffolds, fabricated by a robocasting method. It has been shown that the released oxygen from the scaffolds could maintain cell viability under hypoxic conditions. The results suggested that such scaffolds could be an outstanding candidate in order to promote bone ingrowth, while simultaneously increase the level of oxygen for surrounding tissues, preventing cell death due to hypoxia condition. The findings could assure the higher ability of bone repair for CPO-coated BCP scaffolds were implanted in the segmental defect of rabbit radius and might be an outstanding choice for healing of large and load bearing bone defects. Hence, the system of oxygen-generating coating/scaffold can be regarded as potent treatment for accelerated repairing of bone defects.

6.2 Recommendation

In this study, a BCP composite with the composition of 60% HA and 40% β-TCP was used for fabrication of the robocast scaffold. According to the results of in vivo test, the scaffold didn't experience a full degradation after 6 months of implantation. As the degradation rate increases with the percentage of β-TCP, so it is recommended to repeat the tests of this study with keeping all of the aspects and just altering the percentage of β-TCP and compare its results with the current study to investigate how the composition with more degradability affect the bone regeneration.

In the present study, the oxygen-generating system applied to the scaffolds by coating. Another study can be conducted to use the CPO particles (as an oxygen-generating agent) in the bulk of scaffolds and compare its results with the current study

to explore how the spreading of CPO powders in whole of the scaffolds can impress the bone regeneration.

The scaffolds in this study were implanted into the bone defects without prior cell culturing in them. . It is hoped that more studies can be conducted with culturing of MSCs in the scaffolds before implantation and then compare its results with the present study to assess how the seeding of stem cells in the scaffolds before the implantation can alter the bone regeneration in the defect.

In the present study, CPO particle are encapsulated in PCL, a hydrophobic material, to have sustained oxygen release and slow down the cytotoxicity. A new study can be conducted with a hydrophilic polymer for coating like PLGA and compare the results with the current study to investigate how a hydrophilic material can affect the cell behaviour, bone regeneration, etc.

Another recommendation can be related to the internal structure of the scaffold. For exploring the effect of pore geometry on bone regeneration, the shape of pores in robocast scaffolds can be changed.

REFERENCES

Abarrategi, Ander, Moreno-Vicente, Carolina, Martínez-Vázquez, Francisco Javier, Civantos, Ana, Ramos, Viviana, Sanz-Casado, José Vicente, . . . Miranda, Pedro. (2012). Biological properties of solid free form designed ceramic scaffolds with BMP-2: in vitro and in vivo evaluation. *PloS one, 7*(3), e34117.

Al Hadi, Hadil, Smerdon, Gary R, & Fox, Simon W. (2015). Hyperbaric oxygen therapy accelerates osteoblast differentiation and promotes bone formation. *Journal of dentistry, 43*(3), 382-388.

Albrektsson, T, & Johansson, C. (2001). Osteoinduction, osteoconduction and osseointegration. *European spine journal, 10*(2), S96-S101.

Arcaute, Karina, Mann, Brenda K, & Wicker, Ryan B. (2006). Stereolithography of three-dimensional bioactive poly (ethylene glycol) constructs with encapsulated cells. *Annals of biomedical engineering, 34*(9), 1429-1441.

Arinzeh, T Livingston, Tran, T, Mcalary, J, & Daculsi, G. (2005). A comparative study of biphasic calcium phosphate ceramics for human mesenchymal stem-cell-induced bone formation. *Biomaterials, 26*(17), 3631-3638.

Ashman, O, & Phillips, AM. (2013). Treatment of non-unions with bone defects: which option and why? *Injury, 44*, S43-S45.

Baghbani, F, Moztarzadeh, F, Nazari, A Gafari, Kamran, AH Razavi, Tondnevis, F, Nezafati, N, . . . Mozafari, M. (2012). Biological response of biphasic hydroxyapatite/tricalcium phosphate scaffolds intended for low load-bearing orthopaedic applications. *Advanced Composites Letters, 21*(1), 096369351202100102.

Baker, MA, Assis, SL, Higa, OZ, & Costa, Isolda. (2009). Nanocomposite hydroxyapatite formation on a Ti–13Nb–13Zr alloy exposed in a MEM cell culture medium and the effect of H2O2 addition. *Acta Biomaterialia, 5*(1), 63-75.

Baldeck, Jeremiah D, & Marquis, Robert E. (2008). Targets for hydrogen-peroxide-induced damage to suspension and biofilm cells of Streptococcus mutans. *Canadian journal of microbiology, 54*(10), 868-875.

Bansal, Sanjay, Chauhan, Vijendra, Sharma, Sansar, Maheshwari, Rajesh, Juyal, Anil, & Raghuvanshi, Shailendra. (2009). Evaluation of hydroxyapatite and beta-tricalcium phosphate mixed with bone marrow aspirate as a bone graft substitute for posterolateral spinal fusion. *Indian journal of orthopaedics, 43*(3), 234.

Bao, Quanwei, Chen, Sixu, Qin, Hao, Feng, Jianquan, Liu, Huayu, Liu, Daocheng, . . . Li, Junfeng. (2017). An appropriate Wnt/β-catenin expression level during the remodeling phase is required for improved bone fracture healing in mice. *Scientific Reports, 7*(1), 2695.

Bártolo, Paulo J, Almeida, Henrique A, Rezende, Rodrigo A, Laoui, Tahar, & Bidanda, Bopaya. (2008). Advanced processes to fabricate scaffolds for tissue engineering *Virtual prototyping & bio manufacturing in medical applications* (pp. 149-170): Springer.

Basrani, Bettina, Tjäderhane, Leo, Santos, J Miguel, Pascon, Elizeu, Grad, Helen, Lawrence, Herenia P, & Friedman, Shimon. (2003). Efficacy of chlorhexidine- and calcium hydroxide–containing medicaments against Enterococcus faecalis in vitro. *Oral Surgery, Oral Medicine, Oral Pathology, Oral Radiology, and Endodontology, 96*(5), 618-624.

Billiet, Thomas, Vandenhaute, Mieke, Schelfhout, Jorg, Van Vlierberghe, Sandra, & Dubruel, Peter. (2012). A review of trends and limitations in hydrogel-rapid prototyping for tissue engineering. *Biomaterials, 33*(26), 6020-6041.

Bjarnsholt, Thomas, Kirketerp-Møller, Klaus, Jensen, Peter Østrup, Madsen, Kit G, Phipps, Richard, Krogfelt, Karen, . . . Givskov, Michael. (2008). Why chronic wounds will not heal: a novel hypothesis. *Wound repair and regeneration, 16*(1), 2-10.

Bose, Susmita, Vahabzadeh, Sahar, & Bandyopadhyay, Amit. (2013). Bone tissue engineering using 3D printing. *Materials Today, 16*(12), 496-504.

Bouwman, WF, Bravenboer, N, Frenken, JWFH, Ten Bruggenkate, CM, & Schulten, EAJM. (2017). The use of a biphasic calcium phosphate in a maxillary sinus floor elevation procedure: a clinical, radiological, histological, and histomorphometric evaluation with 9-and 12-month healing times. *International journal of implant dentistry, 3*(1), 34.

Brighton, Carl T, & Krebs, Alfred G. (1972). Oxygen tension of healing fractures in the rabbit. *JBJS, 54*(2), 323-332.

Broggini, Nina, Bosshardt, Dieter D, Jensen, Simon S, Bornstein, Michael M, Wang, Chun-Cheng, & Buser, Daniel. (2015). Bone healing around nanocrystalline hydroxyapatite, deproteinized bovine bone mineral, biphasic calcium phosphate, and autogenous bone in mandibular bone defects. *Journal of Biomedical Materials Research Part B: Applied Biomaterials, 103*(7), 1478-1487.

Calori, GM, Mazza, E, Colombo, M, & Ripamonti, C. (2011). The use of bone-graft substitutes in large bone defects: any specific needs? *Injury, 42*, S56-S63.

Camci-Unal, Gulden, Alemdar, Neslihan, Annabi, Nasim, & Khademhosseini, Ali. (2013). Oxygen-releasing biomaterials for tissue engineering. *Polymer international, 62*(6), 843-848.

Cao, Yang, Mitchell, Geraldine, Messina, Aurora, Price, Lisa, Thompson, Erik, Penington, Anthony, . . . Cooper-White, Justin. (2006). The influence of architecture on degradation and tissue ingrowth into three-dimensional poly (lactic-co-glycolic acid) scaffolds in vitro and in vivo. *Biomaterials, 27*(14), 2854-2864.

Capulli, Mattia, Paone, Riccardo, & Rucci, Nadia. (2014). Osteoblast and osteocyte: games without frontiers. *Archives of biochemistry and biophysics, 561*, 3-12.

Carlier, Aurélie, Geris, Liesbet, van Gastel, Nick, Carmeliet, Geert, & Van Oosterwyck, Hans. (2015). Oxygen as a critical determinant of bone fracture healing—a multiscale model. *Journal of theoretical biology, 365*, 247-264.

Chen, S-H, Lei, M, Xie, X-H, Zheng, L-Z, Yao, D, Wang, X-L, . . . Xiao, D-M. (2013). PLGA/TCP composite scaffold incorporating bioactive phytomolecule icaritin for enhancement of bone defect repair in rabbits. *Acta biomaterialia, 9*(5), 6711-6722.

Cheng, Connie, Trzcinski, Olivia, & Doering, Laurie C. (2014). Fluorescent labeling of dendritic spines in cell cultures with the carbocyanine dye "DiI". *Frontiers in neuroanatomy, 8*, 30.

Cheng, S, Yan, D, Chen, JT, Zhuo, RF, Feng, JJ, Li, HJ, . . . Yan, PX. (2009). Soft-template synthesis and characterization of ZnO2 and ZnO hollow spheres. *The Journal of Physical Chemistry C, 113*(31), 13630-13635.

Chiang, Poney, & Burrows, Lori L. (2003). Biofilm formation by hyperpiliated mutants of Pseudomonas aeruginosa. *Journal of bacteriology, 185*(7), 2374-2378.

Cho, Jung Sang, Chung, Chong-Pyong, & Rhee, Sang-Hoon. (2011). Bioactivity and osteoconductivity of biphasic calcium phosphates. *Bioceramics Development and Applications, 1*.

Council, National Research. (2010). *Guide for the care and use of laboratory animals*: National Academies Press.

Danesh-Sani, Seyed Amir, Shariati-Sarabi, Zhaleh, & Feiz, Mohammad Reza. (2012). Comprehensive review of hyperbaric oxygen therapy. *Journal of Craniofacial Surgery, 23*(5), e483-e491.

de Almeida Gomes, Brenda Paula Figueiredo, Vianna, Morgana Eli, Sena, Neylla Teixeira, Zaia, Alexandre Augusto, Ferraz, Caio Cezar Randi, & de Souza Filho, Francisco José. (2006). In vitro evaluation of the antimicrobial activity of calcium hydroxide combined with chlorhexidine gel used as intracanal medicament. *Oral Surgery, Oral Medicine, Oral Pathology, Oral Radiology, and Endodontology, 102*(4), 544-550.

Dellinger, Jennifer G, Cesarano, Joseph, & Jamison, Russell D. (2007). Robotic deposition of model hydroxyapatite scaffolds with multiple architectures and multiscale porosity for bone tissue engineering. *Journal of Biomedical Materials Research Part A, 82*(2), 383-394.

Dellinger, Jennifer G, Wojtowicz, Abigail M, & Jamison, Russell D. (2006). Effects of degradation and porosity on the load bearing properties of model hydroxyapatite bone scaffolds. *Journal of Biomedical Materials Research Part A: An Official Journal of The Society for Biomaterials, The Japanese Society for Biomaterials, and The Australian Society for Biomaterials and the Korean Society for Biomaterials, 77*(3), 563-571.

Detsch, Rainer, Schaefer, Susannne, Deisinger, Ulrike, Ziegler, Guenter, Seitz, Hermann, & Leukers, Barbara. (2011). In vitro-osteoclastic activity studies on surfaces of 3D printed calcium phosphate scaffolds. *Journal of biomaterials applications, 26*(3), 359-380.

Dimitriou, Rozalia, Jones, Elena, McGonagle, Dennis, & Giannoudis, Peter V. (2011). Bone regeneration: current concepts and future directions. *BMC medicine, 9*(1), 66.

Eisenbud, David E. (2012). Oxygen in wound healing: nutrient, antibiotic, signaling molecule, and therapeutic agent. *Clinics in plastic surgery, 39*(3), 293-310.

Elzein, Tamara, Nasser-Eddine, Mohamad, Delaite, Christelle, Bistac, Sophie, & Dumas, Philippe. (2004). FTIR study of polycaprolactone chain organization at interfaces. *Journal of colloid and interface science, 273*(2), 381-387.

Entezari, Ali, Zhang, Zhongpu, Chen, Junning, & Li, Qing. (2014). Optimization of bone tissue scaffolds fabricated by robocasting technique.

Estrela, Carlos, & Holland, Roberto. (2003). Calcium hydroxide: study based on scientific evidences. *Journal of Applied Oral Science, 11*(4), 269-282.

Fakhry, Maya, Hamade, Eva, Badran, Bassam, Buchet, René, & Magne, David. (2013). Molecular mechanisms of mesenchymal stem cell differentiation towards osteoblasts. *World journal of stem cells, 5*(4), 136.

Farris, Ashley L, Rindone, Alexandra N, & Grayson, Warren L. (2016). Oxygen delivering biomaterials for tissue engineering. *Journal of Materials Chemistry B, 4*(20), 3422-3432.

Florencio-Silva, Rinaldo, Sasso, Gisela Rodrigues da Silva, Sasso-Cerri, Estela, Simões, Manuel Jesus, & Cerri, Paulo Sérgio. (2015). Biology of bone tissue: structure, function, and factors that influence bone cells. *BioMed research international, 2015*.

Forget, Aurelien, Staehly, Camille, Ninan, Neethu, Harding, Frances J, Vasilev, Krasimir, Voelcker, Nicolas H, & Blencowe, Anton. (2017). Oxygen-releasing coatings for improved tissue preservation. *ACS Biomaterials Science & Engineering, 3*(10), 2384-2390.

Franklyn, Melanie, & Field, Bruce. (2013). Experimental and finite element analysis of tibial stress fractures using a rabbit model. *World journal of orthopedics, 4*(4), 267.

Gautam, Sneh, Chou, Chia-Fu, Dinda, Amit Kumar, Potdar, Pravin D, & Mishra, Narayan Chandra. (2014). Fabrication and characterization of PCL/gelatin/chitosan ternary nanofibrous composite scaffold for tissue engineering applications. *Journal of materials science, 49*(3), 1076-1089.

Ghafari-Nazari, Ali, Moztarzadeh, Fathollah, Rabiee, Sayed Mahmood, Rajabloo, Talieh, Mozafari, Masoud, & Tayebi, Lobat. (2012). Antibacterial activity of

silver photodeposited nepheline thin film coatings. *Ceramics International, 38*(7), 5445-5451.

Gholipourmalekabadi, Mazaher, Zhao, Susan, Harrison, Benjamin S, Mozafari, Masoud, & Seifalian, Alexander M. (2016). Oxygen-generating biomaterials: a new, viable paradigm for tissue engineering? *Trends in biotechnology, 34*(12), 1010-1021.

Giuliani, Mauro, Moritz, Wolfgang, Bodmer, Elvira, Dindo, Daniel, Kugelmeier, Patrick, Lehmann, Roger, . . . Weber, Markus. (2005). Central necrosis in isolated hypoxic human pancreatic islets: evidence for postisolation ischemia. *Cell transplantation, 14*(1), 67-76.

Gordillo, Gayle M, & Sen, Chandan K. (2003). Revisiting the essential role of oxygen in wound healing. *The American journal of surgery, 186*(3), 259-263.

Granström, Gösta. (2003). Radiotherapy, osseointegration and hyperbaric oxygen therapy. *Periodontology 2000, 33*(1), 145-162.

Guo, S al, & DiPietro, Luisa A. (2010). Factors affecting wound healing. *Journal of dental research, 89*(3), 219-229.

Harrison, Benjamin S, Eberli, Daniel, Lee, Sang Jin, Atala, Anthony, & Yoo, James J. (2007). Oxygen producing biomaterials for tissue regeneration. *Biomaterials, 28*(31), 4628-4634.

He, Jiawei, Genetos, Damian C, Yellowley, Clare E, & Leach, J Kent. (2010). Oxygen tension differentially influences osteogenic differentiation of human adipose stem cells in 2D and 3D cultures. *Journal of cellular biochemistry*, *110*(1), 87-96.

Heymann, Dominique, Pradal, G, & Benahmed, M. (1999). Cellular mechanisms of calcium phosphate ceramic degradation. *Histology and histopathology, 14*(3), 871-877.

Hollister, Scott J. (2005). Porous scaffold design for tissue engineering. *Nature materials, 4*(7), 518-524.

Holzwarth, Christina, Vaegler, Martin, Gieseke, Friederike, Pfister, Stefan M, Handgretinger, Rupert, Kerst, Gunter, & Müller, Ingo. (2010). Low physiologic oxygen tensions reduce proliferation and differentiation of human multipotent mesenchymal stromal cells. *BMC cell biology, 11*(1), 11.

Houmard, Manuel, Fu, Qiang, Genet, Martin, Saiz, Eduardo, & Tomsia, Antoni P. (2013). On the structural, mechanical, and biodegradation properties of HA/β-TCP robocast scaffolds. *Journal of Biomedical Materials Research Part B: Applied Biomaterials, 101*(7), 1233-1242.

Hsu, Shu-Han, Chen, Chien-Tsun, & Wei, Yau-Huei. (2013). Inhibitory effects of hypoxia on metabolic switch and osteogenic differentiation of human mesenchymal stem cells. *Stem cells, 31*(12), 2779-2788.

Hutmacher, Dietmar W. (2000). Scaffolds in tissue engineering bone and cartilage. *Biomaterials, 21*(24), 2529-2543.

Hwang, Ji-Wan, Park, Jae-Sub, Lee, Jung-Seok, Jung, Ui-Won, Kim, Chang-Sung, Cho, Kyoo-Sung, . . . Choi, Seong-Ho. (2012). Comparative evaluation of three calcium phosphate synthetic block bone graft materials for bone regeneration in rabbit calvaria. *Journal of Biomedical Materials Research Part B: Applied Biomaterials, 100*(8), 2044-2052.

Johnson, Amy J Wagoner, & Herschler, Brad A. (2011). A review of the mechanical behavior of CaP and CaP/polymer composites for applications in bone replacement and repair. *Acta biomaterialia, 7*(1), 16-30.

Kalfas, Iain H. (2001). Principles of bone healing. *Neurosurgical focus, 10*(4), 1-4.

Karageorgiou, Vassilis, & Kaplan, David. (2005). Porosity of 3D biomaterial scaffolds and osteogenesis. *Biomaterials, 26*(27), 5474-5491.

Kargozar, Saeid, Hashemian, Seyed Jafar, Soleimani, Mansooreh, Milan, Peiman Brouki, Askari, Mohammad, Khalaj, Vahid, . . . Latifi, Noorahmad. (2017). Acceleration of bone regeneration in bioactive glass/gelatin composite scaffolds seeded with bone marrow-derived mesenchymal stem cells over-expressing bone morphogenetic protein-7. *Materials Science and Engineering: C, 75*, 688-698.

Kargozar, Saeid, Lotfibakhshaiesh, Nasrin, Ai, Jafar, Samadikuchaksaraie, Ali, Hill, Robert G, Shah, Priyen A, . . . Joghataei, Mohammad Taghi. (2016). Synthesis, physico-chemical and biological characterization of strontium and cobalt substituted bioactive glasses for bone tissue engineering. *Journal of Non-Crystalline Solids, 449*, 133-140.

Karthega, M, Nagarajan, S, & Rajendran, N. (2010). In vitro studies of hydrogen peroxide treated titanium for biomedical applications. *Electrochimica acta, 55*(6), 2201-2209.

Kasten, Philip, Vogel, Julia, Geiger, Florian, Niemeyer, Philipp, Luginbühl, Reto, & Szalay, Krisztian. (2008). The effect of platelet-rich plasma on healing in critical-size long-bone defects. *Biomaterials, 29*(29), 3983-3992.

Kato, Hirohito, Katayama, Nobuhito, Taguchi, Yoichiro, Tominaga, Kazuya, Umeda, Makoto, & Tanaka, Akio. (2013). A synthetic oligopeptide derived from enamel matrix derivative promotes the differentiation of human periodontal ligament stem cells into osteoblast-like cells with increased mineralization. *Journal of periodontology, 84*(10), 1476-1483.

Khoo, Xiaojuan, Hamilton, Paul, O'Toole, George A, Snyder, Brian D, Kenan, Daniel J, & Grinstaff, Mark W. (2009). Directed assembly of PEGylated-peptide coatings for infection-resistant titanium metal. *Journal of the American Chemical Society, 131*(31), 10992-10997.

Kim, Hae-Won, Knowles, Jonathan C, & Kim, Hyoun-Ee. (2004). Development of hydroxyapatite bone scaffold for controlled drug release via poly (ϵ-caprolactone) and hydroxyapatite hybrid coatings. *Journal of Biomedical*

Materials Research Part B: Applied Biomaterials: An Official Journal of The Society for Biomaterials, The Japanese Society for Biomaterials, and The Australian Society for Biomaterials and the Korean Society for Biomaterials, 70(2), 240-249.

Kim, Jun Sung, Kuk, Eunye, Yu, Kyeong Nam, Kim, Jong-Ho, Park, Sung Jin, Lee, Hu Jang, . . . Hwang, Cheol-Yong. (2007). Antimicrobial effects of silver nanoparticles. *Nanomedicine: Nanotechnology, Biology and Medicine, 3*(1), 95-101.

Kim, Tae-Wan, Lee, Hyeong-Shin, Kim, Dong-Hyun, Jin, Hyeong-Ho, Hwang, Kyu-Hong, Lee, Jong Kook, . . . Yoon, Seog-Young. (2012). In situ synthesis of magnesium-substituted biphasic calcium phosphate and in vitro biodegradation. *Materials Research Bulletin, 47*(9), 2506-2512.

Kokubo, Tadashi, & Takadama, Hiroaki. (2006). How useful is SBF in predicting in vivo bone bioactivity? *Biomaterials, 27*(15), 2907-2915.

Krishnan, Venkatesh, Bryant, Henry U, & MacDougald, Ormond A. (2006). Regulation of bone mass by Wnt signaling. *The Journal of clinical investigation, 116*(5), 1202-1209.

Kubarev, OL, Komlev, VS, & Barinov, SM. (2010). Bioactive ceramic composite materials in hydroxyapatite-tricalcium phosphate system. *Inorganic Materials: Applied Research, 1*(3), 182-187.

Lee, Mun-Hwan, You, Changkook, & Kim, Kyo-Han. (2015). Combined effect of a microporous layer and type I collagen coating on a biphasic calcium phosphate scaffold for bone tissue engineering. *Materials, 8*(3), 1150-1161.

LeGeros, RZ, Lin, S, Rohanizadeh, R, Mijares, D, & LeGeros, JP. (2003). Biphasic calcium phosphate bioceramics: preparation, properties and applications. *Journal of materials science: Materials in Medicine, 14*(3), 201-209.

Lewis, Jennifer A, Smay, James E, Stuecker, John, & Cesarano, Joseph. (2006). Direct ink writing of three-dimensional ceramic structures. *Journal of the American Ceramic Society, 89*(12), 3599-3609.

Li, Zhenqing, Guo, Xiaolei, & Guan, Jianjun. (2012). An oxygen release system to augment cardiac progenitor cell survival and differentiation under hypoxic condition. *Biomaterials, 33*(25), 5914-5923.

Lin, Song-Shu, Ueng, Steve WN, Niu, Chi-Chien, Yuan, Li-Jen, Yang, Chuen-Yung, Chen, Wen-Jer, . . . Chen, Jan-Kan. (2014). Hyperbaric oxygen promotes osteogenic differentiation of bone marrow stromal cells by regulating Wnt3a/β-catenin signaling—an in vitro and in vivo study. *Stem cell research, 12*(1), 260-274.

Liu, C, Xia, Z, & Czernuszka, JT. (2007). Design and development of three-dimensional scaffolds for tissue engineering. *Chemical Engineering Research and Design, 85*(7), 1051-1064.

Lu, Chuanyong, Saless, Neema, Wang, Xiaodong, Sinha, Arjun, Decker, Sebastian, Kazakia, Galateia, . . . Hunt, Thomas K. (2013). The role of oxygen during fracture healing. *Bone, 52*(1), 220-229.

Ma, Yong, Zhang, Bo-Tao, Zhao, Lixia, Guo, Guangsheng, & Lin, Jin-Ming. (2007). Study on the generation mechanism of reactive oxygen species on calcium peroxide by chemiluminescence and UV-visible spectra. *Luminescence: The journal of biological and chemical luminescence, 22*(6), 575-580.

Mal, S, Berendt, AR, & Peacock, SJ. (2002). Staphylococcus aureus bone and joint infection. *Journal of infection, 44*(3), 143-151.

Martínez-Vázquez, Francisco J, Perera, Fidel H, Miranda, Pedro, Pajares, Antonia, & Guiberteau, Fernando. (2010). Improving the compressive strength of bioceramic robocast scaffolds by polymer infiltration. *Acta Biomaterialia, 6*(11), 4361-4368.

Martínez-Vázquez, Francisco J, Miranda, Pedro, Guiberteau, Fernando, & Pajares, Antonia. (2013). Reinforcing bioceramic scaffolds with in situ synthesized ε-polycaprolactone coatings. *Journal of Biomedical Materials Research Part A: An Official Journal of The Society for Biomaterials, The Japanese Society for Biomaterials, and The Australian Society for Biomaterials and the Korean Society for Biomaterials, 101*(12), 3551-3559.

Mayr, Helmar, Schlüfter, Susanne, Detsch, Rainer, & Ziegler, Günter. (2008). *Influence of phase composition on degradation and resorption of biphasic calcium phosphate ceramics.* Paper presented at the Key Engineering Materials.

Melchels, Ferry PW, Feijen, Jan, & Grijpma, Dirk W. (2010). A review on stereolithography and its applications in biomedical engineering. *Biomaterials, 31*(24), 6121-6130.

Miranda, Pedro, Pajares, Antonia, & Guiberteau, Fernando. (2008). Finite element modeling as a tool for predicting the fracture behavior of robocast scaffolds. *Acta biomaterialia, 4*(6), 1715-1724.

Miranda, Pedro, Pajares, Antonia, Saiz, Eduardo, Tomsia, Antoni P, & Guiberteau, Fernando. (2007). Fracture modes under uniaxial compression in hydroxyapatite scaffolds fabricated by robocasting. *Journal of Biomedical Materials Research Part A: An Official Journal of The Society for Biomaterials, The Japanese Society for Biomaterials, and The Australian Society for Biomaterials and the Korean Society for Biomaterials, 83*(3), 646-655.

Miranda, Pedro, Pajares, Antonia, Saiz, Eduardo, Tomsia, Antoni P, & Guiberteau, Fernando. (2008a). Mechanical properties of calcium phosphate scaffolds fabricated by robocasting. *Journal of Biomedical Materials Research Part A, 85*(1), 218-227.

Miranda, Pedro, Pajares, Antonia, Saiz, Eduardo, Tomsia, Antoni P, & Guiberteau, Fernando. (2008b). Mechanical properties of calcium phosphate scaffolds fabricated by robocasting. *Journal of Biomedical Materials Research Part A: An Official Journal of The Society for Biomaterials, The Japanese Society for*

Biomaterials, and The Australian Society for Biomaterials and the Korean Society for Biomaterials, 85(1), 218-227.

Mohamed, Alizae Marny. (2008). An overview of bone cells and their regulating factors of differentiation. *The Malaysian journal of medical sciences: MJMS, 15*(1), 4.

Mohammadi, Z, Shalavi, S, & Yazdizadeh, M. (2012). Antimicrobial activity of calcium hydroxide in endodontics: a review. *Chonnam medical journal, 48*(3), 133-140.

Mouriño, Viviana, & Boccaccini, Aldo R. (2009). Bone tissue engineering therapeutics: controlled drug delivery in three-dimensional scaffolds. *Journal of the Royal Society Interface*, rsif20090379.

Mura, Anna, Medda, Rosaria, Longu, Silvia, Floris, Giovanni, Rinaldi, Andrea C, & Padiglia, Alessandra. (2005). A Ca2+/Calmodulin-Binding Peroxidase from Euphorbia Latex: Novel Aspects of Calcium− Hydrogen Peroxide Cross-Talk in the Regulation of Plant Defenses. *Biochemistry, 44*(43), 14120-14130.

Murphy, Ciara M, Haugh, Matthew G, & O'brien, Fergal J. (2010). The effect of mean pore size on cell attachment, proliferation and migration in collagen–glycosaminoglycan scaffolds for bone tissue engineering. *Biomaterials, 31*(3), 461-466.

Northup, Abraham, & Cassidy, Daniel. (2008). Calcium peroxide (CaO2) for use in modified Fenton chemistry. *Journal of Hazardous Materials, 152*(3), 1164-1170.

O'brien, Fergal J. (2011). Biomaterials & scaffolds for tissue engineering. *Materials today, 14*(3), 88-95.

Oh, Se Heang, Ward, Catherine L, Atala, Anthony, Yoo, James J, & Harrison, Benjamin S. (2009). Oxygen generating scaffolds for enhancing engineered tissue survival. *Biomaterials, 30*(5), 757-762.

Okubo, Yasunori, Bessho, Kazuhisa, Fujimura, Kazuma, Konishi, Yasuzo, Kusumoto, Kenji, Ogawa, Yutaka, & Iizuka, Tadahiko. (2000). Osteoinduction by recombinant human bone morphogenetic protein-2 at intramuscular, intermuscular, subcutaneous and intrafatty sites. *International Journal of Oral & Maxillofacial Surgery, 29*(1), 62-66.

Olszta, Matthew J, Cheng, Xingguo, Jee, Sang Soo, Kumar, Rajendra, Kim, Yi-Yeoun, Kaufman, Michael J, . . . Gower, Laurie B. (2007). Bone structure and formation: a new perspective. *Materials Science and Engineering: R: Reports, 58*(3), 77-116.

Ozdemir, Burcu, Kurtis, Bulent, Tuter, Gulay, Senguven, Burcu, & Yildirim, Benay. (2016). Osteocalcin and osteonectin expression after double application of platelet-rich plasma in rabbits. *Journal of Istanbul University Faculty of Dentistry, 50*(2), 1.

Özkadif, S, Eken, E, Beşoluk, K, & Dayan, MO. (2015). Three-dimensional reconstruction of New Zealand rabbit antebrachium by multidetector computed tomography. *Iranian journal of veterinary research, 16*(2), 205.

Park, JH, Park, BH, Kim, HK, Park, TS, & Baek, HS. (2002). Hypoxia decreases Runx2/Cbfa1 expression in human osteoblast-like cells. *Molecular and cellular endocrinology, 192*(1-2), 197-203.

Park, Su A, Lee, Hyo-Jung, Kim, Keun-Suh, Lee, Sang Jin, Lee, Jung-Tae, Kim, Sung-Yeol, . . . Park, Shin-Young. (2018). In vivo evaluation of 3D-printed polycaprolactone scaffold implantation combined with β-TCP powder for alveolar bone augmentation in a beagle defect model. *Materials, 11*(2), 238.

Pedraza, Eileen, Coronel, Maria M, Fraker, Christopher A, Ricordi, Camillo, & Stabler, Cherie L. (2012a). Preventing hypoxia-induced cell death in beta cells and islets via hydrolytically activated, oxygen-generating biomaterials. *Proceedings of the National Academy of Sciences*, 201113560.

Pedraza, Eileen, Coronel, Maria M, Fraker, Christopher A, Ricordi, Camillo, & Stabler, Cherie L. (2012b). Preventing hypoxia-induced cell death in beta cells and islets via hydrolytically activated, oxygen-generating biomaterials. *Proceedings of the National Academy of Sciences, 109*(11), 4245-4250.

Peltola, Sanna M, Melchels, Ferry PW, Grijpma, Dirk W, & Kellomäki, Minna. (2008). A review of rapid prototyping techniques for tissue engineering purposes. *Annals of medicine, 40*(4), 268-280.

Petite, Herve, Viateau, Veronique, Bensaid, Wassila, Meunier, Alain, de Pollak, Cindy, Bourguignon, Marianne, . . . Guillemin, Genevieve. (2000). Tissue-engineered bone regeneration. *Nature biotechnology, 18*(9), 959.

Pfister, Andreas, Landers, Rüdiger, Laib, Andres, Hübner, Ute, Schmelzeisen, Rainer, & Mülhaupt, Rolf. (2004). Biofunctional rapid prototyping for tissue-engineering applications: 3D bioplotting versus 3D printing. *Journal of Polymer Science Part A: Polymer Chemistry, 42*(3), 624-638.

Pham, DT, Dimov, S, & Lacan, F. (1999). Selective laser sintering: applications and technological capabilities. *Proceedings of the Institution of Mechanical Engineers, Part B: Journal of Engineering Manufacture, 213*(5), 435-449.

Popov, VK, Evseev, AV, Ivanov, AL, Roginski, VV, Volozhin, AI, & Howdle, SM. (2004). Laser stereolithography and supercritical fluid processing for custom-designed implant fabrication. *Journal of Materials Science: Materials in Medicine, 15*(2), 123-128.

Prins, Henk-Jan, Braat, A Koen, Gawlitta, D, Dhert, Wouter JA, Egan, David A, Tijssen-Slump, Estel, . . . Martens, Anton C. (2014). In vitro induction of alkaline phosphatase levels predicts in vivo bone forming capacity of human bone marrow stromal cells. *Stem cell research, 12*(2), 428-440.

Qi, Lifeng, Xu, Zirong, Jiang, Xia, Hu, Caihong, & Zou, Xiangfei. (2004). Preparation and antibacterial activity of chitosan nanoparticles. *Carbohydrate research, 339*(16), 2693-2700.

Ragab, HS, Ibrahim, FA, Abdallah, F, Al-Ghamdi, Attieh A, El-Tantawy, Farid, Radwan, Neyara, & Yakuphanoglu, F. (2014). Synthesis and in vitro antibacterial properties of hydroxyapatite nanoparticles. *IOSR J. Pharm. Biol. Sci, 9*, 77-85.

Rajendran, Archana, Barik, Rakesh C, Natarajan, Duraipandy, Kiran, MS, & Pattanayak, Deepak K. (2014). Synthesis, phase stability of hydroxyapatite–silver composite with antimicrobial activity and cytocompatability. *Ceramics International, 40*(7), 10831-10838.

Randorn, Chamnan, Kanta, Acharapun, Yaemsunthorn, Kasidid, & Rujijanakul, Gobwute. (2015). Fabrication of dense biocompatible hydroxyapatite ceramics with high hardness using a peroxide-based route: a potential process for scaling up. *Ceramics International, 41*(4), 5594-5599.

Rawadi, Georges, & Roman-Roman, Sergio. (2005). Wnt signalling pathway: a new target for the treatment of osteoporosis. *Expert opinion on therapeutic targets, 9*(5), 1063-1077.

Rodriguez, Paola G, Felix, Frances N, Woodley, David T, & Shim, Elisabeth K. (2008). The role of oxygen in wound healing: a review of the literature. *Dermatologic surgery, 34*(9), 1159-1169.

Roohani-Esfahani, Seyed-Iman, Nouri-Khorasani, Saied, Lu, Zufu, Appleyard, Richard, & Zreiqat, Hala. (2010). The influence hydroxyapatite nanoparticle shape and size on the properties of biphasic calcium phosphate scaffolds coated with hydroxyapatite–PCL composites. *Biomaterials, 31*(21), 5498-5509.

Russias, J, Saiz, Eduardo, Deville, Sylvain, Gryn, Karol, Liu, G, Nalla, RK, & Tomsia, Antoni P. (2007). Fabrication and in vitro characterization of three-dimensional organic/inorganic scaffolds by robocasting. *Journal of Biomedical Materials Research Part A, 83*(2), 434-445.

Russias, Julie, Saiz, Eduardo, Deville, Sylvain, Gryn, Karol, Liu, G, Nalla, Ravi K, & Tomsia, Antoni P. (2007). Fabrication and in vitro characterization of three-dimensional organic/inorganic scaffolds by robocasting. *Journal of Biomedical Materials Research Part A: An Official Journal of The Society for Biomaterials, The Japanese Society for Biomaterials, and The Australian Society for Biomaterials and the Korean Society for Biomaterials*, *83*(2), 434-445.

Sachlos, E, & Czernuszka, JT. (2003). Making tissue engineering scaffolds work. Review: the application of solid freeform fabrication technology to the production of tissue engineering scaffolds. *Eur Cell Mater, 5*(29), 39-40.

Salim, Ali, Nacamuli, Randall P, Morgan, Elise F, Giaccia, Amato J, & Longaker, Michael T. (2004). Transient changes in oxygen tension inhibit osteogenic differentiation and Runx2 expression in osteoblasts. *Journal of Biological Chemistry*, *279*(38), 40007-40016.

Schumacher, M, Deisinger, U, Detsch, R, & Ziegler, G. (2010). Indirect rapid prototyping of biphasic calcium phosphate scaffolds as bone substitutes: influence of phase composition, macroporosity and pore geometry on mechanical properties. *Journal of Materials Science: Materials in Medicine, 21*(12), 3119-3127.

Sen, Chandan K. (2003). The general case for redox control of wound repair. *Wound Repair and Regeneration, 11*(6), 431-438.

Sharifi, Davood, Khoushkerdar, Hamid Reza, Abedi, Gholamreza, Asghari, Ahmad, & Hesaraki, Saeed. (2012). Mechanical properties of radial bone defects treated with autogenous graft covered with hydroxyapatite in rabbit. *Acta cirurgica brasileira, 27*(3), 256-259.

Sheikh, Zeeshan, Abdallah, Mohamed-Nur, Hanafi, Ahmed, Misbahuddin, Syed, Rashid, Haroon, & Glogauer, Michael. (2015). Mechanisms of in vivo degradation and resorption of calcium phosphate based biomaterials. *Materials, 8*(11), 7913-7925.

Siqueira Jr, JF, & Lopes, HP. (1999). Mechanisms of antimicrobial activity of calcium hydroxide: a critical review. *International endodontic journal, 32*(5), 361-369.

Sladdin, M, & Lynch, JM. (1983). Antimicrobial properties of calcium peroxide in relation to its potential use as a seed dressing. *Microbiology, 129*(7), 2307-2314.

Smay, James E, Cesarano, Joseph, & Lewis, Jennifer A. (2002). Colloidal inks for directed assembly of 3-D periodic structures. *Langmuir, 18*(14), 5429-5437.

Song, Sang-Heon, Yun, Young-Pil, Kim, Hak-Jun, Park, Kyeongsoon, Kim, Sung Eun, & Song, Hae-Ryong. (2014). Bone formation in a rat tibial defect model using carboxymethyl cellulose/BioC/bone morphogenic protein-2 hybrid materials. *BioMed research international, 2014*.

Steg, Hilde, Buizer, Arina T, Woudstra, Willem, Veldhuizen, Albert G, Bulstra, Sjoerd K, Grijpma, Dirk W, & Kuijer, Roel. (2015). Control of oxygen release from peroxides using polymers. *Journal of Materials Science: Materials in Medicine, 26*(7), 1-4.

Stock, Ulrich A, & Vacanti, Joseph P. (2001). Tissue engineering: current state and prospects. *Annual review of medicine, 52*(1), 443-451.

Suchanek, Wojciech, & Yoshimura, Masahiro. (1998). Processing and properties of hydroxyapatite-based biomaterials for use as hard tissue replacement implants. *Journal of Materials Research, 13*(1), 94-117.

Sulaiman, Shamsul Bin, Keong, Tan Kok, Cheng, Chen Hui, Saim, Aminuddin Bin, & Idrus, Ruszymah Bt Hj. (2013). Tricalcium phosphate/hydroxyapatite (TCP-HA) bone scaffold as potential candidate for the formation of tissue engineered bone. *The Indian journal of medical research, 137*(6), 1093.

Tadic, D, & Epple, M. (2004). A thorough physicochemical characterisation of 14 calcium phosphate-based bone substitution materials in comparison to natural bone. *Biomaterials, 25*(6), 987-994.

Touri, Maria, Kabirian, Fatemeh, Saadati, Mahdi, Ramakrishna, Seeram, & Mozafari, Masoud. (2019). Additive manufacturing of biomaterials− the evolution of rapid prototyping. *Advanced Engineering Materials, 21*(2), 1800511.

Touri, Maria, Moztarzadeh, Fathollah, Osman, Noor Azuan Abu, Dehghan, Mohammad Mehdi, & Mozafari, Masoud. (2018a). 3D–printed biphasic calcium phosphate scaffolds coated with an oxygen generating system for enhancing engineered tissue survival. *Materials Science and Engineering: C, 84*, 236-242. doi: https://doi.org/10.1016/j.msec.2017.11.037

Touri, Maria, Moztarzadeh, Fathollah, Osman, Noor Azuan Abu, Dehghan, Mohammad Mehdi, & Mozafari, Masoud. (2018b). Breathable tissue engineering scaffolds: An efficient design-optimization by additive manufacturing. *Materials Today: Proceedings, 5*(7), 15813-15820.

Touri, Maria, Moztarzadeh, Fathollah, Osman, Noor Azuan Abu, Dehghan, Mohammad Mehdi, & Mozafari, Masoud. (2019). Optimisation and biological activities of bioceramic robocast scaffolds provided with an oxygen-releasing coating for bone tissue engineering applications. *Ceramics International, 45*(1), 805-816.

Touri, R, Moztarzadeh, F, Sadeghian, Z, Bizari, D, Tahriri, M, & Mozafari, M. (2013). The use of carbon nanotubes to reinforce 45S5 bioglass-based scaffolds for tissue engineering applications. *BioMed research international, 2013*.

Tsao, Yu-Tzu, Huang, Yi-Jeng, Wu, Hao-Hsiang, Liu, Yu-An, Liu, Yi-Shiuan, & Lee, Oscar K. (2017). Osteocalcin mediates biomineralization during osteogenic maturation in human mesenchymal stromal cells. *International journal of molecular sciences, 18*(1), 159.

Tuncay, Orhan C, Ho, Daphne, & Barker, Melissa K. (1994). Oxygen tension regulates osteoblast function. *American Journal of Orthodontics and Dentofacial Orthopedics, 105*(5), 457-463.

Utting, JC, Robins, SP, Brandao-Burch, A, Orriss, IR, Behar, J, & Arnett, TR. (2006). Hypoxia inhibits the growth, differentiation and bone-forming capacity of rat osteoblasts. *Experimental cell research, 312*(10), 1693-1702.

Verras, Meletios, Papandreou, Ioanna, Lim, Ai Lin, & Denko, Nicholas C. (2008). Tumor hypoxia blocks Wnt processing and secretion through the induction of endoplasmic reticulum stress. *Molecular and cellular biology, 28*(23), 7212-7224.

Wandiyanto, Jason V, Truong, Vi Khanh, Al Kobaisi, Mohammad, Juodkazis, Saulius, Thissen, Helmut, Bazaka, Olha, . . . Ivanova, Elena P. (2019). The fate of osteoblast-like mg-63 cells on pre-infected bactericidal nanostructured titanium surfaces. *Materials, 12*(10), 1575.

Wang, Junping, Zhu, Yizhou, Bawa, Harinder K, Ng, Geoffrey, Wu, Yong, Libera, Matthew, . . . Yu, Xiaojun. (2010). Oxygen-generating nanofiber cell scaffolds with antimicrobial properties. *ACS applied materials & interfaces, 3*(1), 67-73.

Wang, Junping, Zhu, Yizhou, Bawa, Harinder K, Ng, Geoffrey, Wu, Yong, Libera, Matthew, . . . Yu, Xiaojun. (2011). Oxygen-generating nanofiber cell scaffolds with antimicrobial properties. *ACS applied materials & interfaces, 3*(1), 67-73.

Westendorf, Jennifer J, Kahler, Rachel A, & Schroeder, Tania M. (2004). Wnt signaling in osteoblasts and bone diseases. *Gene, 341*, 19-39.

Wu, Mengrui, Deng, Lianfu, Zhu, Guochun, & Li, Yi-Ping. (2010). G Protein and its signaling pathway in bone development and disease. *Front Biosci, 15*, 957-985.

Xie, Denghui, Guo, Jinshan, Mehdizadeh, M Reza, Tran, Richard T, Chen, Ruisong, Sun, Dawei, . . . Yang, Jian. (2015). Development of injectable citrate-based bioadhesive bone implants. *Journal of Materials Chemistry B, 3*(3), 387-398.

Xie, L, Yu, H, Deng, Y, Yang, W, Liao, L, & Long, Q. (2016). Preparation and in vitro degradation study of the porous dual alpha/beta-tricalcium phosphate bioceramics. *Materials Research Innovations, 20*(7), 530-537.

Yeong, Wai-Yee, Chua, Chee-Kai, Leong, Kah-Fai, & Chandrasekaran, Margam. (2004). Rapid prototyping in tissue engineering: challenges and potential. *TRENDS in Biotechnology, 22*(12), 643-652.

Yong Liang, SU, & Wang, Xiao Yan. (2016). Inhibition of Enterococcus faecalis by Calcium Peroxide. *Chin J Dent Res, 19*(2), 109-113.

Yoshida, Kazuya, Bessho, Kazuhisa, Fujimura, Kazuma, Kusumoto, Kenji, Ogawa, Yutaka, Tani, Yoshiaki, & Iizuka, Tadahiko. (1998). Osteoinduction capability of recombinant human bone morphogenetic protein-2 in intramuscular and subcutaneous sites: an experimental study. *Journal of cranio-maxillo-facial surgery, 26*(2), 112-115.

Zhao, Hong, Miranda, Pedro, Lawn, Brian R, & Hu, Xiaozhi. (2002). Cracking in ceramic/metal/polymer trilayer systems. *Journal of materials research, 17*(5), 1102-1111.

Zhou, Kui, Dong, Chunfa, Zhang, Xianglin, Shi, Lei, Chen, Zhichao, Xu, Yanlin, & Cai, Hao. (2015). Preparation and characterization of nanosilver-doped porous hydroxyapatite scaffolds. *Ceramics International, 41*(1), 1671-1676.

Zou, Fen, Zhao, Naru, Fu, Xiaoling, Diao, Jingjing, Ma, Yijuan, Cao, Xiaodong, . . . Wang, Yingjun. (2016). Enhanced osteogenic differentiation and biomineralization in mouse mesenchymal stromal cells on a β-TCP robocast scaffold modified with collagen nanofibers. *RSC Advances, 6*(28), 23588-23598.